VALIDATION OF ENDPOINTS AS BIOMARKERS OF LOW-DOSE RADIATION DAMAGE

Maria Susanna Rossouw

Dissertation submitted to the fulfillment of the requirements for the Master's Degree in Technology (Biomedical Technology) in the Faculty of Applied Sciences at the Cape Technikon

November 2004

Supervisor: Dr K A Meehan
Faculty of Applied Sciences
Cape Technikon

Co-supervisor: Dr W A Groenewald
Department of Radiation Oncology
Tygerberg Hospital

God's creation never
ceases to amaze me ...

Declaration

I, the undersigned hereby declare that the work contained in this dissertation is my own original work and has not previously in its entirety or in part been submitted to any University or Technikon for a degree.

..... 7/12/04

Signature Date

Table of contents

Abstract

The need for radiobiological research was born from the discovery that high doses of radiation could cause cancer and other health effects. However, recent developments in molecular biology uncovered the effects of low doses of radiation on different biological systems and as a result new techniques have been developed to measure these effects.

The aim of this study was thus to validate biomarkers of initial DNA strand breaks, micronucleus formation, and the different phases of apoptosis as biological indicators of low-dose radiation damage. Furthermore, the difference in response of blood cells to different qualities and doses of radiation was investigated by irradiating cells with low- and high-LET radiation simultaneously.

Blood from one donor was irradiated with doses between 0 and 4 Gy gamma- and neutron radiation. The alkaline single-cell gel electrophoresis (comet) assay was performed on different cell preparations directly after irradiation for the detection of initial DNA strand breaks. Radiation-induced cytogenetic damage was investigated using the cytokinesis-blocked micronucleus assay while different features of apoptosis were investigated by measuring caspase activation, enzymatic DNA fragmentation, and cellular morphology.

The comet assay was sensitive enough to detect DNA strand breaks above 0.25 Gy and showed that the lymphocyte isolation process induced some endogenous damage in cells, detected by the formation of highly damaged cells and hedgehogs in

isolated cell preparations only.

Although the micronucleus assay was not sensitive enough to detect significant radiation damage below 0.5 Gy in either of the two radiation qualities, the difference in energy deposition between low- and high-LET radiation was confirmed. The potential therefore exists to use the assay as a biomarker of radiation damage above 0.5 Gy. It was apparent that the quality of PHA could induce a positive correlation with the NDI and micronucleus frequency and needs to be investigated further.

The detection of very low levels of caspase activation in irradiated lymphocytes led to the conclusion that irradiated lymphocytes do not follow the well-known caspase proteolytic pathway as major route of apoptosis but rather the more unknown proteasome/ubiquitin pathway. The TUNEL Assay was very sensitive to neutron and gamma doses below 0.5 Gy and proved to be the only assay sensitive enough to detect the effect of low- and high-LET radiation doses in the very low-dose region. Although cellular morphology was not validated for use as indicator of radiation damage, it confirmed the apoptotic response of lymphocytes to radiation.

Although the comet-, CBMN- and caspase 3/7 assays produced significant dose-response relationships after exposure to low- and high LET radiation, they would not be sensitive enough for use as biological dosimeters in the very low-dose (<0.5 Gy) region. However, once standardised, the Apo-Direct Assay may prove to be suitable as a biological indicator of radiation damage as well as a predictor of radiosensitivity.

Acknowledgements

When I started out on this project, I could not imagine how much I would learn in the process. I not only learnt a lot about radiobiology, tissue culture and radiation, but also learnt that there are still people in the scientific world that are really proud of their work and who would not hesitate to help others to achieve their goals and to reach their dreams. I would like to thank…

- *Professor Fred Vernimmen for allowing me to undertake this study and to use the facilities and equipment of the Department of Radiation Oncology at Tygerberg Hospital.*
- *Dr Wilhelm Groenewald, head of Medical Physics at Tygerberg Hospital and co-supervisor of the project, who encouraged me with his sincere interest in my study and who shared in my excitement whenever I discovered yet another interesting concept of radiobiology. Thank you for allowing me to rearrange my work schedule around my experiments and for your constructive comments on the manuscript.*
- *Dr Kathy Meehan, my study leader and source of inspiration. She introduced me to the field of genetic toxicology and inspired me with her enthusiasm about the lessons she learnt from her bats. She has secured the funds from the NRF and the Thuthuka Project to support the study and has introduced me to several experts in the field, creating a valuable platform for the exchange of knowledge and expertise.*
- *Dr Kobus Slabbert at the Radiobiology Laboratory, iThemba LABS, for hour-long discussions on the experimental approach of the study. I have learnt invaluable lessons from him and appreciate the time and effort he put in. My sincere thanks to Timothy, the medical physicists and the radiographers for their technical assistance and for the nursing staff who drew countless tubes of blood.*

- *Dr Tony Serafin at the Department of Radiobiology, Tygerberg Hospital who was always willing to help with the preparation of reagents and who, together with Dr Kobus Slabbert, educated me in the finer aspects of tissue culture. I would like to thank Dr John Michie who allowed me to use the equipment in the radiobiology laboratory and for his input.*
- *Mr Christo Muller from the Department of Anatomy and Physiology who handled the analysis of samples on the highly sophisticated flow cytometer. Without him I would have been lost.*
- *Dee Blackhurst from the Faculty of Medicine at UCT for the use of their spectrofluorometer and for the many hours she sacrificed to assist me with the read-out of samples. It is hard to thank someone for so much kindness – thank you, Dee.*
- *Kathy Smit, my co-student and friend with whom I have shared many hours of hard work and little sleep. It was assuring to know she was there, sharing the same dreams and ideals and working to the same goal. Thanks for your encouragement and pep talks, Kathy. I really enjoyed working with you.*
- *My husband, Joos, who drove me around at night and kept me company at the lab while everybody else was sleeping. I appreciate your love and support.*

This was an experience that enriched my life with new knowledge and new friends and I am truly grateful to everyone who has contributed to the success of this project. Thank you.

- Anne-Mari -

List of Tables

List of Figures

List of Abbreviations

µg	microgram
µl	microliter
ATP	adenosine triphosphate
BN	binucleated
Bq	becquerel
CA	chromosome aberrations
CBMN	cytokinesis-blocked micronucleus assay
cGy	centigray
CV	coefficient of variation
DMSO	dimethyl sulfoxide
DNA	deoxy ribonucleic acid
DSB	double strand break
EDTA	ethylene diamine tetra-acetic acid
FCS	foetal calf serum
FISH	fluorescence in situ hybridisation
FITC	fluorescein isothiocyanate
FLICA	*fluorescent inhibitor of caspases*
Gy	gray
HDC	highly damaged cell
HH	hedgehog
ICRP	International Commission On Radiological Protection
keV	kilo electron volt
LAA	leukocyte apoptosis assay
LET	linear energy transfer

LMPA	low melting point agarose
LNT	linear-no-threshold
mA	milli-ampere
meV	milli-electron volt
MN	micronucleus
mSv	millisievert
NAD	nicotinamide adenine dinucleotide
NADH	nicotinamide adenine dinucleotide hydrogen
NDI	nuclear division index
NMA	normal melting point agarose
PARP	poly-ADP-ribose polymerase
PBS	phosphate buffered saline
PHA	phytohaemagglutinin
PI	propidium iodide
PS	phosphatidyl serine
RBE	radiobiological effectiveness
RPMI	Roswell Park Memorial Institute
SCE	sister chromatid exchange
SD	standard deviation
SSB	single strand break
SSD	source surface distance
TNF	tumour necrosis factor
TUNEL	terminal deoxynucleotidyl transferase dutp nick end labelling
V	volt

LMPA	low melting point agarose
LNT	linear-no-threshold
mA	milli-ampere
meV	milli-electron volt
MN	micronucleus
mSv	millisievert
NAD	nicotinamide adenine dinucleotide
NADH	*nicotinamide adenine dinucleotide hydrogen*
NDI	nuclear division index
NMA	normal melting point agarose
PARP	poly-ADP-ribose polymerase
PBS	phosphate buffered saline
PHA	phytohaemagglutinin
PI	propidium iodide
PS	phosphatidyl serine
RBE	radiobiological effectiveness
RPMI	*Roswell Park Memorial Institute*
SCE	sister chromatid exchange
SD	standard deviation
SSB	single strand break
SSD	source surface distance
TNF	tumour necrosis factor
TUNEL	terminal deoxynucleotidyl transferase dutp nick end labelling
V	volt

Chapter 1

Introduction

1.1. Background to biological dosimetry

The exposure of individuals to ionising radiation and the possible detrimental effects on human health is of great concern to role players in the medical and industrial environment. Damage to DNA and other biological systems after environmental and occupational exposure could be important in the initiation and progression of cancer and other diseases; therefore effective genetic biomonitoring of human populations exposed to low-level radiation is essential as an early warning system for such diseases. Possible risk factors could be identified early enough for control measures to be implemented before irreversible DNA damage has been inflicted. Cellular responses to radiation are often measured in peripheral lymphocytes as these cells can be acquired in a non-invasive manner and, being a non-dividing cell, have the ability to carry genotoxic insult throughout their lifespan of roughly 1500 days (Chang *et al.*, 1999).

Although effective radiation protection programmes are in place to protect individuals against dangerous levels of radiation exposure, the influence of continuous doses of low-level radiation is still under investigation (Undeger *et al.*, 1999; Wojewódzka *et al.*, 1998; He *et al.*, 2000; Touil *et al.*, 2000; Chang *et al.*, 1999). Because estimates of risk for low doses of radiation over long periods of time are made by extrapolation of data relating to risk after acute doses, much uncertainty still exists about these

extrapolated estimates of risk. However, scientific advances in biology may lead to new genetic analysis techniques that can identify radiation-induced tumours above the general background of cancer incidence (Cunningham *et al.*, 1994).

1.2. Biomarkers of genotoxicity

The measurements obtained from biomonitoring procedures are referred to as biomarkers, defined as "cellular or molecular indicator(s) of exposure, health effects, or susceptibility" (Looney, 2002). Before biomarkers can be used for biomonitoring purposes, they first have to be developed, characterised and validated as biomarkers relevant to environmental carcinogenesis (Albertini, 1999). The validity of a biomarker is defined as "the extent to which it measures what it is intended to measure" (Looney, 2002). Adequate *validity* means that the result of the biomarker can be substituted for the result of the gold standard, but in the absence of a gold standard, the term *consistency* is used to describe the agreement between the gold standard and the other method used (Looney, 2002).

Chromosome aberrations (CA) have been extensively validated as the gold standard for cytogenetic markers of exposure to acute doses of ionising radiation (Albertini, 1999). However, these aberrations (dicentrics and rings) are unstable and disappear within six months following radiation exposure (Turai, 2000). The development of the fluorescence *in situ* hybridisation (FISH) assay for the detection of stable chromosome abnormalities (translocations) provided a method for retrospective biological dosimetry by which the true dose received during accidental or occupational radiation exposure can be estimated (Camparoto *et al.*, 2003).

The cytokinesis-blocked micronucleus (CBMN) assay detects radiation-induced chromosome breaks in cells by identifying chromosome fragments that lagged behind during mitosis. Micronuclei appear as small bodies in the cytoplasm resembling the nuclear material in morphology and staining pattern. Micronuclei show a clear dose-response relationship (Touil *et al.*, 2000); therefore an increased frequency of micronuclei in a cell is an indication of permanent genotoxic damage and is therefore a useful assay for biological dosimetry.

Since it is widely believed that DNA strand breaks are the critical lesion induced by ionising radiation (Steel, 2002), much research has gone into developing methods by which they can be measured. Some of the older methods employed sedimentation and filtration techniques (Steel, 2002), but the single-cell gel electrophoresis (comet) assay has emerged as a sensitive, cost-effective assay for the detection of DNA migration in an electric field (Rojas *et al.*, 1999). Negatively charged DNA fragments, embedded in agarose, migrate to the positive anode in an electric field, producing comet-shaped structures that are visible with fluorescence microscopy. The main advantage of this assay is the rapid processing of small cell numbers and the ability of the assay to detect low levels of DNA damage accurately.

Another complex phenomenon being studied widely is apoptosis, defined as "programmed cell death". As apoptosis is a complex process involving a variety of biological systems, different assays have been developed to measure different proteins and enzymes involved in the cascade, e.g. Annexin V (Wilkins *et al.*, 2002), FLICA (fluorescent inhibitor of caspase) (Smolewski *et al.*, 2002a), TUNEL (terminal deoxynucleotidyltransferase [TdT] dUTP nick end labelling) (Bebb *et al.*, 2001) and caspases (Louagie *et al,* 1999). Defects in genes that control apoptosis can promote cancer development or result in autoimmune disease. Based on the response of

lymphocytes to different types and doses of radiation, apoptosis assays have great potential as predictor of individual radiosensitivity of cancer patients and radiation workers (Crompton *et al.,* 1999).

1.3. Aim of study

The neutron facility at iThemba LABS near Faure, South Africa, is one of only four operational high-energy neutron therapy centres in the world. The beam of each neutron facility is unique in its physical and energy characteristics and the radiobiological effects of such a beam are therefore also unique. The availability of a nearby neutron facility provided the opportunity to expand the study by including a high-LET radiation source in addition to the more readily available gamma beams.

The main aim of the study was to validate biomarkers of direct DNA breakage (comet assay), micronucleus formation, and different stages of apoptosis as biological indicators of radiation-induced DNA damage. By measuring the sensitivity, reliability, and accuracy of each biomarker, the potential of each endpoint to be employed as biological dosimeter in the radiation protection environment could be evaluated.

In order to evaluate the assays for future implementation as biomarkers of radiation damage, the sensitivity of peripheral lymphocytes to reflect the mechanism of damage induced by different qualities and increasing doses of radiation was analysed. Dose-response relationships were established by irradiating cells with a low-LET ^{60}Co γ-beam and a high-LET 66 MeV p(66)/Be(40) neutron beam.

1.4. Methodology

Fresh blood from one healthy female donor was collected in Vacutainer tubes containing either EDTA or lithium heparin as anticoagulant. Different cell preparations were irradiated *in vitro* with ^{60}Co γ-rays and 66 MeV p(66)/Be(40) neutrons respectively to measure cell response in terms of DNA fragmentation, micronucleus formation and apoptosis. Three independent experiments were performed for each assay unless stated otherwise.

Gamma irradiation was carried out using two Cobalt units, i.e. the Theratron 780C treatment unit at the Department of Radiation Oncology at Tygerberg Hospital and the Eldorado 76 research unit at iThemba LABS. Neutron irradiation was performed using the cyclotron at iThemba LABS. Gamma and neutron doses ranging between 0 and 4.0 Gy were used for all experiments except for cell morphology where only 0 and 4 Gy gamma doses were used.

Great care was taken to ensure identical experimental conditions for both radiation qualities to provide the same radiation background for each experiment. To prevent variation in cell number for the caspase experiments, cells were pooled after isolation and split prior to irradiation. Control samples (unirradiated cells) were included in each experiment to measure inherent DNA damage.

The alkaline comet assay was applied for the detection of DNA strand breaks in whole blood, isolated lymphocytes, and cryopreserved isolated lymphocytes. Cells were embedded in agarose on slides, irradiated, and electrophoresed under high alkaline conditions. After neutralisation and drying, slides were stained with a DNA binding dye and analysed using a fluorescence microscope. Comets were classified

into 5 categories of DNA damage. DNA damage was presented by means of histograms and dose-response curves.

Micronucleus formation in isolated lymphocytes was studied by employing the cytokinesis-blocked micronucleus (CBMN) assay. Cells were isolated, stimulated with a mitogen, irradiated, and incubated at 37°C and 5% CO_2 for 44 hours after which cytokinesis was blocked with Cytocalasin B. After a total incubation period of 72 hours, cells were harvested and prepared for analysis. Micronuclei were analysed with fluorescence microscopy and dose-response curves were constructed.

The induction of apoptosis was studied by measuring caspase 3/7 activity using a spectrofluorometer, DNA fragmentation by endonucleases (flow cytometry), and cellular morphology by means of fluorescence microscopy. Cells were isolated, irradiated and incubated at 37°C under conditions of 5% CO_2 for between 6 and 90 hours after which cells were harvested and samples analysed.

1.5. Significance of study

The field of radiobiology came into existence with the discovery that high doses of radiation could cause cancer and other health effects. In recent years, the focus of radiobiology was directed towards research in the low dose region and phenomena such as the bystander effect, adaptive response, changes in gene expression etc. were reported (Washington State University, online). New techniques have made it possible to determine how molecules, cells, tissues, animals and humans respond to low doses of radiation. These new insights may provide a link between molecular studies and radiation-induced cancer.

Occupational and accidental exposure to radiation will always be an emotional and physical threat to employees and employers in the nuclear and medical industry and although well regulated, radiation protection policy makers would welcome more sensitive and reliable biomonitoring procedures. Not much data is available on the radiobiological effects of neutron radiation on radiation workers in the relevant industries; therefore most of the results obtained in this study will be original and reported for the first time. The outcome of this study may provide new information on biomonitoring procedures and possible new biomarkers.

Chapter 2

Radiation

2.1. Introduction

Radioactivity is the spontaneous transformation of an unstable nucleus to a stable or unstable daughter nucleus with emission of energy in the form of particles and/or photons. This process is most frequently accomplished by the emission of alpha particles (helium nuclei), beta particles (electrons and positrons), or gamma radiation (electromagnetic waves of very high frequency). The unit for measuring activity is the becquerel (Bq). One becquerel is the activity of a radioactive element in which there is one nuclear disintegration per second.

Ionising radiation is energy in the form of high-speed particles and electromagnetic rays. This energy is enough to knock electrons from atoms during its passage, thereby changing their physical state and causing the atoms to become electrically charged, or ionised. The presence of such ions in living tissues has the potential to disrupt normal biological processes. The principle unit for expressing the dose of radiation absorbed in a living tissue is the gray (Gy). One gray represents one joule of radiation energy absorbed per kilogram of tissue.

2.2. Types of radiation

2.2.1 Electromagnetic radiation

X-rays are generated in an electric device that accelerates electrons to high kinetic energy and stops them abruptly in a target, usually made of tungsten or gold. On the other hand, gamma rays are emitted by radioactive nuclides, representing excess energy given off in the decay process (Hall, 2000).

X- and gamma rays do not differ in their properties, they merely differ in the way they are produced. X-rays may be thought of as waves of electrical and magnetic energy or "packets" of energy. These "packets" of energy are called photons and each one contains an amount of energy. This concept of "packets of energy" is important to the radiobiologist, as the biological effect of the x-rays is not determined by the amount of energy absorbed, but by the energy of the individual "packages" (Hall, 2000).

2.2.2 Particulate radiation

Neutrons are produced when a charged particle collides with a suitable target material, e.g. beryllium. Neutrons are uncharged particles that produce a densely ionising radiation track, causing more severe damage than x- or gamma rays.

The alpha particle is a heavy, positively charged particle producing high-LET radiation. Because of their relatively large size, alpha particles collide readily with matter and lose their energy quickly. They therefore do not penetrate tissue very deeply (only 0.04 mm) (Van Rooyen, 2002), and because they give up their energy over such a short distance, alpha particles can inflict more severe biological damage

than other types of radiation. They are particularly harmful to lung tissue when inhaled.

Beta particles are fast moving negative (negatron) or positive (positron) electrons. Being much smaller and having a smaller charge than alpha particles, they move faster and can penetrate up to one centimetre of water or tissue.

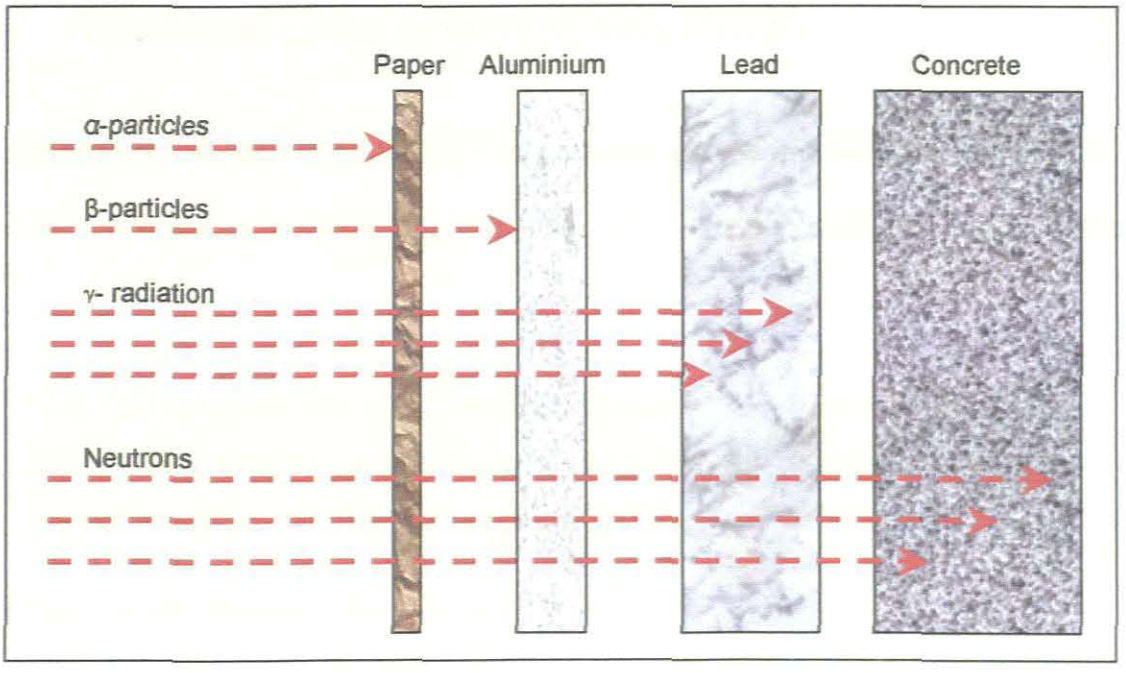

***Figure 2-1**: Graphic illustration of penetration abilities of different types of radiation (Redrawn from Van Rooyen, 2002).*

2.3. Background radiation

Humans are continuously being exposed to radiation from natural sources in the earth's crust, building materials, food, and cosmic radiation from the sun. Small quantities of radioactive materials are normally present in the human body of which only potassium-40 makes an appreciable contribution to human exposure from

ingestion. However, with a dose-rate of about 0.2 mSv per year it could be a possible source of mutations (Hall, 2000).

The total average effective radiation dose to the population is 3.6 mSv per person per year. Approximately 15% of this is contributed by medical radiation, 84% by natural background radiation and less than 1% by the nuclear industry (Van Rooyen, 2002).

2.4. Radiobiological Effectiveness (RBE)

The difference between different types of radiation producing the same biological effect is expressed in the RBE (Fajardo *et al.* 2001). The definition of RBE is given as:

> *"The RBE of some test radiation (r) compared with x-rays is defined by the ratio D_{250}/D_r, where D_{250} and D_r are, respectively, the doses of x-rays and the test radiation required for equal biological effect." (Hall, 2000)*

This could be expressed in the following formula:

$$RBE = \frac{\text{Dose in Gy from 250 keV x-ray}}{\text{Dose in Gy from another radiation delivered under the same conditions that produces the same biological effect}}$$

(Travis, 1989)

It is important to note that the biological response and not the radiation dose is the constant. The biological effectiveness of radiations with different LETs is measured and therefore RBE will only be a meaningful value if both the test system and the biological end point measured are identical (Travis. 1989). RBE is highly dose-dependent and therefore a different RBE could be expected for each dose point measured.

2.5. Linear Energy Transfer (LET)

Linear Energy Transfer can be defined as the rate at which energy is deposited per unit distance of the path travelled by a particle (keV/μm) (Travis, 1989) and depends on the mass, the charge and the velocity of the particle. Low-LET radiation, e.g. gammas and electrons, produces sparse ionisations separated by long distances while high-LET radiation, e.g. neutrons and alphas, produces dense ionisations in very short distances, giving rise to concentrated columns of ionisations along the tracks (**Figure 2-2**). Radiobiological differences between low- and high-LET radiations will be discussed in more depth in Chapter 3.

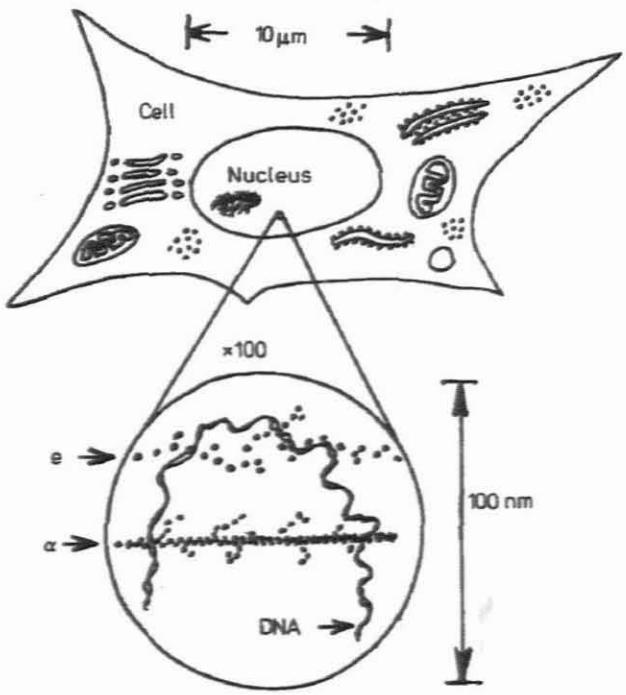

Figure 2-2: *Illustration of the track structure of low-LET (gammas) and high-LET (neutrons) radiation through a small part of a nucleus (Fowler, 1981).*

2.6. Radiation protection

The biological effect on humans can be somatic or genetic. Somatic effects appear in the person irradiated while genetic effects only affect their offspring. The acute effects of radiation occur after a single dose received in a relatively short period of time and can range from nausea to death. The chronic effects of radiation are due to relatively small incremental doses received over a long period of time. Low radiation doses are defined as total doses less than 10 mSv, received at high dose rates in single events, or dose rates less than 20 mSv per year, received continuously (Testard and Sabatier, 2000). The biological effects of radiation depend upon the size of the dose received, the extent of the body irradiated, the part of the body irradiated, and the type of radiation (Samarin, 2001).

The detrimental effects of radiation on man are classified into stochastic and non-stochastic (deterministic) effects. Stochastic effects occur by chance and the probability of the effect occurring is a function of dose without a threshold. Examples of these effects are cancer and genetic disorders. The severity of deterministic effects on the other hand varies with dose and the effects have a threshold value. Cataract formation, depletion of bone marrow and impaired fertility are examples of such effects (Pizzarello and Witcofsky, 1982).

Radiation protection standards are based on the conservative assumption that risk is directly proportional to the dose, even at the lowest levels, though there is no evidence of risk at low levels. This is called the "Linear no-threshold (LNT) hypothesis". Most countries have adopted their own systems of radiological protection that are mostly based on the recommendations of the International Commission on Radiological Protection (ICRP) (ICRP 60, 1990; ICRP 75, 1997).

South African radiation protection regulations and codes of practice are based on the latest recommendations of the ICRP. The four key points of the ICRP's recommendations are:

Justification	*No practice should be adopted unless its introduction produces a positive net benefit*
Optimisation	*All exposures should be kept as low as reasonably achievable (ALARA), economic and social factors taken into account*
Limitation	*The exposure of individuals should not exceed the limits recommended for the appropriate circumstances*
Risk limits	*The risk of potential exposure should be minimised*

The ICRP recommends that the maximum permissible dose for occupational exposure should be 20 mSv per year averaged over five years with a maximum of 50 mSv in any one year. For public exposure, the limit is 1 mSv per year, averaged over five years. These figures exclude background levels and medical exposure.

Chapter 3

Biological effects of radiation

3.1. Introduction

The challenge of radiobiological research today lies in the uncertainty of possible health effects induced by low doses of radiation. Previously it was necessary to estimate the biological effects of low doses from high-dose effects, such as cancer development in atomic bomb survivors. Recent scientific advances such as the sequencing of the human genome and newly developed radiobiology techniques have made it possible to determine how molecules, cells, tissues, animals and humans respond to low doses of radiation. This information could be instrumental in the development of new methods for using radiation in the treatment of disease on the one hand, and to provide a scientific basis for radiation protection on the other (Washington State University, online).

3.2. Interaction of radiation with matter

When ionising irradiation interacts with matter, ionisations and excitations are produced in macromolecules or in the cellular medium. Direct ionisation occurs when a particle is absorbed by a **macromolecule** (i.e. DNA) with the ejection of an electron. This is the most probable mechanism of biologic effect for high-LET radiation such as neutrons. The secondary charged particles that are produced, result in a dense column of ionisations more likely to interact with DNA (**Figure 3-1**B)

Indirect ionisation involves the absorption of ionising radiation in the **cellular medium** (i.e. water), resulting in the formation of ion pairs and unstable free radicals. This mode of action is dominant for low-LET radiation such as x-rays and gamma rays (**Figure 3-1**A). Free radicals have the ability to initiate other chemical reactions and could thus cause damage throughout the cell (Travis, 1989). Since biological systems consist largely of water, water molecules are the most probable targets of indirect ionising radiation.

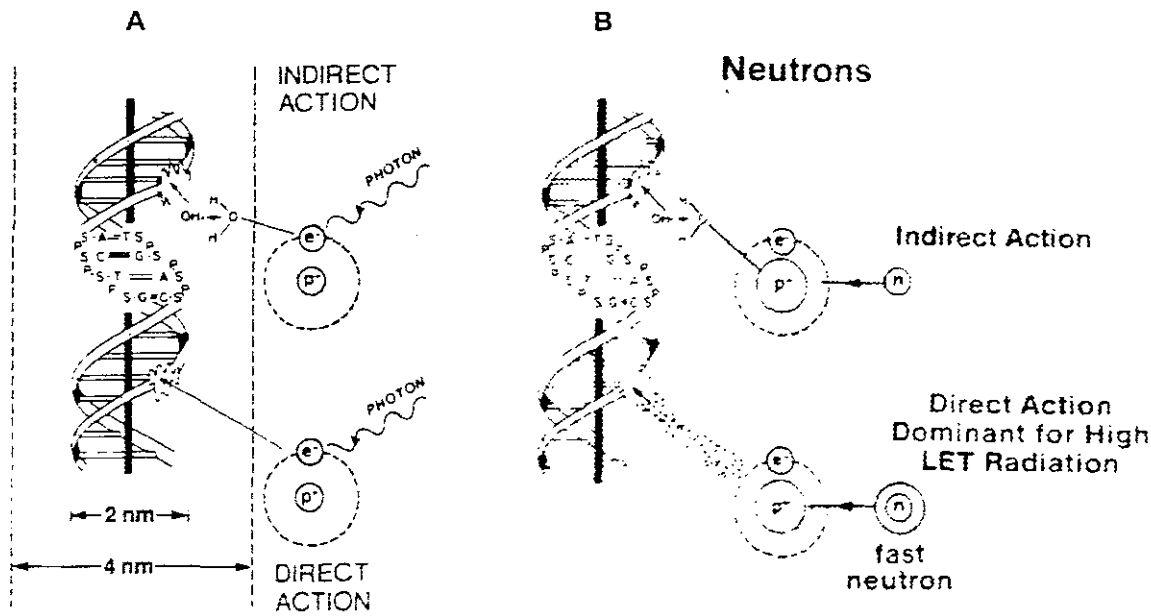

***Figure 3-1**: Direct and indirect actions of radiation. Low-LET radiation mainly invokes indirect DNA damage (A), while the heavy, densely ionising high-LET particles produce mostly direct DNA damage (Hall, 2000).*

3.3. Factors influencing radiation response

3.3.1 Physical factors

The most important physical factors that affect the degree and type of biological response are the **type** of radiation, the total **dose** administered and the **time** frame in which the dose was given (Fajardo *et al.*, 2001).

After irradiation with very large doses, mostly DSB are introduced and all cellular functions cease and the cell undergoes immediate cell death (interphase death). Cell death is defined as "the irreversible loss of reproductive capacity". With lower doses delivered to dividing cells, mostly SSB are introduced with the result that a proportion of the cells lose their capacity for division or proliferation (Tubiana *et al.*, 1990).

3.3.2 Chemical factors

Chemical substances may either protect cells against the effect of radiation or enhance destruction. High oxygen levels have an inducing effect on cell killing while low levels have a protective effect. Halogenated pyrimidines increase the radiosensitivity of cells while the sulfhydrylamines serves to protect cells against radiation-induced injury (Fajardo *et al.*, 2001)

3.3.3 Biological factors

Two of the most important biological factors influencing the response of cells to radiation are the ability of cells to **repair** damage and the timing of exposure in terms of the **cell cycle**. Cells are most sensitive during the G_2 phase and least sensitive in the last part of the S phase. Repair is much more effective after low-LET radiation than after high-LET radiation (Fajardo *et al.*, 2001).

3.4. Cellular responses to radiation

When ionising radiation interacts with cells it triggers a sequence of processes that will ultimately result in one of the following end points:

Cells are undamaged by the dose
Cells are damaged, repair the damage, and operate normally
Cells are damaged, repair the damage, and operate abnormally
Cells die as a result of the damage (Samarin, 2001).

These processes are divided into three distinct phases, i.e., a physical phase, a chemical phase, and a biological phase (Steel, 2002).

The **physical phase** (induction phase) is marked by interactions between the charged particle and the molecules in the tissue or medium, giving rise to either ionisations or excitations.

The **chemical phase** (processing phase) describes the reaction of damaged atoms and molecules (free radicals) with other cellular components in an attempt to stabilise the electronic charge equilibrium in the cell. At the same time, the cell tries to repair the damage by other means, which could lead to permanent chemical changes in biologically important molecules.

All the processes that follow the first two phases are regarded as the **biological phase** (manifestation phase) of radiation repair. The vast majority of DNA lesions are successfully repaired by enzymatic reactions and will have no permanent influence on the viability of the cell. Some lesions however will not be repaired and these would eventually lead to cell death. The sequence of processes following exposure to ionising radiation is summarised in **Figure 3-2**.

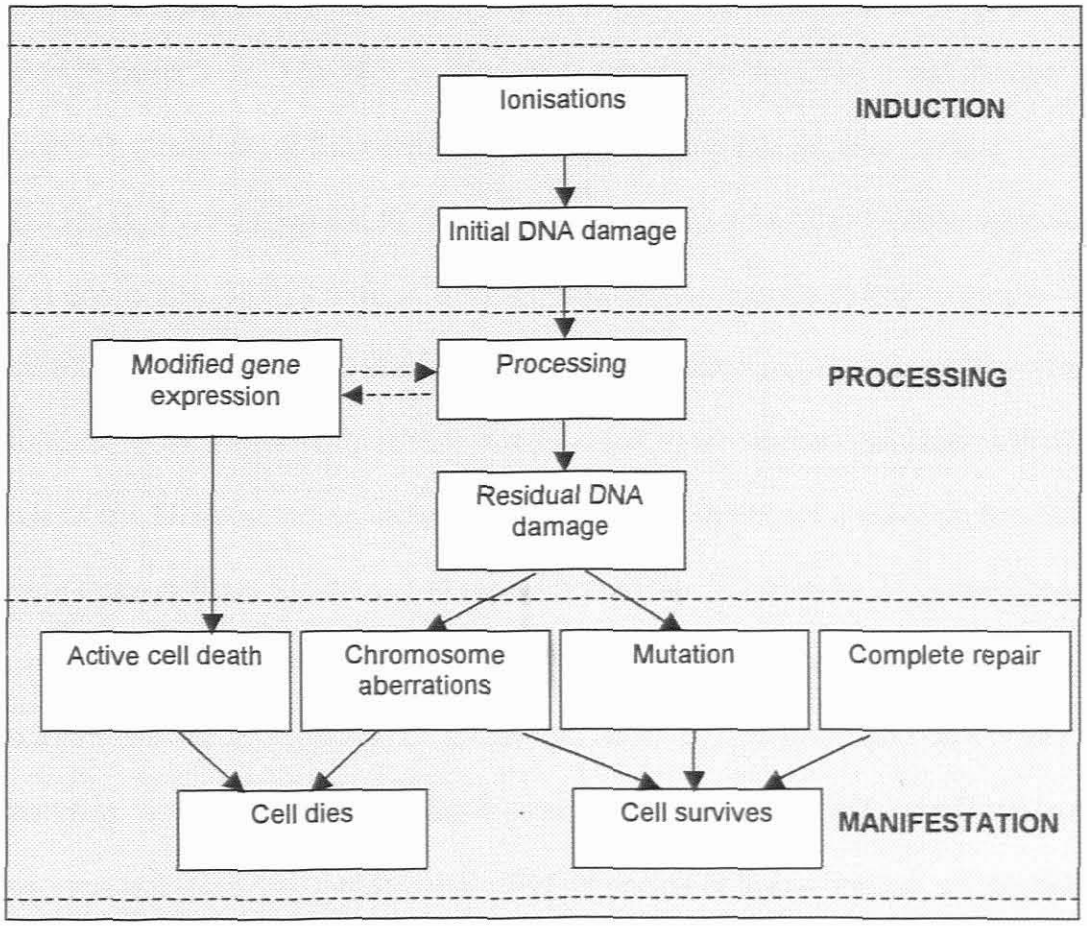

***Figure 3-2**: The sequence of processes taking place in cells after radiation (Redrawn from Steel, 2002).*

3.5. Radiation effects on the DNA molecule

Deoxyribunucleic acid (DNA) is a large molecule with a characteristic double helix structure. Each strand is made up of nucleotides, arranged in a specific sequence to specify the genetic code. Nucleotides are subunits consisting of a base, a sugar group, and a phosphate group. The two strands are held together by hydrogen bonds between the bases. The long DNA molecule is organised in a highly super coiled structure, becoming visible as chromosomes during mitosis (Steel, 2002).

Many different types of damage can occur in the DNA molecule as a consequence of radiation (**Figure 3-3**). The loss or change of a **base** on the DNA chain always results in the alteration of the base sequence, changing the genetic code of the cell. This could be of consequence to the cell, giving rise to a mutation. When **breaks** occur in one of the DNA chains, it is not of great consequence to the molecule because it is usually repaired within minutes after irradiation, using the other strand as template. If the repair is incorrect, it may result in a mutation. Breaks in **both strands** of the DNA molecule, however, can have a significant impact on the cell, making it more difficult for the cell to repair accurately. These double strand breaks are the most likely lesion produced by radiation, resulting in strand separation and subsequent cell killing, mutation or carcinogenesis. **Cross-links** can be formed between two regions on the same DNA strand, two regions on different strands or between two different DNA molecules. The influence of these lesions on the cell is unclear, but it could be detrimental if not repaired properly.

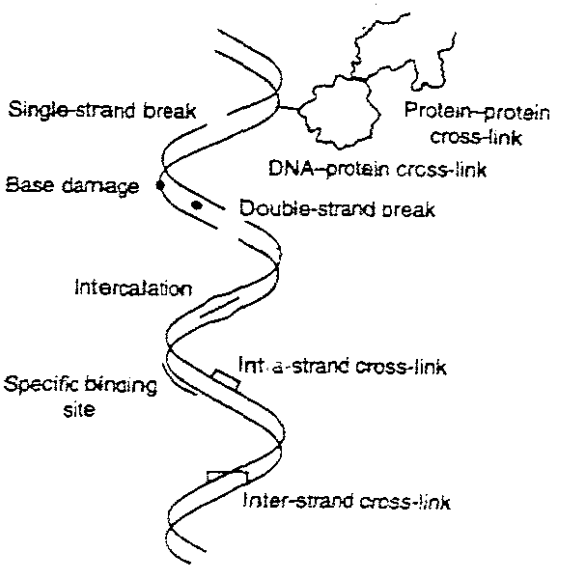

Figure 3-3: Types of DNA damage induced by radiation (Steel, 2002)

3.6. Chromosomes

Radiation can induce chromosome breaks in somatic cells and germ cells, which can be transmitted during mitosis and meiosis. When chromosomes break, "sticky ends" are produced, resulting in broken ends sticking together. Breaks may rejoin in original configuration without any influence on cell function or they may rejoin incorrectly and give rise to an aberration, producing a deletion at the next mitosis. Broken ends may also join other broken ends, giving rise to distorted chromosomes (Hall, 2000).

Chromatid aberrations are produced when irradiation occurred after DNA synthesis and only one arm of a chromosome has been affected. Chromosome aberrations, on the other hand, are produced when cells are exposed to radiation before DNA synthesis. A chromosome break will be replicated if not repaired before DNA synthesis and the damage will be visible in both daughter cells (Hall, 2000).

When a break occurs in each arm of a chromosome, the "sticky" ends rejoin incorrectly to form a **ring** and an **acentric** fragment (**Figure 3-4**A). A second chromosome is formed without a centromere and will be lost at the next mitosis. When two separate chromosomes join to form an interchange, a new chromosome with two centromeres is formed, termed a **dicentric** (**Figure 3-4**B). Symmetrical translocations are not lethal to the cell, but are associated with several human malignancies caused by the activation of an oncogene, e.g. Burkitt's lymphoma (Kumar, 1997). When a break is produced in two different chromosomes, broken pieces are exchanged between the two chromosomes and the "sticky" ends rejoin to form a translocation (**Figure 3-4**B). **Translocations** are visible with fluorescent *in situ* hybridisation (FISH or whole chromosome painting). Probes are available for

specific chromosomes, which are then visible as fluorescent signals against a dark background.

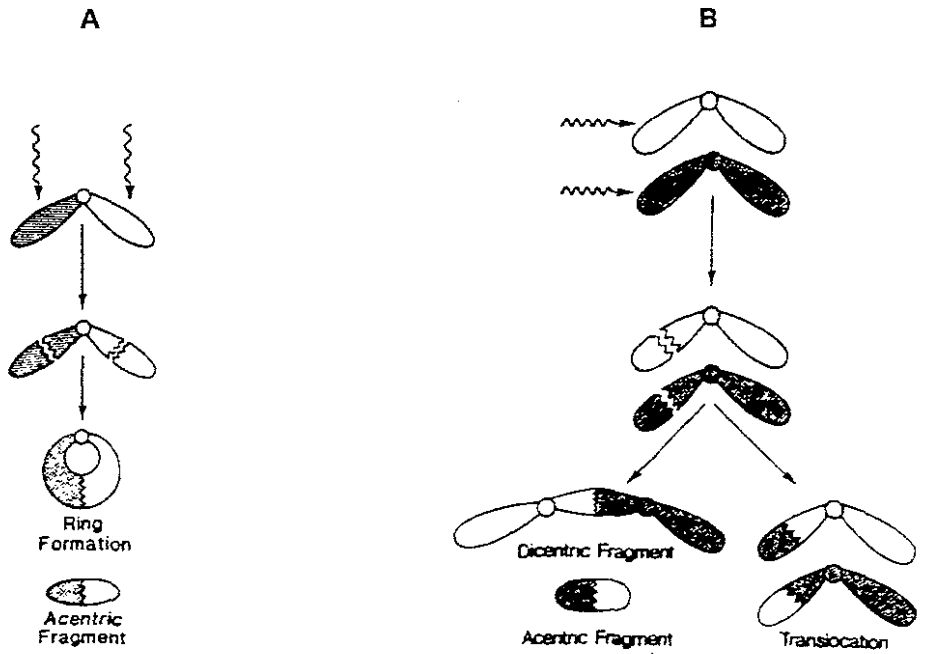

Figure 3-4: *Radiation-induced breaks in both arms of a chromosome can result in an acentric fragment and/or the formation of a ring (A). A break in one arm of two different chromosomes may result in the formation of a dicentric and an acentric fragment (B) (Travis, 1989).*

3.7. The haemopoietic system

Ionising radiation impairs haemopoiesis through a variety of mechanisms. Damage to the stem cells of the bone marrow results in a dose-dependent decrease in the production of and increase in apoptosis of mature haemopoietic cells. Moreover, ionising radiation also alters gene expression and interferes with intracellular and intercellular signalling pathways. This could lead to the induction of leukaemia, the most significant haematological complication arising in atomic bomb survivors in Japan (Dainaik, 2002).

Essentially blood consists of plasma, erythrocytes (red blood cells), leucocytes and thrombocytes (platelets). Leucocytes are nucleated cells and consist of neutrophils (65-70%), lymphocytes (25-35%), monocytes (5-10%), eosinophils (1%) and basophils (<1%) (Hendry and Lord, 1995). Lymphocytes are derived from the same pluripotential stem cells as the other haemopoietic cell lines and consist of B- and T-lymphocytes.

Peripheral red blood cells, granulocytes, and platelets are fairly radioresistent while lymphocytes show a spectrum of radiosensitivities. In general, B cells are more radiosensitive than T cells while subpopulations of T cells have varying radiosensitivities (Tubiana *et al.*, 1990). Total body irradiation leads to a rapid fall in the number of circulating B and T lymphocytes and regeneration is accomplished by proliferation and differentiation of bone marrow stem cells. Many lymphocytes die within hours of radiation, providing a useful indicator of the dose received after a radiation accident (Hendry and Lord, 1995).

Chromosomal aberrations in human lymphocytes have been widely used as biomarkers of radiation exposure because the lifespan of a peripheral lymphocyte could be 1500 days (Hall, 2000) reflecting the total amount of chromosomal damage induced in that period of time. The amount of dicentrics and rings in lymphocytes of exposed persons usually reflects the radiation dose received. Symmetrical translocations are classified as stable and can be detected in lymphocytes for many years after induction because they are not lethal to the cell and are passed on to the progeny. It was shown in a study on atomic bomb survivors of Hiroshima and Nagasaki that chromosomal aberrations can persist for as long as 25 years, proving the value of translocations as biological dosimeter (Pizzarello and Witcofsky, 1982).

3.8. Apoptosis

Two major mechanisms of cell death exist, namely apoptosis and necrosis. Necrosis occurs as a response to injury during which cells swell and lyse, eliciting an inflammatory response. Apoptosis on the other hand, involves the activation of a genetic program and no inflammatory response is produced. Morphologically, cells undergoing apoptosis display membrane blebbing and nuclear and cytoplasmic condensation (Schimmer *et al.*, 2001).

Apoptosis is triggered by a variety of stimuli, including cell surface receptors such as Fas, mitochondrial responses to stress, cytotoxic T cells, and radiation. All apoptotic triggers lead to a final pathway where cells reach the point of irreversible commitment to death. Activation of caspases, calcium influx and loss of mitochondrial membrane potential result in depletion of ATP and NAD/NADH, changes in intracellular signalling, oxidative damage to cellular membranes, disruption of intracellular compartments, dilatation of endoplasmic reticulum, crosslinking of cytoplasmic proteins

and cell shrinkage. Within the nucleus endonucleases are activated, resulting in DNA fragmentation (Tannock and Hill, 1998).

Radiation-induced cell death is highly cell-type dependent with cells from the haemopoietic and lymphoid systems particularly sensitive to radiation. In contrast to the classical pathways of apoptosis, the induction of apoptosis by radiation is less well studied, but it has been shown that *in vitro* gamma irradiation induces apoptosis in peripheral lymphocytes (Louagie *et al.*, 1999).

Different cells use different apoptosis pathways and the critical determinant of whether a cell will live or die depends on the regulatory mechanism that determines whether the pathway is activated or repressed (Lewin, 2000). **Figure 3-5** summarises the classical pathway for activation of apoptosis via a protease cascade.

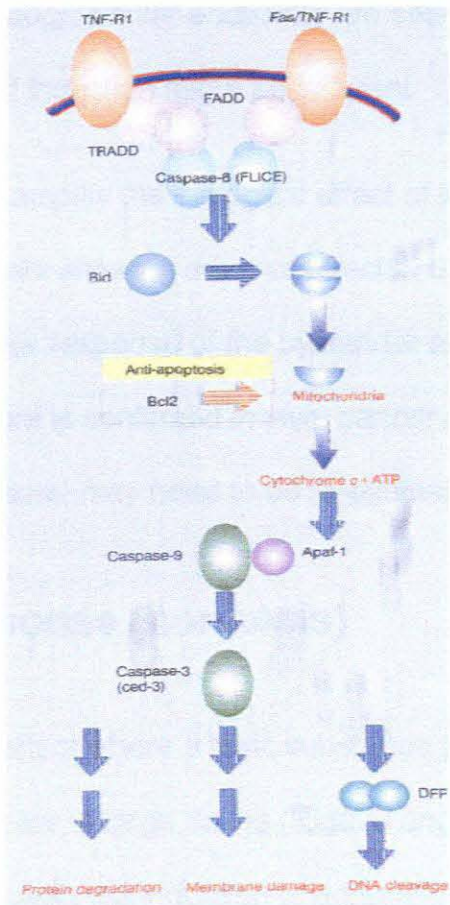

***Figure 3-5**: Classical pathway for activation of apoptosis via a protease cascade (Lewin, 2000).*

3.9. Bystander effect

The term "bystander effect" was given to the phenomenon in which damage was induced in cells not traversed by radiation. Bystander effects occur in cells receiving cell-, medium-, or blood borne signals from many types of cells following exposure to low- and high-LET radiation (Mothersill and Seymour, 2003). Numerous experimental studies have been undertaken and some general features were identified: bystander effects are observed at very low doses, do not increase significantly with dose and do not contribute significantly to total damage at higher doses (Ballarini *et al.*, 2002). Although the underlying mechanisms are still unknown, cellular communication seems to play a key role, inducing damage by cell killing, gene mutations, and modifications in gene expression. Mothersill and Seymour (2003) suggested that, although similar endpoints are seen for low- and high-LET radiation, the mechanism of induction might be different.

The bystander effect could amplify the biological effect of low dose radiation by increasing the number of cells showing adverse effects. Ballarini *et al.* (2002) commented on the non-linear response of the bystander effect at low doses and speculated that, if this feature is confirmed *in vivo*, cancer risk models at low doses, such as occupational exposure, may need to be re-evaluated.

3.10. Adaptive response (hormesis)

Hormesis is defined as an effect where a toxic substance acts like a stimulant in small doses, but as an inhibitor in large doses (Rigaud and Moustacchi, 1996). Olivieri *et al.* (1984) investigated the induction of adaptation by low doses of ionising radiation on lymphocytes that had incorporated tritiated thimidine and showed that

cells exposed to thimidine produced only half the chromosome aberrations induced in cells not exposed to the radioisotope before irradiation (Cited in Medical Radiation Physics, online). Vijayalaxmi *et al.* (1995) assessed the induction of adaptive response in lymphocytes by measuring the frequencies of chromosome aberrations and micronuclei after an adaptive dose of 1cGy and a challenge dose of 150 cGy. Their findings confirmed the heterogeneity in adaptive response to irradiation between individuals. The strong positive correlation between chromosome aberrations and micronuclei promotes the use of micronuclei as the method of choice over the more tedious chromosome aberration examination.

Although research on adaptive response is ongoing, it is not yet clear what the exact mechanism is. The working hypothesis is that an inducible molecular process, possibly mutagenic adaptation, is triggered by low doses and leads to cell protection against subsequent higher doses (Rigaud and Moustacchi, 1996).

Additional information concerning chronic exposure over long periods of time would be of great interest and relevance to the radiation protection community. The bystander effect and adaptive response are important in determining the biological responses at low doses of radiation and could have a significant influence on the shape of the dose-response relationship.

3.11. Carcinogenesis

A carcinogen may be defined as an agent that increases the risk of cancer development compared to development of the same cancer without exposure to the agent. Ionising radiation is seen as a general carcinogen, capable of inducing

tumours in almost all tissues of mammals, irrespective of species (Pizzarello and Witcofski, 1982).

Although radiation tends to increase the incidence of tumours arising naturally in the population, radiation-induced tumours cannot be distinguished from these (Pizzarello and Witcofski, 1982). The exact mechanisms by which genetic instability is induced by radiation are still uncertain but probably include mutations in genes involved in DNA synthesis and repair, induction of chromosome instability and aberrant production of oxygen radicals that can damage DNA. Two groups of genes play major roles in the development of cancer: proto-oncogenes and tumour suppressor genes.

Proto-oncogenes are positive growth regulators, promoting the proliferation and differentiation of normal cells. **Tumour suppressor genes** code for proteins that restrain cell growth. Cancer is a multistage process, involving the activation of proto-oncogenes and the inactivation of tumour suppressor genes (Anderson *et al.*, 2000).

Human data on carcinogenesis has been derived from occupational exposures, therapeutic exposures, accidental exposures, and studies of the atomic bomb survivors in Hiroshima and Nagasaki and from studies of exposure to pregnant women during medical x-ray examinations (Tannock and Hill, 1998). Estimates of risk for low doses of radiation and for low exposures over long periods of time are made by extrapolation of data relating to risk after larger (acute) doses. Radiation risk is defined as the increase in the number of cancer deaths over that expected for an unirradiated population. Although there is considerable uncertainty about these extrapolated estimates of risk, a Nordic Study Group examined a cohort of 3182 healthy adults for the presence of chromosome aberrations, micronuclei and sister

chromatid exchanges (SCE) and found "a highly statistically significant linear trend for a positive association (p = 0.009) between chromosomal damage in peripheral lymphocytes and subsequent cancer risk" (Anderson *et al.*, 2000).

3.12. Biological indicators of genotoxicity

The measurements obtained from biomonitoring procedures are referred to as biomarkers. They may be biomarkers of exposure, effect, or susceptibility (Anderson *et al. 2000).*

Biomarkers of exposure indicate exposure of bio'ogical material, e.g. proteins and DNA, to chemicals. Biomarkers of effect are used to measure processed biological activities, e.g. chromosome aberrations and gene mutations. Biomarkers of susceptibility should provide an indication of individual differences in response to genotoxic influence, e.g. polymorphic metabolising genes. These genes may influence the expression of biological effects and the development of cancer (Anderson *et al.*, 2000).

Before biomarkers can be used for human population research, they must have been developed, characterised and validated as biomarkers relevant to environmental carcinogenesis (Albertini, 1999). Inter-laboratory standardisation of assays for biomarkers is absolutely essential to ensure reliability, precision, and accuracy before they can be employed as indicators of DNA damage.

Physical monitoring of radiation dose is difficult or impossible after exposure when monitoring equipment was not in place. An alternative is to measure the level of exposure by measuring the biological effect rather than the agents itself (Gray *et al.*,

1995). However, it would be unrealistic to assume that a single biomarker will be able to measure all biological effects after exposure to radiation.

The full biological impact of occupational exposure to low-dose radiation is still unknown; therefore a multiple-assay approach was followed in this study, measuring a variety of endpoints associated with radiation damage. It is envisaged that this approach will identify biomarkers that are suitable for the accurate detection of radiation-induced genotoxic damage.

Chapter 4

Single-cell gel electrophoresis (comet) assay

4.1. Introduction and literature review

A variety of techniques for the detection of DNA damage are being used to identify genotoxic agents and to investigate DNA repair. Over the past two decades the comet assay has developed into a sensitive, reliable genotoxic test to detect single strand breaks (SSB) and double strand breaks (DSB) in human, animal and plant cells (Rojas *et al.*, 1999).

Radiation and chemicals can damage the DNA molecule, producing DNA fragments of varying lengths. The principle of the comet assay is based on the fact that negatively charged DNA fragments, embedded in agarose, migrate to the positive anode in an electric field, producing comet-shaped DNA structures that are visible with fluorescence microscopy. Alkaline treatment facilitates the unwinding and denaturation of DNA molecules, allowing the detection of single strand breaks. The extent of this migration is proportional to the amount and type of DNA damage as smaller DNA fragments migrate further in the gel than larger fragments.

The neutral microgel electrophoresis technique was first developed by Östling and Johanson (1984) and was able to detect DSB in individual mammalian cells. Singh *et al.* (1988) modified the neutral method, introducing an alkaline version to detect SSB, DSB, alkali-labile sites and incomplete excision repair sites. Olive introduced

another version of the alkaline comet assay in which unwinding and electrophoresis were conducted at a pH of 12.3 (Cited in Rojas *et al.*, 1999). Although the Singh and Olive methods are identical in principle, the Singh method appears to be more sensitive (Rojas *et al.*, 1999).

Low-dose ionising radiation is of specific concern in human biomonitoring and therefore the effects on radiation- and nuclear workers have been studied extensively. Touil (2002) studied a group of nuclear workers and found no difference in comet formation between study and control groups. Total exposure to the study group was estimated from personnel dosimeter records and ranged from 19.54 to 242 mSv. Wojewódska *et al.* (1998) and Ündeger *et al.* (1999) however, studied comet formation in radiation workers in hospitals and both found significant differences between their study- and control groups. The significance of these studies is the fact that none of the radiation workers received a radiation dose of >50 mSv per year on their personal radiation dosimeters but still displayed comet formation in lymphocytes.

The comet assay has also been applied in DNA repair studies (Bergqvist *et al.*, 1998; Mustonen *et al.*, 1999 and Collins *et al.*, 1997). Mendiola-Cruz and Morales-Ramirez (1999) investigated the repair kinetics of gamma ray-induced DNA damage in mice leukocytes at certain time intervals after irradiation. They found 80% of DNA damage visible after 3 minutes of treatment and complete repair after 120 minutes. Their findings proved the rapid repair capacity of leukocytes *in vivo* and proposed a useful method for determination of *in vivo* repair mechanisms with the comet assay. Malcolmson *et al.* (1995) reported the same tendency with an *in vitro* study on lymphocytes stating "the most damage is repaired within the first 15 minutes of

incubation, with a second slower repair completed after 120 minutes".

Various research groups have studied the effects of harmful substances in the environment. Ivancsits *et al.* (2002b) studied the influence of intermittent exposure to electromagnetic fields on human diploid fibroblasts, and Carere and co-workers (2002) investigated the genotoxic effects of urban air.

Although the comet assay is a relatively simple method to perform, technical variables such as the agarose concentration, temperature, pH, composition of the lysing solution, electrophoresis buffer, electrophoretic conditions of voltage, amperage, and unwinding and running time may effect the sensitivity of the assay (Rojas *et al.*, 1999). Speit *et al.* (1999) investigated the influence of temperature and found that performing the experiment at room temperature lead to significantly higher sensitivity of the comet assay, although the inter-experimental variability also increased. They concluded that standardised and constant experimental conditions are an absolute requirement for reliable comet assay results. Rojas *et al.* (1999) confirmed this finding in his review of the comet assay, stating that an unwinding and electrophoresis temperature of 15°C appears to give maximum sensitivity without comet formation in controls.

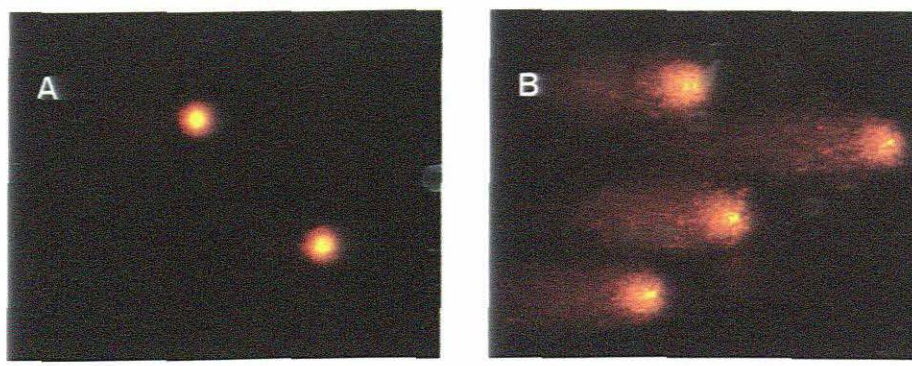

Figure 4-1: *Photomicrographs of comet formation in unirradiated lymphocytes after treatment with the alkaline comet assay. A: electrophoresis at 13°C, B: electrophoresis at 21°C.*

Thus, technical variability of the comet assay necessitated careful standardisation to compensate for individual research requirements. De Boeck *et al.* (2000) investigated the inclusion of a positive (ethyl methanesulfonate-treated cells) and negative internal standard (untreated cells) and found a negative internal standard to be more reliable due to its inter-experimental stability.

Quantification of DNA damage is mostly done by means of dedicated image analysis software. Tail moment, originally defined by Olive as the average distance migrated by the DNA multiplied by the fraction of DNA in the comet tail, is a popular and sensitive endpoint, but also varies between laboratories. However, when any part of an image becomes saturated (too much fluorescence), the amount of DNA in the comet cannot be quantified accurately, making the calculation of the tail moment inaccurate (Olive, 1999).

Although visual scoring of comets may be subjective, Collins *et al.* (1995) found a clear relationship between the percentages of DNA in the tail as measured by image analysis software (Komet 2.2, Kinetic Imaging LTD.) and visually classifying comets into five categories of DNA damage. Gutiérrez *et al.* (1998) compared comet length as measured by an ocular scale to visually classified comets and found a correlation coefficient (r) of 0.93 ($p < 0.001$) and 0.84 ($p < 0.001$) for pre- and post-treatment samples respectively.

Ivancsits *et al.* (2002b) used another method of visual scoring in a study on electromagnetic fields whereby a "comet tail factor" was calculated after a thousand comets per dose point were classified into five categories of DNA damage. The tail factor reflects weighted DNA damage and makes it possible to quantify and compare

DNA damage as a single figure.

The correlation between the comet assay and other genotoxic endpoints is still under investigation. Although Malcolmson *et al.* (1995) found a positive correlation between the comet- and micronucleus assays in the lymphocytes of severely radiosensitive cancer patients, they admitted that the use of the lymphocyte might be limited in reflecting variability in normal tissue at risk during radiotherapy. However, they reported an association between the determination of repair proficiency in the comet assay and the micronucleus assay. Touil (2002) compared the comet assay with the micronucleus assay and fluorescent *in situ* hybridisation (FISH) and concluded that a "positive correlation between mechanistically related biomarkers has confirmed the relevance of these biomarkers to assess genotoxic effects after exposure to ionising radiation".

4.2. Aim of study

The aim of this experiment was to validate the alkaline comet assay for the detection of initial DNA strand breaks induced by low-level gamma and neutron radiation between 0 and 4 Gy. Experimental conditions were adjusted to produce comets with <5% DNA migration in control (0 Gy) samples. Different qualities and doses of radiation were used to establish *in vitro* dose response relationships and to evaluate the efficiency of the comet assay to distinguish between different doses of gamma and neutron irradiation. Different cell preparations were used to investigate comet formation in viz., isolated lymphocytes, cryopreserved isolated lymphocytes, and whole blood.

4.3. Methodology

4.3.1 Cell preparation

Fresh blood from one healthy female donor was used throughout the study. Five millilitres of blood was drawn into Vacutainer tubes containing EDTA (ethylene diamine tetra-acetic acid) as anticoagulant and processed within one hour.

Three different cell preparations were analysed. **Firstly**, peripheral lymphocytes were isolated with Histopaque-1077 (Sigma), washed with Mg^{++} and Ca^{++} free Dulbecco's phosphate buffered saline (PBS, Sigma) and diluted in 10 ml RPMI 1640, supplemented with 5% heat inactivated foetal calf serum (FCS) to produce a cell count of 1.4×10^6 cells/ml of medium. A cell viability test was performed by mixing 100 µl cell suspension with 100 µl 0.4% Trypan Blue stain. Cells were counted in a haemocytometer and the percentage of dead cells was calculated.

Secondly, isolated lymphocytes were resuspended in 1.8 ml RPMI plus 0.2 ml DMSO and cryopreserved at –70°C. After three weeks the cell suspension was thawed in a 37°C water bath, resuspended in 8 ml RPMI, and pelleted by centrifugation. The pellets were resuspended in 2 ml RPMI and pooled for a Trypan Blue cell viability test.

Lastly, undiluted EDTA blood was processed and irradiated within one hour of collection.

4.3.2 Preparation of slides

Preparation of reagents and slides was performed according to the method described by Tice and Vasquez (1999). Buffer temperature and electrophoresis time were adjusted to produce controls with <5% DNA in the tail.

One percent normal melting point agarose (NMA, Sigma) and 0.5% low melting point agarose (LMPA, Sigma) were diluted in Ca^{++} Mg^{++} free PBS and carefully heated in a microwave oven until the agarose was just dissolved. NMA was used hot and the LMPA was cooled and maintained at 37°C for use. Fresh NMA and LMPA were prepared for each experiment.

Clear microscope slides with frosted ends (76 x 26 mm, B & C, Germany) were dipped into hot NMA and left to dry at room temperature. Duplicate slides were prepared for each dose point and labelled before coating. Twenty microliters (µl) of isolated cell suspension or 5 µl of undiluted whole blood was mixed with 75 µl of LMPA (37°C), dropped onto the coated slides, and covered with a cover slip (24 x 50 mm, Marienfield). Care was taken to prevent formation of air bubbles in the agarose. Slides were left on ice for 3-5 minutes to solidify before the cover slip was removed and another layer of 75 µl LMPA was added. Slides were cover-slipped, covered with tin foil, and returned to ice until irradiated. All steps involving cells were performed under yellow light or in the dark to prevent further DNA damage. An illustration of the preparation of cell layers is given in **Figure 4-2**.

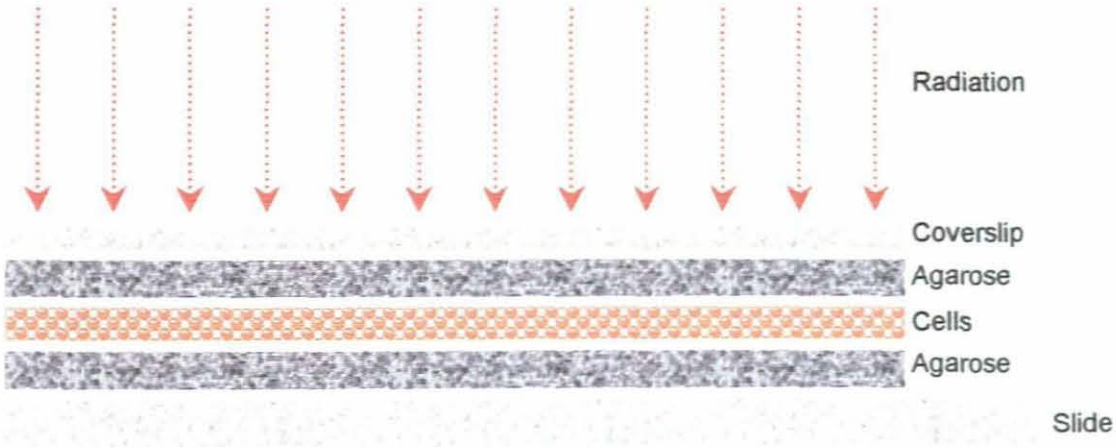

***Figure 4-2**: Layering of cells and agarose on microscope slide before electrophoresis.*

4.3.3 Irradiation procedure

Gamma irradiation was performed using a ^{60}Co γ-source (Theratron 780C, Theratronix International), delivering a dose-rate of 0.5 Gy/min at a source surface distance (SSD) of 100 cm, a field size of 10 x 10 cm^2 and a gantry angle of 0°. Slides were placed side-by-side in the centre of the radiation beam on a water phantom and covered by 0.5 cm build-up material. The dose at the position of the slides was verified by using a 0.6 cm^3 thimble Farmer ionisation chamber, type 2505/3 and a Farmer electrometer, model 2570. The dosimetry system was calibrated against a national standard at the CSIR in Pretoria, South Africa.

Neutron irradiation was performed using the cyclotron at iThemba LABS at Faure, using a dose rate of 0.35 Gy/min produced by 66 MeV protons bombarding a 19.6 mm thick beryllium target. The p(66)/Be(40) neutron beam generated had a large spectrum of energy with a maximum value of 64.15 MeV (Schreuder, 1992). A field

size of 20 x 20 cm^2 and SSD of 150 cm was used at a gantry angle of 0°. Slides were placed side-by-side in the centre of the beam on a 10 cm thick perspex block with 2 cm nylon as build-up material and 6 cm Perspex as backscatter. The dose at the position of the slides was verified by means of an 80 cm^3 Far West (model IC-80) ionisation chamber (Far West Technology) and a BNC Portanim (model AP-2H) current digitiser (Berkeley Nucleomics, Corporation, USA).

Doses of 0.25, 0.5, 1.0, 2.0, and 4.0 Gy were applied for both types of irradiation and for all cell preparations. Control samples (0 Gy) were treated identical but sham irradiated. Slides were irradiated at room temperature, but were returned to ice immediately after irradiation.

Cover slips were removed and slides were placed in cold lysing solution consisting of 2.5 M sodium chloride (NaCl, Merck); 100 mM ethylene diamine tetra-acetic acid (EDTA, Merck); 10 mM Tris hydroxymethyl aminomethane (Merck); 1% Triton X-100 (t-octylphenoxypolyethoxyethanol, Sigma) and 10% DMSO (Merck) at 4°C overnight in the dark.

4.3.4 Electrophoresis

Slides were removed from the lysing solution and put side-by-side on the horizontal gel box in an electrophoresis tank (MAX Electrophoresis gel unit, model HE 99, Hoefer Scientific Instruments) filled with fresh, chilled electrophoresis buffer consisting of 10 N sodium hydroxide (NaOH: Merck) and 200 mM EDTA with a pH of >13. The buffer temperature was maintained at <12 °C throughout the procedure by means of ice packs around the tank. As the tank could only accommodate 12 slides at a time, one slide per dose point for each radiation type was electrophoresed in

each of two batches to reflect intra-experimental variation. Slides were left in the tank for 30 minutes to unwind at a temperature of 7-10°C. The power supply (PS 500X DC Power Supply, Hoefer Scientific Instruments) was turned to 25 V and the current was adjusted to 300 mA by lowering or raising the buffer level in the tank. Slides were electrophoresed for 25 minutes at a temperature of 10-12°C, drained, and neutralised by submerging the slides in 3 changes of neutralising buffer (0.4 M Tris) for 5 min each. The fixation with ethanol as described by Tice and Vasquez (1999) was omitted to prevent DNA clumping (Singh and Stephens, 1997). Slides were drained and left to dry at room temperature, stained with 60-75 µl of ethidium bromide (20µg/ml), covered with a cover slip, and scored within an hour. Care was taken to prevent the formation of air bubbles under the cover slip.

4.3.5 Microscopic analysis

Comets were analysed using a 40x objective on a Nikon Labophot-2 microscope with an Episcopic EFD-3 fluorescence unit equipped with an excitation filter of 515-560 nm and a barrier filter of 590 nm. One hundred comets were scored per slide. A Nikon Coolpix 990 digital camera was used to capture photomicrographs.

Comets were visually classified into five grades of DNA damage corresponding to the approximate amount of DNA in the tail. **Grade 1** comets (**Figure 4-3 A**) had a tight nucleus with very little DNA in the tail. **Grade 2** comets (**Figure 4-3 B**) also displayed very little migrated DNA, but a few DNA fragments were clearly visible around the nucleus. **Grade 3** comets (**Figure 4-3 C**) showed more DNA migration in the tail with a nucleus that was starting to unravel, but still had clear nuclear boundaries. **Grade 4** comets (**Figure 4-3 D**) had only a small visible nuclear area with almost all the DNA

migrated into a longer tail. **Grade 5** comets (**Figure 4-3 E**) had no visible nucleus with a long diffuse tail of DNA fragments. **Hedgehogs** (**Figure 4-3 F**) were classified as cells containing a small, bright area of condensed DNA (head) and a large fan-shaped tail (Choucroun *et al.*, 2001).

Results were expressed as comet tail factors, calculated according to Ivancsits *et al.* (2002a). Tail factors made it possible to quantify weighted DNA damage as a single figure. Tail factors were calculated according to the following formula:

$$\text{Tail factor} = \frac{AF_A + BF_B + CF_C + DF_D + EF_E}{\text{Cells counted}}$$

Where:

A – E = number of cells classified as grade 1 to grade 5

F_A = average % of migrated DNA in grade 1 (2.5%)

F_B = average % of migrated DNA in grade 2 (12.5%)

F_C = average % of migrated DNA in grade 3 (30%)

F_D = average % of migrated DNA in grade 4 (67.5%)

F_E = average % of migrated DNA in grade 5 (>97.5%)

Hedgehogs (ghost cells) were reported but not included in calculation of tail factor.

Figure 4-3 on the following page shows the different DNA migration patterns that were used in grading criteria.

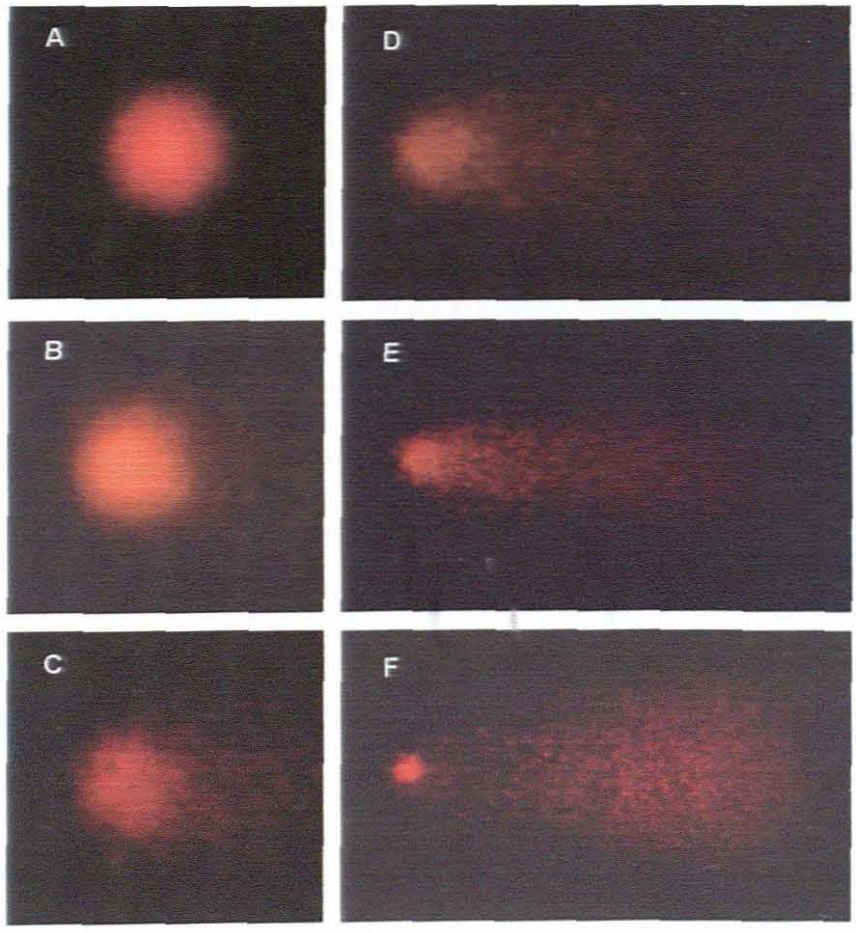

Figure 4-3: *Photomicrographs of comets displaying the DNA migration pattern of each grading category. A to E represent comets classified into grade 1 to 5 as described in 4.3.5 and F shows a cell classified as a hedgehog.*

4.4. Statistical analysis

Dose-response curves and histograms were generated with Microsoft ® Excel 2000 (9.0.2720). Standard deviations (SD) and averages of tail factors were calculated from three experiments using the STDEV and AVERAGE statistical functions respectively. p-Values were calculated using the two-sample student's t-test (TTEST function), assuming unequal variances. Coefficients of variation were calculated as

measure of inter-experimental variability using the following formula:

CV = SD/Mean x 100

4.5. Results

The alkaline comet assay was performed on freshly isolated peripheral lymphocytes, cryopreserved isolated lymphocytes, and fresh whole blood. Isolated lymphocytes and whole blood samples were irradiated with doses ranging from 0 to 4 Gy gammas and neutrons, but cryopreserved isolated lymphocytes were only irradiated with gammas.

All graphs have been constructed from the data summarised in Tables 4.1 to 4.5. Dose-response curves were compiled by plotting average tail factors as function of radiation dose. Tail factors were calculated according to the formula explained in section 4.3.5 of this chapter. All data points represent the average values of three independent experiments. Error bars represent ± one standard deviation

DNA distribution is represented by means of histograms, displaying the percentage of cells classified into each category of DNA damage for all cell preparations and radiation qualities. One hundred comets were scored per slide. Radiation doses of 0, 0.25, 0.5, 1.0, 2.0, and 4.0 Gy were applied for both radiation qualities.

4.5.1 Cell viability

Cell viability was tested in isolated lymphocytes and cryopreserved isolated lymphocytes by means of a Trypan Blue viability test. Cell viability was 99.3% for

isolated lymphocytes and 96.7% for cryopreserved isolated lymphocytes.

4.5.2 Inter-experimental variability

The average values of three independent experiments are summarised in **Table 4–1** to **Table 4–5**. The data in columns G1 to G5 of each table represent the number of comets observed in 200 cells multiplied by the relevant weighting factors (explained in section 4.3.5). The values in blue represent the percentage of cells classified into each category of DNA damage. p-Values indicate the significance of the difference between the control value and a specific dose point and p-values < 0.05 are indicated by an asterisk.

The inter-experimental variability of cell analysis in the different cell preparations is illustrated in **Figure 4-4** to **Figure 4-8** by plotting the tail factors of three individual experiments as function of radiation dose. Control (0 Gy) values were not subtracted in order to compare comet formation in unirradiated samples. Standard deviation (SD) and coefficient of variation (CV) of tail factors were calculated from three independent experiments.

Three experiments were carried out in which **isolated lymphocytes** were exposed to gamma and neutron irradiation. Average values are presented in **Table 4–1** and **Table 4–2** and inter-experimental variability of experiments is illustrated in **Figure 4-4** and **Figure 4-5**. The CVs for isolated lymphocytes ranged from 6% (4 Gy) to 30% (0.25 and 2 Gy) for gammas and 6% (1 Gy) to 38% (0 Gy) for neutrons.

Cryopreserved isolated lymphocytes were only exposed to gamma radiation. The average values of three experiments are displayed in **Table 4–3** and inter-

experimental variability of experiments is graphically displayed in **Figure 4-6**. CVs ranged from 1% (4Gy) to 27% (0.25 Gy).

Whole blood samples were irradiated with both gammas and neutrons with the results of three experiments summarised in **Table 4–4** and **Table 4–5**. Gamma-irradiated **whole blood** produced the least inter-experimental variability with CVs ranging from 3% for the 2 Gy-sample and 19% for the 0.25 Gy-sample while CVs for neutron-irradiated whole blood ranged from 7% (2 Gy) to 45% (0.5 Gy). Results are graphically illustrated in **Figure 4-7** and **Figure 4-8**.

Table 4-1: *Average values of three experiments in which isolated lymphocytes were irradiated with different doses of ^{60}Co-γ-rays. Values in the first column of each grade display the results of weighted DNA damage while values in blue represent the average percentage of cells classified into each category of DNA damage. p-Values indicate the significance of the difference between the control value and a specific dose point.*

Isolated Lymphocytes – Gammas

Dose (Gy)	G1		G2		G3		G4		G5		HH	TF	SD	CV
0	408	81	167	7	210	4	765	6	488	2	2	10	0.8	8
0.25	404	81	246	10	230	4	518	3	325	2	1	9	2.7	30
0.5	255	51	892	36	360	6	810	6	260	1	1	13	2.0	15
1.0	11	2	2013	81	530	9	878	6	390	2	2	19*	3.3	18
2.0	0	0	1025	39	2640	35	1755	23	390	3	2	29	14.9	30
4.0	2	0	21	1	870	15	11025	81	520	3	2	62*	4.2	6

*G1-G5: Grade 1 to Grade 5; HH: Hedgehogs/100 comets; TF: Tail factor; SD: ± One Standard Deviation; CV: Coefficient of variation; * = p-value<0.05.*

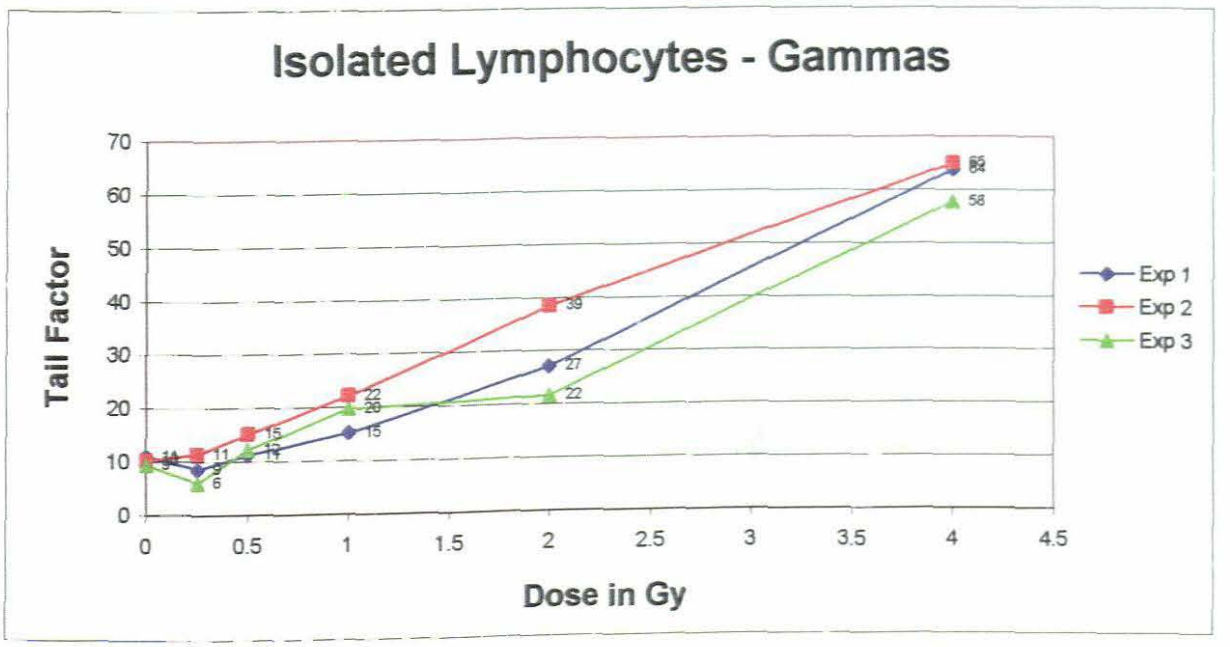

Figure 4-4: *Dose-response curves of isolated lymphocytes after exposure to gamma irradiation. Tail factors are plotted as function of dose and illustrate the reproducibility of comet scoring in three individual experiments. Tail factors are given next to each data point.*

Table 4–2: *Average values of three experiments in which isolated lymphocytes were irradiated with different doses of 66 MeV neutrons. Values in the first column of each grade display the results of weighted DNA damage while values in blue represent the average percentage of cells classified into each category of DNA damage. p-Values indicate the significance of the difference between the control value and a specific dose point*

Isolated Lymphocytes – Neutrons

Dose (Gy)	G1		G2		G3		G4		G5		HH	TF	SD	CV
0	398	80	208	8	120	2	1170	9	260	1	1	11	4.23	38
0.25	356	71	479	19	120	2	878	7	228	1	3	10	2.53	25
0.5	219	44	992	40	220	4	1463	10	390	2	3	16	3.52	22
1.0	57	11	1763	71	430	7	1283	9	293	2	4	19	1.05	6
2.0	2	0	1904	76	580	10	1553	12	455	2	3	22*	3.88	18
4.0	6	1	413	17	3290	55	3398	25	455	2	5	38*	6.76	18

*G1-G5: Grade 1 to Grade 5; HH: Hedgehogs/100 comets; TF: Tail factor; SD: ± One Standard Deviation; CV: Coefficient of variation; * = p-value<0.05.*

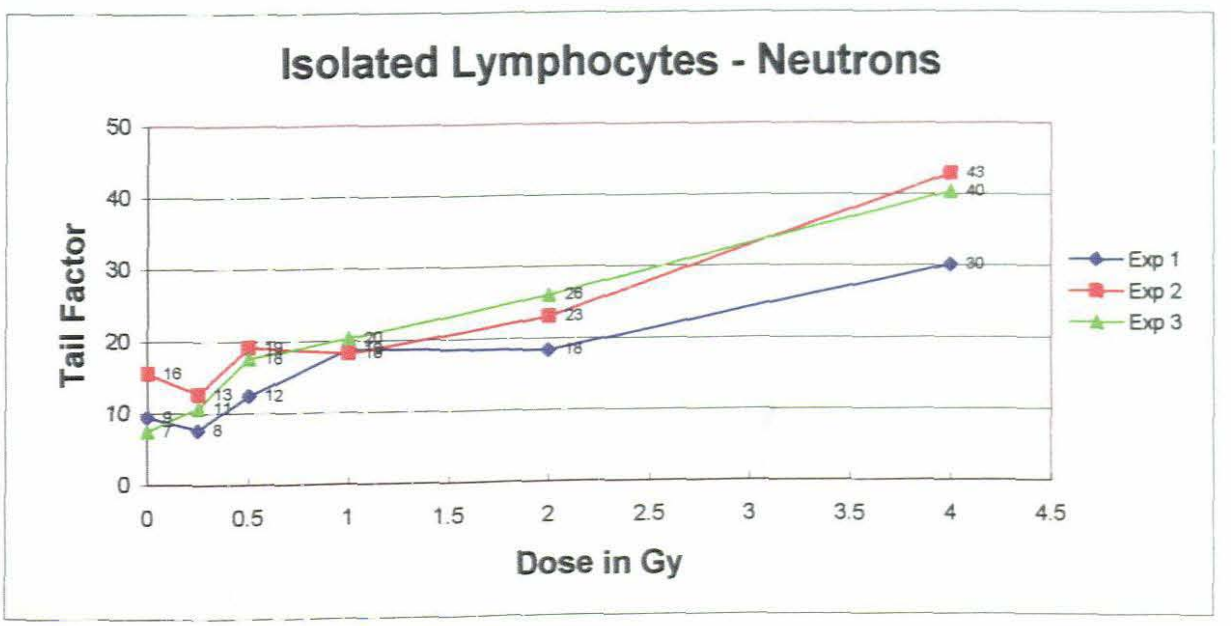

Figure 4-5: *Dose-response curves of isolated lymphocytes after exposure to neutron radiation. Tail factors are plotted as function of dose and illustrate the reproducibility of comet scoring in three individual experiments. Tail factors are shown without control (0 Gy) values subtracted.*

***Table 4-3**: Average values of three experiments in which cryopreserved isolated lymphocytes were irradiated with different doses of ^{60}Co-γ-rays. Values in the first column of each grade display the results of weighted DNA damage while values in blue represent the average percentage of cells classified into each category of DNA damage. p-Values indicate the significance of the difference between the control value and a specific dose point*

Cryopreserved lymphocytes - Gammas

Dose (Gy)	G1		G2		G3		G4		G5		HH	TF	SD	CV
0	378	76	333	13	120	2	563	4	975	5	6	12	1.3	11
0.25	193	39	1317	53	160	2	540	4	423	2	8	13	3.6	27
0.5	35	7	1913	76	350	6	878	7	813	4	9	20*	2.8	14
1.0	0	0	1546	73	680	15	923	8	650	4	10	23*	2.0	9
2.0	0	0	13	1	2900	60	4388	36	390	3	9	45*	7.5	17
4.0	0	0	0	0	60	1	12015	89	1950	10	12	70*	0.7	1

*G1-G5: Grade 1 to Grade 5; HH: Hedgehogs/100 comets; TF: Tail factor; SD: ± One Standard Deviation; CV: Coefficient of variation; * = p-value<0.05.*

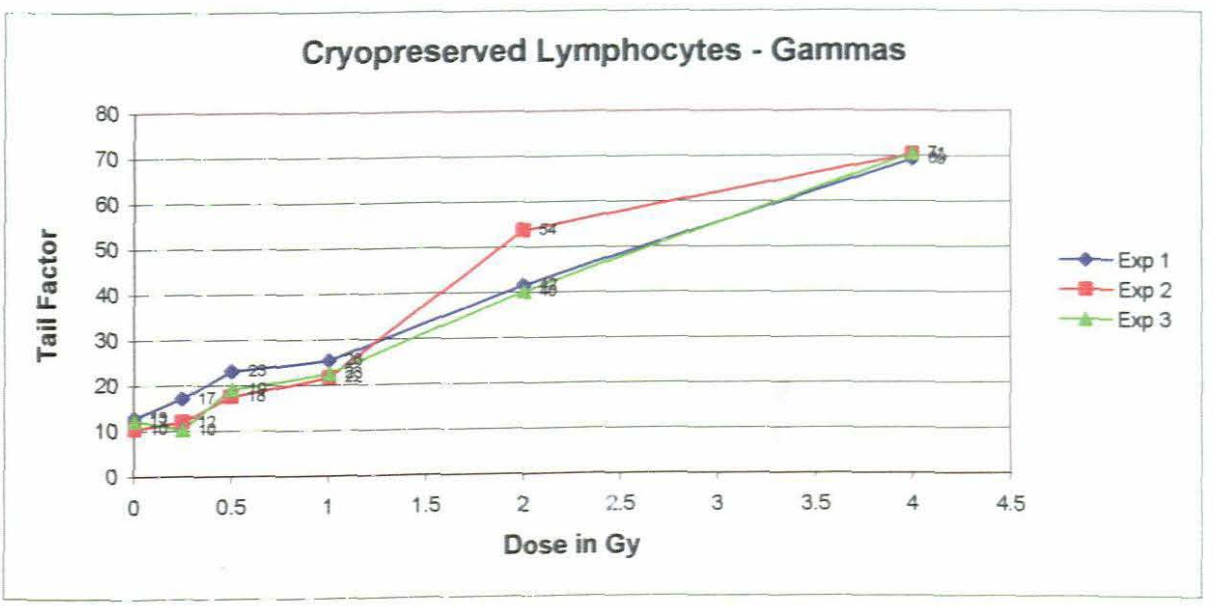

***Figure 4-6:** Dose-response curves of cryopreserved isolated lymphocytes after exposure to gamma radiation. Tail factors are plotted as function of dose and illustrate the reproducibility of comet scoring in three individual experiments. Tail factors are shown without control (0 Gy) values subtracted.*

Table 4-4: *Average values of three experiments in which whole blood was irradiated with different doses of gamma radiation. Values in the first column of each grade display the results of weighted DNA damage while values in blue represent the average percentage of cells classified into each category of DNA damage. p-Values indicate the significance of the difference between the control value and a specific dose point*

Whole blood – Gammas

Dose (Gy)	G1		G2		G3		G4		G5		HH	TF	SD	CV
0	483	96	88	4	0	0	0	0	0	0	0	3	0.4	13
0.25	289	58	1046	42	20	0	0	0	0	0	0	7*	1.3	19
0.5	18	4	2363	94	50	1	23	0	163	1	0	13*	0.7	5
1.0	23	5	2167	86	420	7	90	1	195	1	0	14*	1.7	12
2.0	0	0	263	10	5080	85	270	2	553	3	0	30*	0.8	3
4.0	1	0	4	0	330	6	12150	90	813	4	0	64*	3.0	5

*G1-G5: Grade 1 to Grade 5; HH: Hedgehogs/100 comets; TF: Tail factor; SD: ± One Standard Deviation; CV: Coefficient of variation; * = p-value<0.05.*

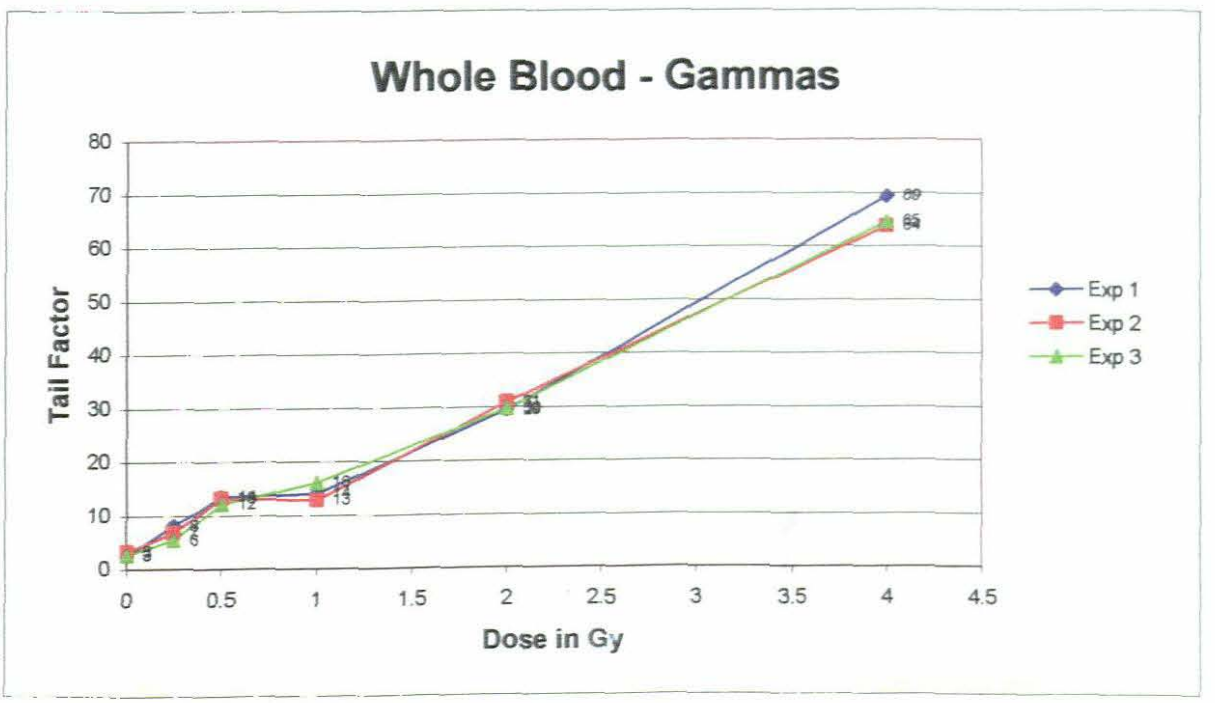

Figure 4-7: *Dose-response curves of whole blood after exposure to gamma radiation. Tail factors are plotted as function of dose and illustrate the reproducibility of comet scoring in three individual experiments. Tail factors are shown without control (0 Gy) values subtracted.*

***Table 4–5**: Average values of three experiments in which whole blood was irradiated with different doses of neutrons. Values in the first column of each grade display the results of weighted DNA damage while values in blue represent the average percentage of cells classified into each category of DNA damage. p-Values indicate the significance of the difference between the control value and a specific dose point*

Whole blood – Neutrons

Dose (Gy)	G1		G2		G3		G4		G5		HH	TF	SD	CV
0	478	96	104	4	0	0	45	0	0	0	0	3	0.33	11
0.25	293	59	1013	40	30	1	45	0	0	0	0	7	3.04	43
0.5	162	33	1613	65	80	1	180	1	33	0	0	10	4.49	45
1.0	42	8	2246	90	80	1	23	1	65	0	0	12*	1.51	13
2.0	3	1	2379	95	230	4	23	0	65	0	0	13*	0.87	7
4.0	0	0	225	9	4400	73	2363	18	33	0	0	35*	12.01	34

*G1-G5: Grade 1 to Grade 5; HH: Hedgehogs/100 comets; TF: Tail factor; SD: ± One Standard Deviation; CV: Coefficient of variation; * = p-value<0.05.*

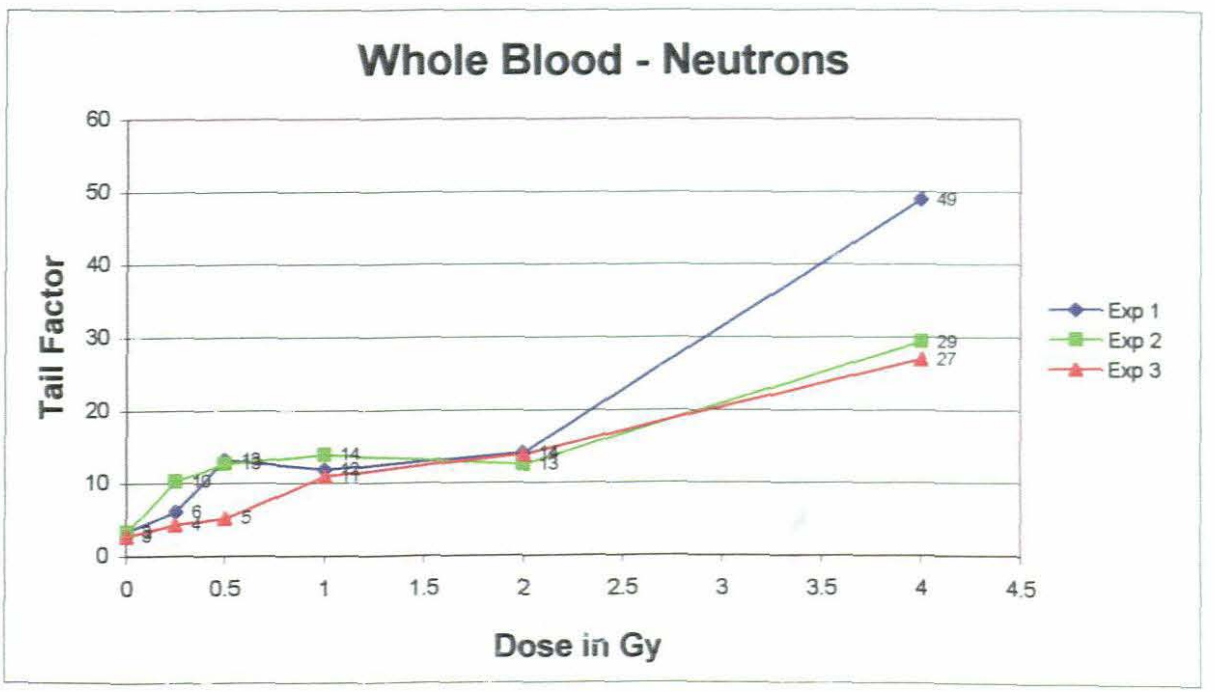

***Figure 4-8:** Dose-response curves of whole blood after exposure to neutron radiation. Tail factors are plotted as function of dose and illustrate the reproducibility of comet scoring in three individual experiments. Tail factors are shown without control (0 Gy) values subtracted.*

4.5.3 Distribution of damage

Figure 4-9 and **Figure 4-10** display histograms of the distribution of DNA damage in freshly isolated lymphocytes from ^{60}Co γ-rays and a 66 MeV neutron beam respectively. Solid lines in red represent the tail factors for each dose point with error bars indicating ± one standard deviation.

Eighty percent of unirradiated samples were classified as grade 1 while the percentage decreased to 0% in samples irradiated with 4 Gy gammas. The distribution of DNA damage in neutron-irradiated samples was similar with 80% of control cells classified as grade 1 and only 1% classified as grade 1 in the 4 Gy samples.

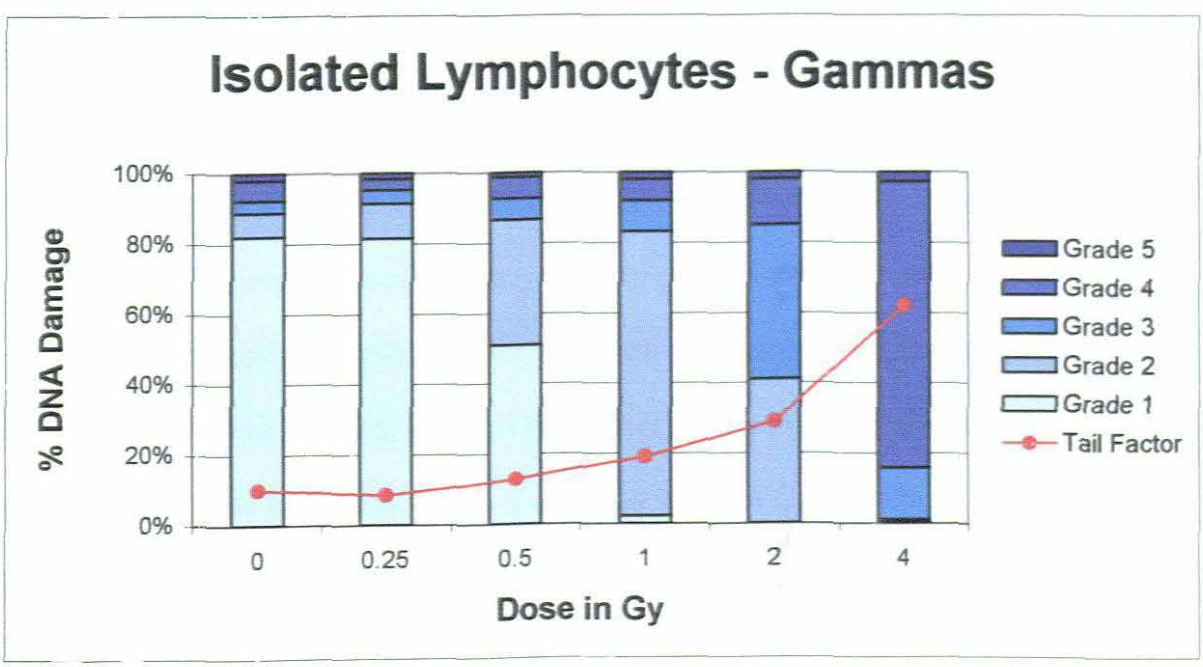

Figure 4-9: *Distribution of DNA damage for isolated lymphocytes irradiated with ^{60}Co γ-rays. Histograms display the percentage of cells classified into each category of DNA damage per dose point. The solid line in red represent the tail factor for each dose point with error bars indicating ± one standard deviation.*

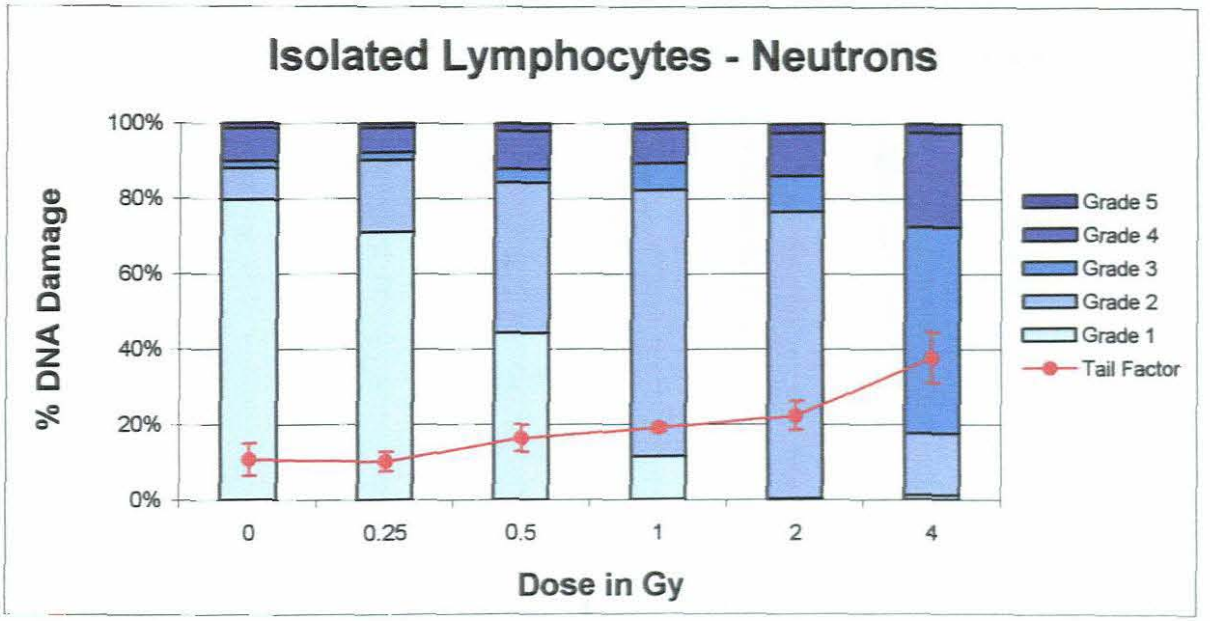

Figure 4-10: *Distribution of DNA damage for isolated lymphocytes exposed to neutrons. Histograms display the percentage of cells classified into each category of DNA damage per dose point. The solid line in red represent the tail factor for each dose point with error bars indicating ± one standard deviation.*

Figure 4-11 displays histograms of the distribution of DNA damage in cryopreserved isolated lymphocytes irradiated with ^{60}Co γ-rays. Solid lines in red represent the tail factors for each dose point with error bars indicating ± one standard deviation. Cryopreserved samples were only exposed to gammas and displayed more damage in control samples than fresh lymphocytes with 76% and 13% comets classified as Grade 1 and Grade 2 respectively. This higher radiosensitivity was also observed in irradiated samples with 89% Grade 4 damage in the 4 Gy-sample.

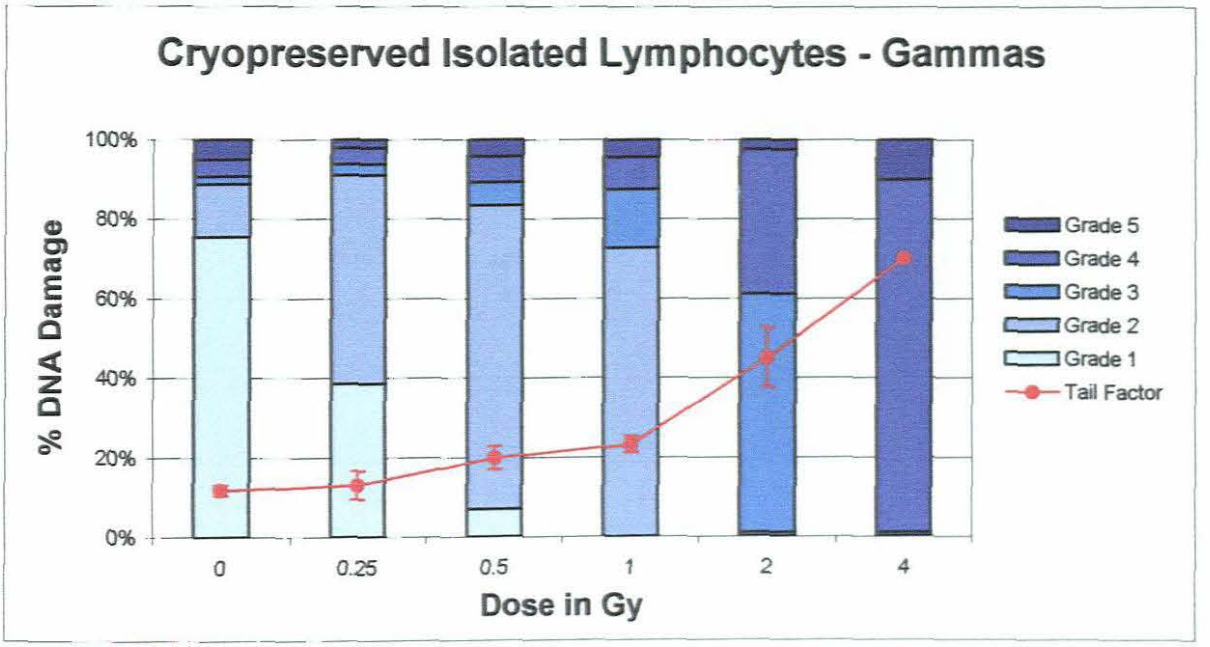

***Figure 4-11**: Distribution of DNA damage for cryopreserved isolated lymphocytes exposed to ^{60}Co γ-rays. Histograms display the percentage of cells classified into each category of DNA damage per dose point. The solid line in red represent the tail factor for each dose point with error bars indicating ± one standard deviation.*

Figure 4-12 and **Figure 4-13** display DNA damage in whole blood induced by gamma- and neutron irradiation. Compared to DNA damage in isolated lymphocytes, much less damage was observed in control samples (96% versus 81% Grade1), but whole blood displayed more radiosensitivity in the high-dose (4 Gy) samples (90% versus 81%). The same tendency was observed in neutron-irradiated cells.

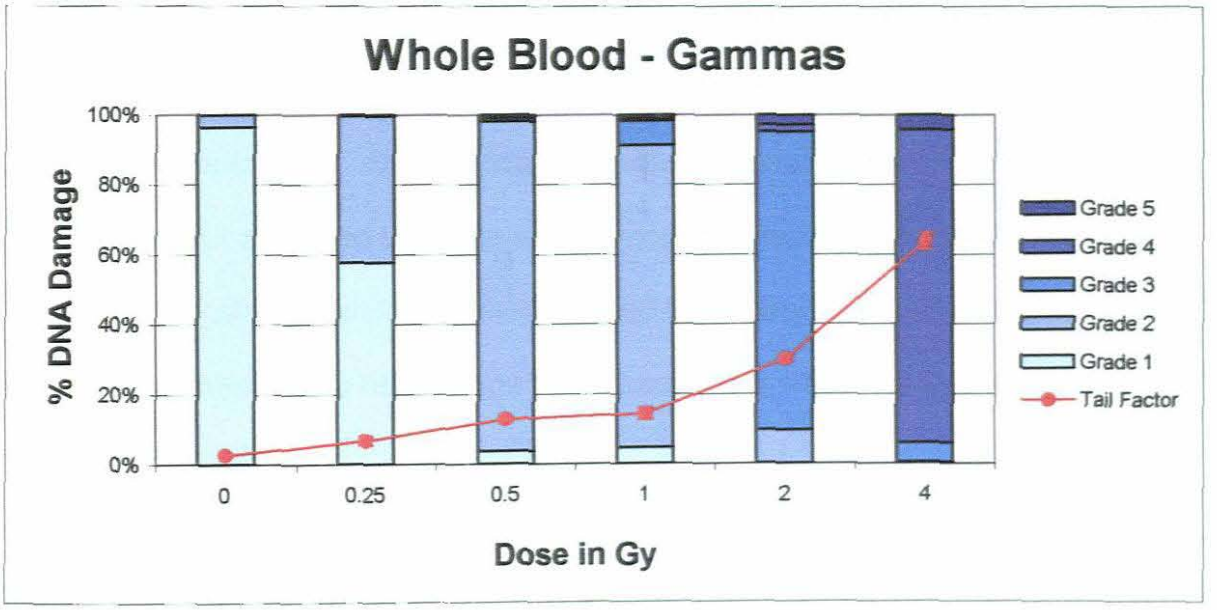

Figure 4-12: *Distribution of DNA damage for whole blood irradiated with ^{60}Co γ-rays. Histograms display the percentage of cells classified into each category of DNA damage per dose point. The solid line in red represent the tail factor for each dose point with error bars indicating ± one standard deviation.*

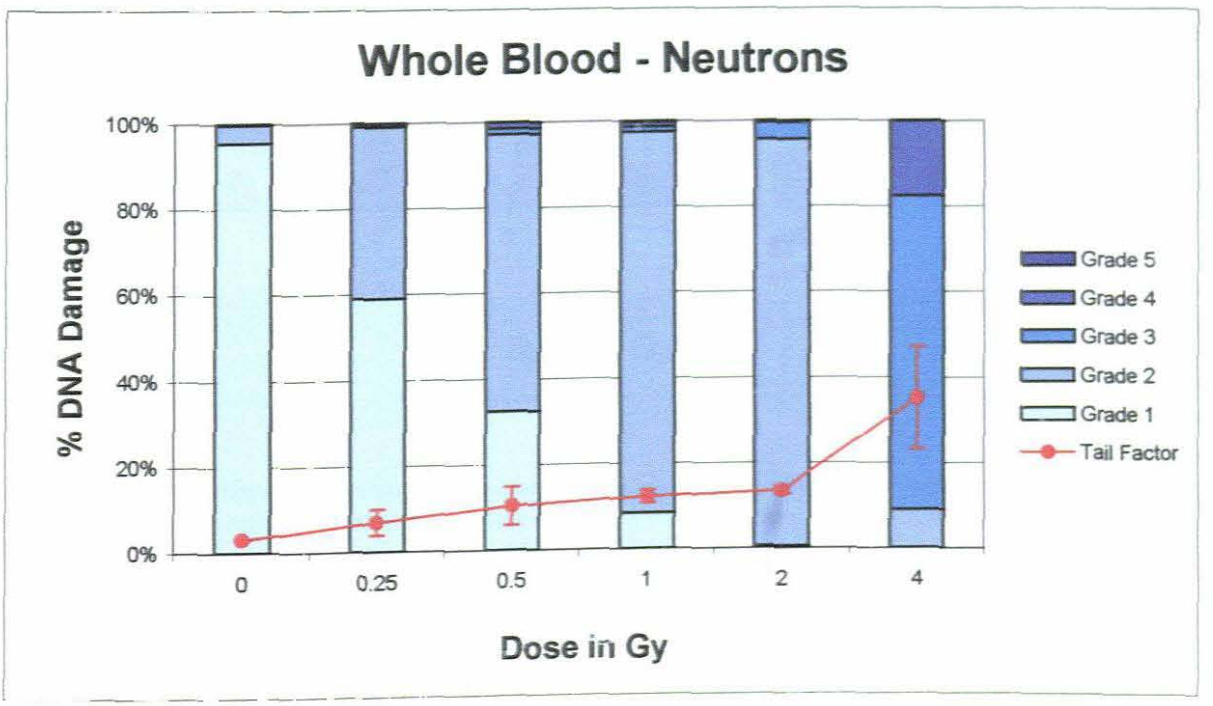

Figure 4-13: *Distribution of DNA damage for whole blood exposed to neutrons. Histograms display the percentage of cells classified into each category of DNA damage per dose point. The solid line in red represent the tail factor for each dose point with error bars indicating ± one standard deviation.*

Figure 4-14 shows the observation of hedgehogs in gamma- and neutron-irradiated isolated lymphocytes. Hedgehogs were counted but not included in the 200 comets classified per dose point. Both radiation qualities induced hedgehogs in isolated lymphocytes but a marked increase was observed in neutron-irradiated cells with a total of 19 hedgehogs per 100 comets induced by neutrons and 10 hedgehogs induced by gammas. No hedgehogs were observed in whole blood samples.

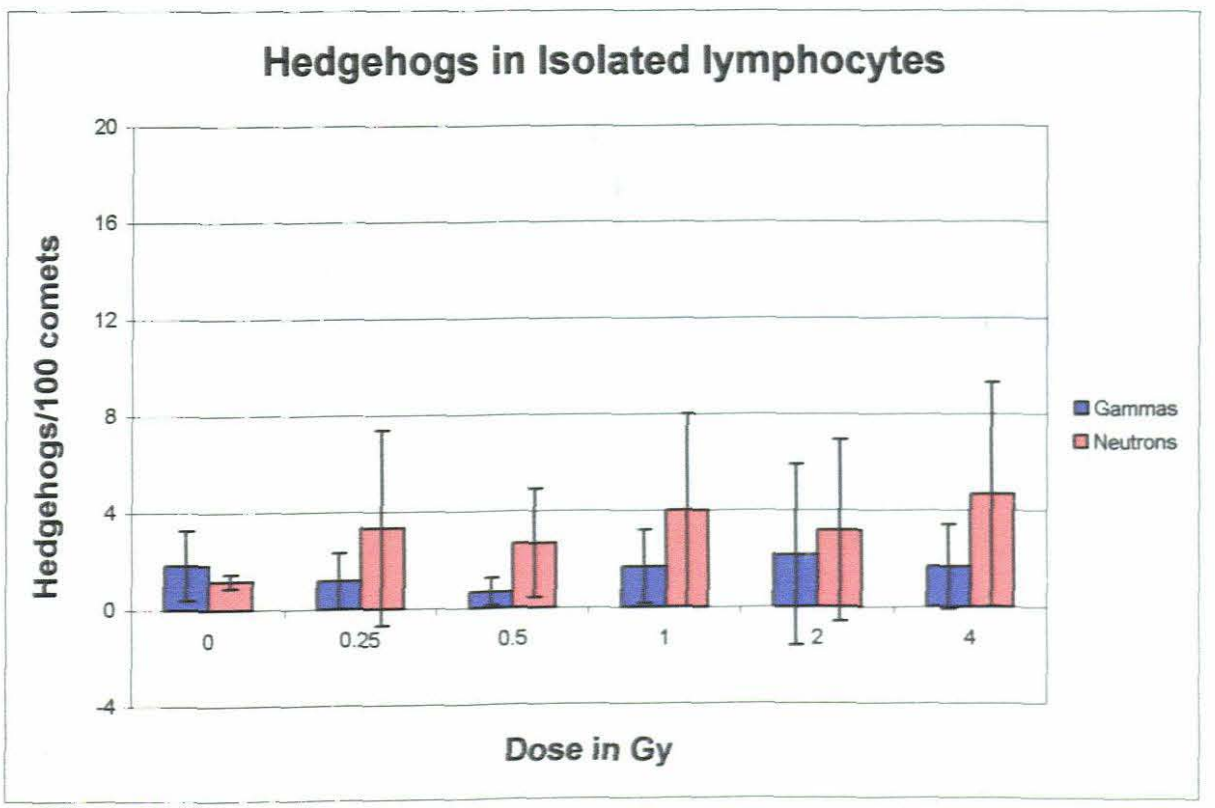

***Figure 4-14**: Hedgehogs observed in gamma-and neutron-irradiated isolated lymphocytes while scoring one hundred comets. Histograms display the average number of hedgehogs in three experiments and are plotted as function of dose. Error bars indicate ± one standard deviation.*

Figure 4-15 shows the observation of hedgehogs in isolated lymphocytes, cryopreserved isolated lymphocytes and whole blood exposed to gamma radiation. Compared to freshly prepared isolated lymphocytes, the number of hedgehogs

observed per 100 comets in cryopreserved isolated lymphocytes was on average 5.4 times higher (54 versus 10). Cryopreserved isolated lymphocytes were only exposed to gamma radiation. No hedgehogs were observed in whole blood samples.

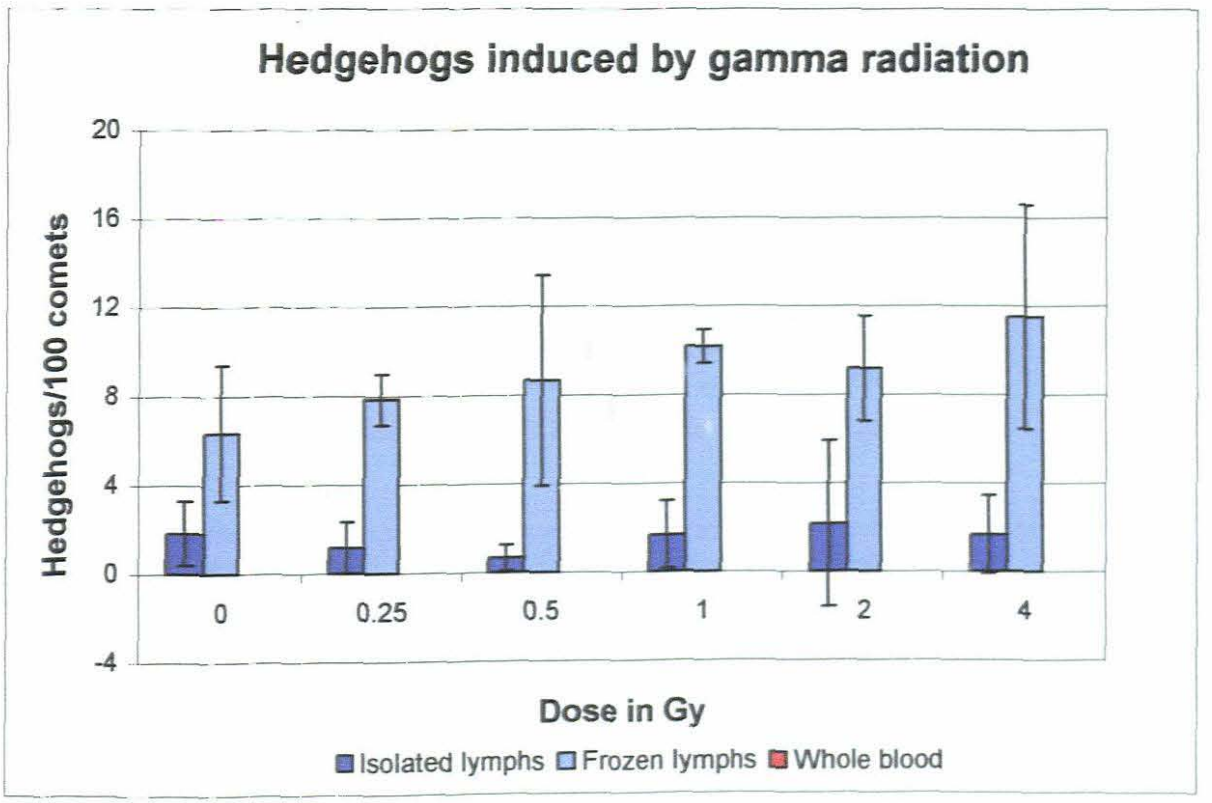

Figure 4-15: *Hedgehogs observed in isolated lymphocytes, cryopreserved isolated lymphocytes and whole blood exposed to gamma radiation while scoring one hundred comets. Histograms display the average number of hedgehogs in three experiments and are plotted as function of dose. Note: No hedgehogs were observed in whole blood samples, therefore no bars are shown.*

Figure 4-16 shows DNA damage observed in unirradiated (0 Gy) samples of all cell suspensions. Whole blood displayed the least amount of damage in control samples with all the cells classified as either Grade 1 (96%) or Grade 2 (4%) while isolated lymphocytes (81% Grade 1, 7% Grade 2, 4% Grade 3, 6% Grade 4, 2% Grade 5) and cryopreserved isolated lymphocytes (76% Grade 1, 13% Grade 2, 2% Grade 3, 4% Grade 4, 5% Grade 5) produced comets in all categories of DNA damage.

4.5.4 Dose-response relationships

Figure 4-17 compares dose-response relationships of all cell suspensions in response to gamma- and neutron irradiation. Control (0 Gy) values have not been subtracted from tail factors in order to compare the formation of comets in unirradiated samples.

All cell suspensions showed statistically significant dose-response relationships in response to both qualities of radiation with tail factors of whole blood samples ranging from 3 to 65 for gammas and 3 to 35 for neutrons. Isolated lymphocytes expressed higher background damage with tail factors ranging from 10 to 62 (gammas) and 11 to 38 (neutrons). Cryopreserved isolated lymphocytes produced slightly higher tail factors of 12 to 70 for gamma-irradiated samples.

Neutron-irradiated samples of whole blood and isolated lymphocytes were less radiosensitive to radiation doses above 1 Gy, expressing consistently lower tail factors than gamma-irradiated samples. Tail factors of 4 Gy-irradiated samples were 62 (gammas) and 38 (neutrons) for isolated lymphocytes, and 64 (gammas) and 35 (neutrons) for whole blood samples.

The difference between tail factors for gamma- and neutron-exposed cells was significant only in the 4 Gy-sample of isolated lymphocytes ($p = 0.007$). Both the 2 and 4 Gy samples of whole blood displayed a significant difference with p-values of 0.00002 and 0.048 respectively.

The difference between control samples and irradiated samples was most significant in gamma-irradiated whole blood with a p-value of 0.026 in the 0.25 Gy-sample and

highly significant in the 4 Gy sample with a p-value of 0.00006. Other cell preparations were only significant above 1 Gy.

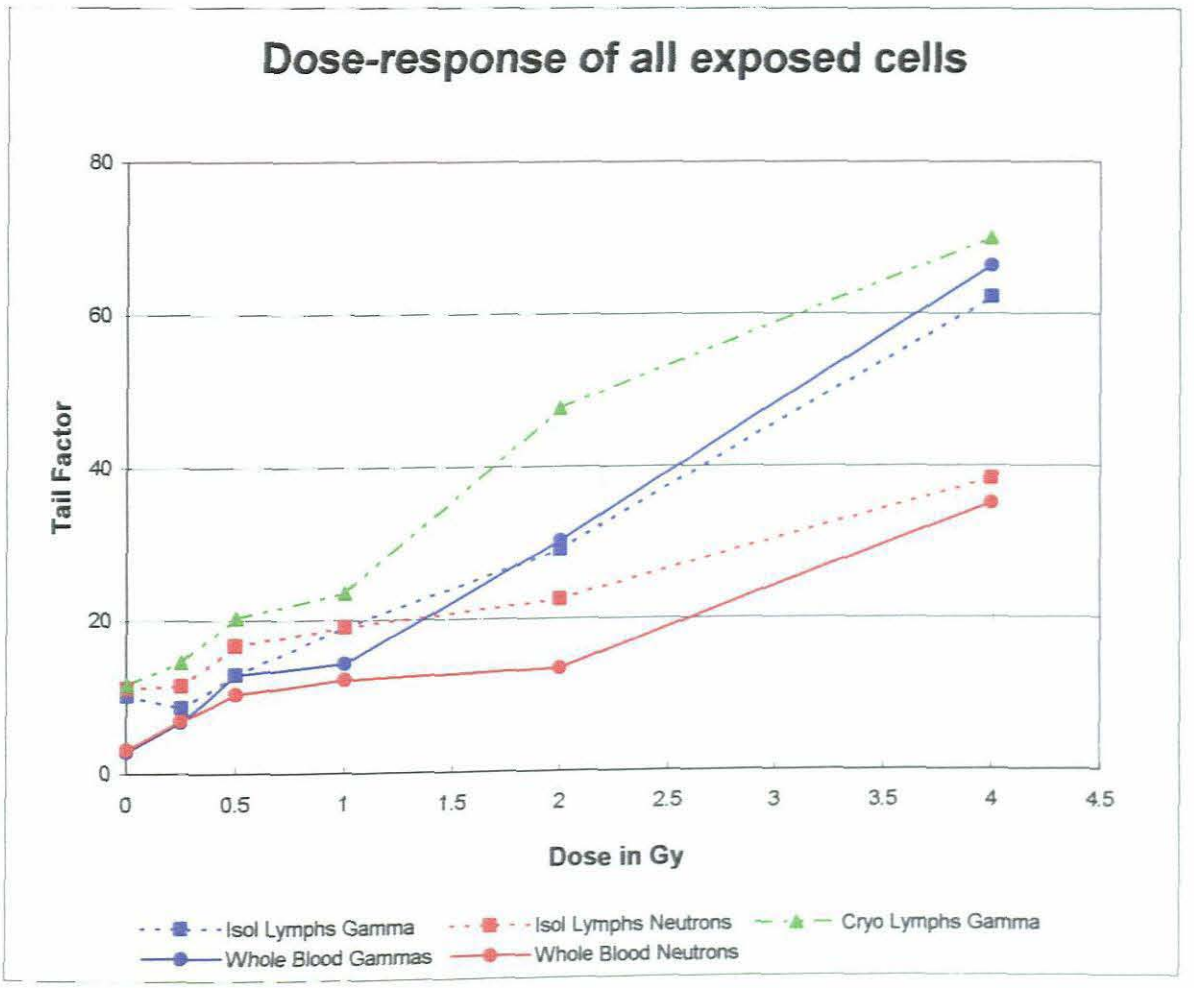

***Figure 4-17**: Dose- response relationship of all cell preparations in response to gamma- and neutron radiation. Data points represent the average tail factors of three independent experiments.*

4.6. Discussion

4.6.1 Methodology

The alkaline comet assay was validated for the detection of initial DNA strand breaks in lymphocytes and leukocytes induced by gamma- and neutron irradiation. Although the principle of the method is relatively simple and easy to perform, a small variation in certain experimental conditions can influence the outcome of the assay significantly.

The temperature of the electrophoresis buffer is one such variable that acts directly on the consistency of the agarose and ultimately determines the migration pattern of DNA fragments. It was found that a buffer temperature of 21°C produced controls with too much DNA in the tail (tail factor not calculated) but a temperature of 7 to 13°C proved to be optimum for the experimental conditions of this study (**Figure 4-1**). Rojas *et al.* (1999) confirmed this result, stating that *an unwinding and electrophoresis temperature of 15°C appeared to give maximum sensitivity without comet formation in controls.*

It was also found that an incorrect method of neutralisation could affect the appearance and hamper the identification of comets. Slides were first dropped with neutralisation buffer as suggested by Tice and Vasquez (1999), but unevenly coated slides produced comets with an unclear migration pattern, making it difficult to classify comets into a category of damage. Submersing the slides in neutralisation buffer rather than dropping the buffer onto the slides appeared to have solved the

problem, but great care had to be taken to prevent gels from slipping off the slides.

4.6.2 Dose-response

Dose-response curves indicating initial DNA damage were established by irradiating cells with different doses of gamma- (low LET) and neutron (high LET) radiation. Cells irradiated with neutron doses above 1 Gy displayed less damage than gamma-irradiated cells. This could be attributed to the fact that low-LET radiation produces DNA breaks throughout the nucleus while neutrons produce concentrated lesions, known as "locally multiply damage sites" (LMDS) (Dainiak, 2002; Hill, 1999). The higher quantity of smaller DNA fragments induced by low-LET radiation was visible as highly damaged cells with resultant higher tail factors. Although the lesions are more lethal, less DNA fragments are produced by high-LET radiation resulting in lower tail factors. This tendency was observed in all cell preparations. No significant difference in dose-response was observed in the 0 to 1 Gy dose region ($p = >0.05$).

4.6.3 Distribution of damage

Damage distribution histograms displayed distinct differences in the pattern of damage in the three cell preparations. Whole blood samples displayed very few hedgehogs (HH) and highly damaged cells (HDC) in control samples but the presence of high numbers of hedgehogs and HDCs in all samples of cryopreserved- and freshly isolated lymphocytes was a surprising observation.

Most studies on the comet assay have used image analysis software that excluded HDCs and hedgehogs from analysis (Lebailly *et al.*, 1997;) and groups either did not comment on their observation (Wojewódzka *et al.*, 1998) or did not encounter these

cells at all. One group that mentioned HDCs in their discussion was Banath *et al.* (1998). They used whole blood and isolated lymphocytes in their study on the repair of DNA strand breaks and confirmed the findings of this study that isolated lymphocytes showed more DNA damage than whole blood samples. They speculated that the isolation procedure and/or the presence of radioprotective substances in whole blood could be the reason for the difference in response. However, the presence of radioprotective substances could not have influenced the response of whole blood cells to radiation in the present study, as only 5 µl of whole blood was suspended in 75 µl of agarose and would have no radioprotective effect in such a high dilution. It is more likely that endogenous damage to cells has led to HDCs. Giovannelli *et al.* (2003) measured DNA strand breaks in polymorphonuclear and mononuclear cells separately and also found more damage in isolated cells than whole blood. They reported, "... breakage of DNA strands is the type of DNA damage that appears to be specifically sensitive to gradient separation, whereas oxidation of DNA bases does not seem to be affected".

Banath *et al.* (1998) did not comment on hedgehogs as such, but classified HDCs as apoptotic or necrotic cells "since almost all of the DNA migrates away from the comet head". These cells were excluded from their calculation of mean tail moment. Due to the fact that only initial DNA damage was measured in the present study, the classification of HDCs and hedgehogs as apoptotic or necrotic cells would not apply here. The high viability (99.3%) of isolated cells proves that these cells are not dead, rather merely badly damaged. The fact that HDCs and hedgehogs appeared in all dose points of both lymphocyte preparations in a dose responsive manner suggests that the isolation process made isolated cells more vulnerable to the effects of

radiation than whole blood cells.

Although the distribution of DNA damage differed greatly among different cell preparations, the dose-response relationships did not vary significantly. The use of only one DNA damage parameter in analysis of genotoxic agents, e.g. tail factor or mean tail moment, could thus confound the actual pattern of DNA damage that could otherwise have been valuable in the assessment of the genotoxic potential of a substance or agent.

4.7. Conclusion

The comet assay has been employed for the detection of DNA strand breaks after different cell preparations were exposed to different qualities and doses of radiation. Although the assay could not distinguish between cells irradiated with different qualities of radiation in the low-dose (< 1Gy) region, the assay is sensitive enough to detect comet formation in whole blood exposed to gamma doses above 0.25 Gy. Doses below 1 Gy did not produce statistically significant dose-response curves for any of the other cell preparations.

The isolation procedure and cryopreservation of lymphocytes proved to play an influential role in the induction of HDCs and/or hedgehogs and needs to be investigated in more depth. It was also shown that the observation of hedgehogs is not an indication of apoptosis as this study was conducted immediately after irradiation before an apoptotic response could have been elicited.

Once standardised for specific experimental conditions, the alkaline comet assay is a sensitive and reliable method for the detection of radiation-induced DNA strand

breaks in individual cells. The assay could be useful as indicator of radiation damage analysed in whole blood for doses above 0.25 Gy.

Chapter 5

Cytokinesis-blocked micronucleus (CBMN) assay

5.1. Introduction and literature review

Ionising radiation is one of few agents that cause direct DNA breakage in a cell (Fenech, 2000). *In vitro* exposure of peripheral lymphocytes to these agents results in chromosome aberrations that may persist for the lifetime of the cell (Albertini *et al.*, 2000).

Classical cytogenetic analysis of chromosome aberrations in metaphases has been the gold standard of biological dosimetry for many years, but the complexity and tediousness of this technique has led to the development of the much faster and simpler cytokinesis-blocked micronucleus (CBMN) assay developed by Fenech and Morley (1985).

Micronuclei are small bodies in the cytoplasm resembling the nuclear material in morphology and staining pattern. They are formed when a broken chromosome or chromosome fragment cannot travel to the spindle during mitosis and is thus not included in either daughter nuclei (Albertini *et al.*, 2000). An increased frequency of micronuclei in a cell may be considered as a biomarker of permanent genotoxic damage, reflecting either clastogenic or aneugenic modes of action (Albertini *et al.*, 2000).

Micronuclei are ideally scored in binucleated cells and can only be expressed in dividing eukaryotic cells (Fenech, 2000). They are mostly studied in cultured isolated

lymphocytes after being stimulated to divide by a mitogen, e.g.phytohaemagglutinin. Cytochalasin-B is an inhibitor of actin polymerisation, preventing the formation of the microfilament ring that constricts the cytoplasm between two daughter nuclei during cytokinesis (Fenech, 2000). This action prevents the accumulation of binucleated cells in almost all dividing cells. The use of Cytochalasin-B was introduced into the original micronuclei assay to enable reliable comparisons of chromosome damage between cells with different cell cycle kinetics (Fenech, 2000).

The combination of the CBMN assay with immunochemical labelling of kinetochores or pancentromeric probes allowed the identification of the most important mechanisms of micronuclei induction. Fluorescent *in situ* hybridisation (FISH) with a pan-centromeric DNA probe can be used to distinguish micronuclei originating from chromosome breakage and those from chromosome loss (Sari-Minodier *et al.*, 2002).

Despite considerable variation in methods and variables influencing the measurement such as incubation periods, reagents and cell fixation, the induction of micronuclei is accepted as an effective biomarker of DNA damage. However, to validate the assay as a reliable biomarker of genotoxicity, the International Collaborative Project on Micronucleus frequency in Human Population (HUMN) was initiated to compare data on micronuclei frequency in different populations and cell types (Fenech, 1999). As a result, a protocol has been developed and published (Kirsch-Volders *et al.*, 2003) while Fenech *et al.* (2003a) compiled detailed scoring criteria for the CBMN assay, using isolated lymphocyte cultures as reference.

The CBMN assay is not only employed in the field of genetic toxicology, but also for human biomonitoring studies (Chang *et al.*, 1999; Kryscio *et al.*, 2001; Sari-Minodier *et al.*, 2002; Thierens *et al.*, 1999 and 2000; Laffon *et al.*, 2002), and in investigations

of intrinsic radiosensitivity (Floyd and Cassoni, 1994; Jones *et al.*, 1994 and 1995; Vral *et al.* 2002; Widel *et al.*, 2003).

The CBMN assay has also been applied in clinical studies and was able to detect cytogenetic damage in lymphocytes from patients treated with 131-Iodine (Guiterrez *et al.*, 1999). Fenech *et al.* (1998) investigated the effect of folate and vitamin B12 on DNA damage and plasma homocystein and found that elevated homocystein levels could be a risk factor for chromosome damage.

Due to the technical variability of the CBMN assay, it needs to be validated and standardised for each laboratory to ensure consistent results. The aim of this experiment was thus to perform the CBMN assay according to a protocol used by the radiobiology laboratory at iThemba LABS at Faure (Slabbert, 2004, personal communication) and evaluate the results in terms of accuracy, repeatability and consistency. The experiment was also aimed at establishing dose response curves for ^{60}Co γ-rays and a 66MeV neutron beam for doses between 0 and 4 Gy

5.2. Methodology

5.2.1 Cell preparation

EDTA-blood from one healthy female donor was used throughout the study. Peripheral lymphocytes were sterilely isolated with Histopaque 1077 (Sigma), washed with phosphate buffered saline (PBS) and diluted in 10 ml RPMI 1640 (Roswell Park Memorial Institute), supplemented with 15% heat inactivated foetal calf serum (FCS). Five millilitres of cell suspension were pipetted into round-bottom culture tubes.

5.2.2 Irradiation

Gamma irradiation was performed using a ^{60}Co γ-source (Eldorado 76, Atomic Energy of Canada Ltd.), delivering a dose-rate of 0.29 Gy/min at a source surface distance (SSD) of 70 cm, a field size of 30 x 30 cm^2 and a gantry angle of 180°. Tubes were placed side-by-side in the centre of the radiation beam on a 0.5 mm-thick Perspex sheet with a 5 cm thick Perspex block on spacers serving as backscatter material. The dose at the position of the tubes was verified by using a 0.6 cc thimble Farmer ionisation chamber, type 2571 and a Farmer electrometer, model 2570/1 (NE Technology). The dosimetry system was calibrated against a national standard at the CSIR. The experimental set-up was also verified by irradiating seventeen calibrated thermoluminescent dosimeters (TLDs) with a dose of 2 Gy. The average TLD-dose registered after read-out in a TOLEDO dosimetry system was 2.055 Gy.

Neutron irradiation was performed with the cyclotron at iThemba LABS at Faure, using a dose rate of 0.35 Gy/min with 66 MeV protons bombarding a 19.6 mm thick beryllium target. The p(66)/Be(40) neutron beam generated had a large spectrum of energy with a maximum value of 64.15 MeV (Schreuder, 1992). A field size of 20 x 20 cm^2 and SSD of 150cm was used at a gantry angle of 0°. Tubes were placed side-by-side in the centre of the beam on a 10cm thick perspex block with 2cm nylon as build-up material and 6 cm Perspex as backscatter. The dose at the position of the cells was verified by means of an 80 cc Far West (model IC-80) ionisation chamber (Far West Technology) and a BNC Portanim (model AP-2H) current digitiser (Berkeley Nucleomics. Corporation. USA).

Doses of 0.25, 0.5, 1.0, 2.0, and 4.0 Gy were applied for both types of irradiation. Control samples (0 Gy) were treated identical but sham irradiated.

5.2.3 Incubation and cell harvest

Immediately after irradiation, lymphocytes were stimulated to divide by adding 50 µl of the mitogen, lyophilised phytohaemagglutinin (PHA, Gibco, 3109) at a concentration of 3 mg/ml. Three different lots of PHA were used for different experiments. Tubes were incubated at 37°C with loose lids in a humidified atmosphere containing 5% CO_2. After 44 hours, 150 µl (3 µg/ml) of Cytochalasin B (Cyt-B, Sigma) was added to each culture tube to block cytokinesis. Cultures were then re-incubated for a further 28 hours (72 hours total incubation time). Tubes were removed from the incubator and centrifuged for 5 min at 300 x g. Supernatant was removed carefully and the cell pellet was gently mixed. Five millilitres of 0.075 M KCl were added drop-wise while tubes were either vortexed at low speed or shaken by hand. Tubes were centrifuged for 8 minutes after which the supernatant was discarded and the cell pellet resuspended in the remaining fluid. Five millilitres of freshly prepared Carnoy's fluid (methanol:acetic acid 3:1) were added in the same manner as the KCl. Tubes were placed in the fridge at 4°C until slides were prepared for analysis.

5.2.4 Slide preparation

Tubes were centrifuged, the supernatant discarded and the cells resuspended in remaining fluid. Ten drops of cell suspension were dropped onto clean, labelled, microscope slides and left on a flat surface at room temperature to dry for at least 24 hours. Slides were stained with acridine orange (TAAB Lab Equipment) at a concentration of 40 µg/ml for 1 minute, washed in distilled water and pH 6.8 buffer (Gurr) for 1 minute, covered with a cover slip, and sealed with Entalan to prevent drying. Slides were analysed immediately using a fluorescence microscope.

5.2.5 Microscopic analysis

Two hundred viable cells were analysed and reported as containing 1, 2, 3, 4, or more nuclei per cell. The nuclear division index (NDI) is an indication of the efficiency of the PHA to stimulate lymphocytes in G_0 to undergo mitotic division.

The formula for the calculation of the NDI is:

$$NDI = \frac{N_1 \times 1 + N_2 \times 2 + N_3 \times 3 + N_4 \times 4}{\text{total cells counted}}$$

where N_{1-4} indicates scorable cells containing 1 to 4 nuclei.

Five hundred binucleated (BN) cells per slide were examined for the presence of *micronuclei* and were reported as containing 0, 1, 2, 3, 4 or more micronuclei per BN cell.

The formula for the calculation of the total number of micronuclei present in the cell sample was as follows:

$$MN/500\ cells = \frac{BN_1 \times 1 - BN_2 \times 2 - BN_3 \times 3 - BN_4 \times 4}{\text{total BN cells counted}} \times 500$$

where BN_{1-4} indicates binucleated cells containing 1 to 4 micronuclei.

The total number of micronuclei and the NDI were calculated for each dose point.

5.2.6 Scoring criteria

The scoring criteria adopted by the HUMN project were used for analysis of micronuclei in this study (Fenech *et al.*, 2003a). Only binucleated cells with both

nuclei situated in the same cytoplasm were scored. The nuclei were more or less equal in size with intact cytoplasm. The diameter of the micronuclei was not greater than a third of the main nucleus and had the same staining intensity as the main nucleus. Micronuclei could touch but not overlap the nucleus. Apoptotic and necrotic cells were identified by chromatin condensation and cytoplasmic vacuoles respectively and were excluded from analysis.

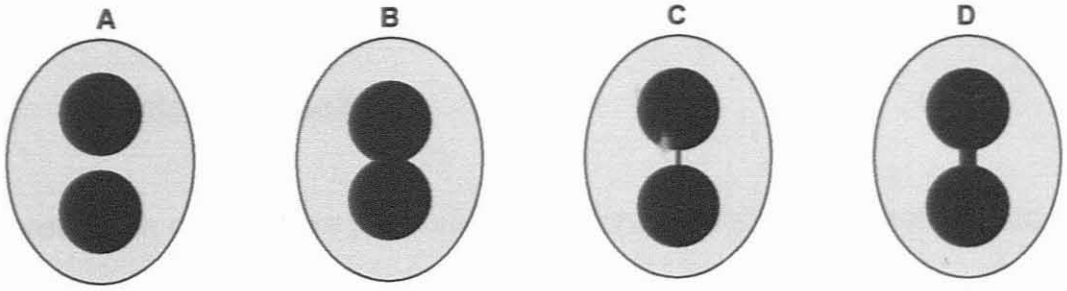

***Figure 5-1**: Criteria for choosing binucleated (BN) cells in the CBMN assay. A: Ideal BN cell; B: BN cell with touching nuclei; C & D: BN cell with nucleoplasmic bridges. All of the above cells can be scored for micronuclei (Redrawn from Fenech, 2003a).*

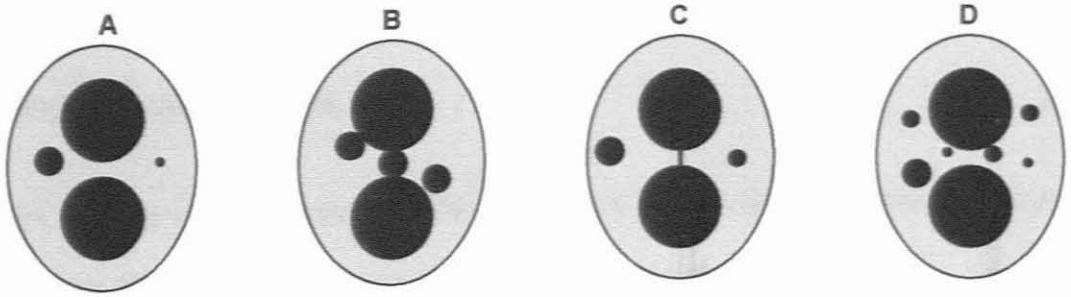

***Figure 5-2:** Typical appearance and relative size of MN in BN cells. A: Cell with two micronuclei; B: Micronuclei touching but not overlapping; C: Binucleated cell with nucleoplasmic bridge; D: Binucleated cell with six micronuclei (Redrawn from Fenech, 2003a).*

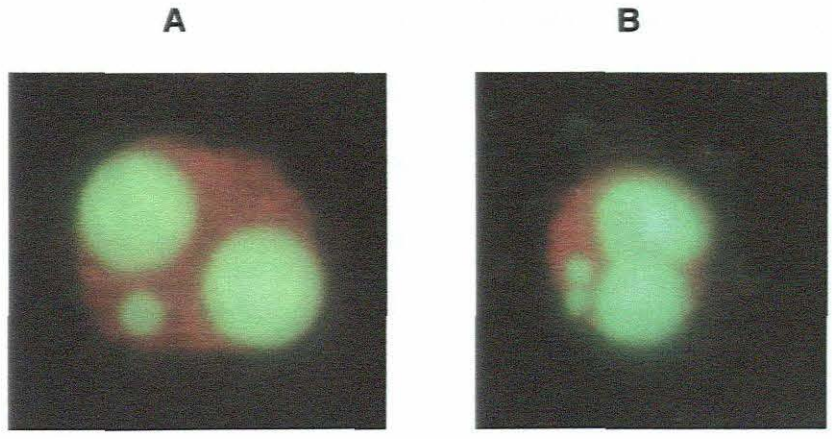

***Figure 5-3**: Photomicrographs of BN lymphocytes containing one (A) and two (B) micronuclei.*

5.2.7 Statistical analysis

Dose-response curves were generated with Microsoft ® Excel 2000 (9.0.2720). Standard deviations and averages were calculated using the STDEV and AVERAGE statistical functions respectively. Coefficients of variation were calculated using the following formula:

CV = SD/Mean x 100

p-Values were calculated using the two-sample student's t-test (TTEST function), assuming unequal variances.

Analysis of dose-response curves was performed with GraphPad Prism version 3.0 for Windows (GraphPad Software, San Diego, California, USA).

5.3. Results

Three experiments were carried out in which lymphocytes were exposed to gamma and neutron doses ranging from 0 to 4 Gy. Two slides were prepared per dose point and ideally 500 cells were scored per slide. All graphs have been constructed from

data displayed in **Table 5–1** to **Table 5–6**. Dose-response curves were compiled by plotting the number of micronuclei per 500 binucleated cells as function of radiation dose. The nuclear division index (NDI) and the number of micronuclei per 500 binucleated cells were calculated according to the formulas explained in section 5.2.5 of this chapter. The data displayed in columns 1 to 5 represent the number of micronuclei scored in the total number of cells analysed.

To compare the micronucleus yield distributions relative to Poisson distribution, the relative variance (σ^2/y), and the dispersion index (μ) were determined. Negative μ values indicate under dispersion and positive μ values indicate over dispersion of an observed Poisson distribution. A μ value of >1.96 is regarded as significantly different from Poisson.

Table 5–1: Results of micronucleus frequencies in lymphocytes exposed to 0 to 4 Gy gamma radiation. MN = Micronucleus; NDI = Nuclear division index; $\sigma^2 y$ = relative variance; μ = dispersion index.

Experiment 1 - Gammas

Dose in Gy	Number of MN in binucleated cells						Cells scored	MN/ 500 cells	NDI	σ^2/y	μ
	0	1	2	3	4	5					
0	484	16	0	0	0	0	500	16	1.70	0.97	-0.49
0.25	482	17	1	0	0	0	500	19	1.67	1.07	1.13
0.5	500	29	2	0	0	0	531	31	1.65	1.06	1.01
1.0	1114	121	15	2	0	0	1252	63	1.67	1.14	3.59
2.0	784	204	46	3	0	0	1037	147	1.75	1.07	1.54
4.0	257	317	254	113	60	14	1015	726	1.81	1.03	0.72
Average									**1.71**	**1.06**	**1.25**

Table 5–2: Results of micronucleus frequencies in lymphocytes exposed to 0 to 4 Gy neutron radiation. MN = Micronucleus; NDI = Nuclear division index; $\sigma^2 y$ = relative variance; μ = dispersion index.

Experiment 1 - Neutrons

Dose in Gy	Number of MN in binucleated cells						Cells scored	MN/ 500 cells	NDI	σ^2/y	μ
	0	1	2	3	4	5					
0	965	27	8	0	0	0	1000	22	1.78	1.33	7.47
0.25	922	67	11	0	0	0	1000	45	1.68	1.16	3.58
0.5	869	111	18	2	0	0	1000	77	1.72	1.16	3.63
1.0	729	222	38	11	0	0	1000	166	1.88	1.10	2.22
2.0	493	336	117	39	14	1	1000	374	1.70	1.13	2.91
4.0	195	370	283	98	43	11	1000	729	1.55	0.84	-3.55
Average									**1.72**	**1.12**	**2.71**

***Table 5–3**: Results of micronucleus frequencies in lymphocytes exposed to 0 to 4 Gy gamma radiation. MN = Micronucleus; NDI = Nuclear division index; σ^2/y = relative variance; μ = dispersion index.*

Experiment 2 - Gammas

Dose in Gy	Number of MN in binucleated cells						Cells scored	MN/ 500 cells	NDI	σ^2/y	μ
	0	1	2	3	4	5					
0	583	17	0	0	0	0	600	14	1.17	0.97	-0.48
0.25	969	26	5	0	0	0	1000	18	1.39	1.24	5.51
0.5	953	43	3	1	0	0	1000	26	1.38	1.18	1.06
1.0	967	27	6	0	0	0	1000	20	1.26	1.27	6.11
2.0	821	161	17	1	0	0	1000	99	1.31	1.01	0.11
4.0	571	302	100	26	1	0	1000	292	1.32	1.05	1.06
Average									**1.31**	**1.12**	**2.22**

***Table 5–4**: Results of micronucleus frequencies in lymphocytes exposed to 0 to 4 Gy neutron radiation. MN = Micronucleus; NDI = Nuclear division index; σ^2/y = relative variance; μ = dispersion index.*

Experiment 2 - Neutrons

Dose in Gy	Number of MN in binucleated cells						Cells scored	MN/500 cells	NDI	σ^2/y	μ
	0	1	2	3	4	5					
0	981	18	1	0	0	0	1000	10	1.28	1.08	1.86
0.25	964	34	2	0	0	0	1000	19	1.24	1.07	1.55
0.5	916	75	7	2	0	0	1000	48	1.34	1.18	4.04
1.0	643	131	23	1	0	0	800	115	1.12	1.08	1.52
2.0	585	237	66	12	0	0	900	225	1.19	1.06	1.17
4.0	204	188	77	28	3	0	500	438	1.1	0.94	-0.90
Average									**1.21**	**1.07**	**1.54**

***Table 5–5**: Results of micronucleus frequencies in lymphocytes exposed to 0 to 4 Gy gamma radiation. MN = Micronucleus; NDI = Nuclear division index; σ^2/y = relative variance; μ = dispersion index.*

Experiment 3 - Gammas

Dose in Gy	Number of MN in binucleated cells						Cells scored	MN/ 500 cells	NDI	σ^2/y	μ
	0	1	2	3	4	5					
0	985	13	2	0	0	0	1000	9	1.61	1.22	5.06
0.25	1073	27	0	0	0	0	1100	12	1.45	0.98	-0.57
0.5	949	43	8	0	0	0	1000	30	1.29	1.21	4.81
1.0	930	66	4	0	0	0	1000	37	1.40	1.04	0.80
2.0	714	170	16	0	0	0	900	112	1.18	0.94	-1.38
4.0	256	219	76	11	6	0	568	377	1.22	0.93	-1.25
Average									**1.36**	**1.05**	**1.25**

***Table 5–6**: Results of micronucleus frequencies in lymphocytes exposed to 0 to 4 Gy neutron radiation. MN Micronucleus; NDI = nuclear division index; $\sigma^2 y$ = relative variance; μ = dispersion index.*

Experiment 3 - Neutrons

Dose in Gy	Number of MN in binucleated cells						Cells scored	MN/ 500 cells	NDI	σ^2/y	μ
	0	1	2	3	4	5					
0	974	26	0	0	0	0	1000	13	1.19	0.98	-0.57
0.25	962	35	3	0	0	0	1000	21	1.44	1.11	2.41
0.5	900	87	13	0	0	0	1000	57	1.54	1.12	2.65
1.0	794	175	26	5	0	0	1000	121	1.33	1.10	2.19
2.0	458	184	48	7	3	0	700	224	1.18	1.11	2.07
4.0	69	72	44	10	5	0	200	525	1.12	0.95	-0.55
Average									**1.30**	**1.06**	**1.37**

The MN data has been analysed by means of a second-degree polynomial fit. The coefficients reflect the alpha and beta parameters of a linear quadratic model (**Table 5–7**). Alpha values represent lethal damage and beta values reparable damage.

Table 5–7: *Statistical data on micronucleus frequencies in lymphocytes exposed to gamma and neutron radiation. Alpha and beta values of dose response curves were derived from a linear quadratic model.*

	Gammas		**Neutrons**	
	α – value (Gy^{-1})	**β – value (Gy^{-2})**	**α – value (Gy^{-1})**	**β – value (Gy^{-2})**
Experiment 1	0	43.71	150.8	6.79
Experiment 2	0	17.57	106.4	0
Experiment 3	12.77	19.80	86.95	10.24
SD	47.8 *(All)*	15.4 *(Exp 2 & 3)*	49.7 *(All)*	12.7 *(Exp 2 & 3)*
CV	31 *(All)*	24 *(Exp 2 & 3)*	32 *(All)*	9 *(Exp 2 & 3)*

5.3.1 Inter-experimental variability

Standard deviations and coefficients of variation of all three experiments are displayed in **Table 5–7**. Micronucleus frequencies in experiment 1 were consistently higher than in the other two experiments resulting in CVs ranging from 9% to 55% for gammas and 21% to 51% for neutrons. If experiment 1 was excluded from the calculation of CVs, the values decreased to between 9% and 44% for gammas and 0.5% and 18% for neutrons. The average NDI for experiment 1 (1.72) was also 32% higher than the average NDI of 1.30 for the other two experiments.

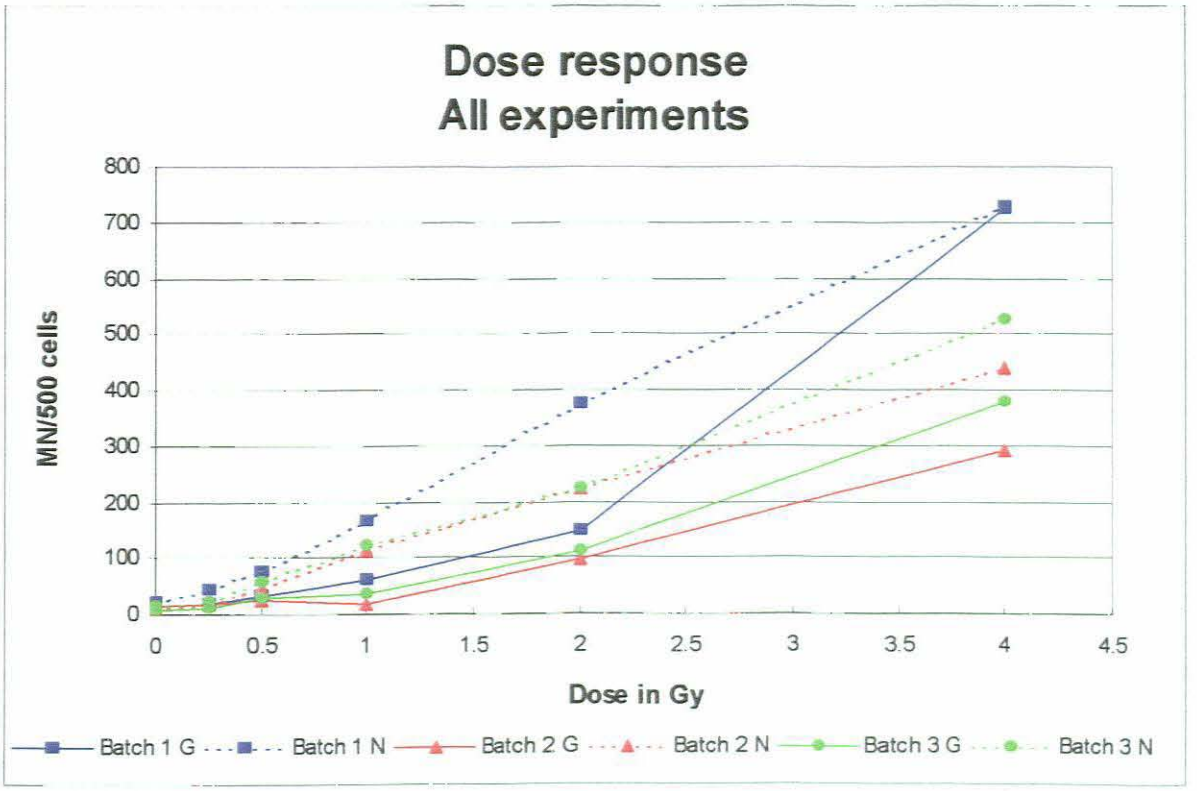

***Figure 5-4**: Dose-response curves of micronucleus frequencies of lymphocytes exposed to gamma and neutron radiation. All data points represent the values of one experiment. Control values (0 Gy) have not been subtracted from data points.*

5.3.2 Dose-response

Both radiation qualities induced micronuclei formation in lymphocytes in a dose-responsive manner (**Table 5–1** to **Table 5–6** and **Figure 5-4**), ranging on average from 12 micronuclei per 500 cells in unirradiated samples to 335 in gamma- and 482 in 4 Gy neutron-irradiated samples. Neutron data produced linear dose-response curves, while gamma data displayed linear-quadratic curves.

Alpha values for neutron-exposed samples ranged from 86.95 to 150.8 and were consistently higher than gamma-exposed samples, which ranged from 0 to 12.77. An alpha value of zero was assigned when the estimate was not significantly different from zero and inter-experimental variability was too high.

5.3.3 Dispersion of micronuclei

Over the three experiments micronucleus frequencies were over dispersed (> 1.96) in 5 dose points for gammas and 10 dose points for neutrons and under dispersed in 5 dose points for gammas and 4 for neutrons. The average relative variances (σ^2/y) ranged from 1.05 to 1.12 across both radiation qualities with no significant difference in the values for gammas and neutrons.

5.4. Discussion

High inter-experimental variability was observed between experiment 1 and the other two experiments; the influence of different lots of PHA could have contributed to this observation. It was conspicuous that experiment 1, apart from higher micronucleus frequencies, also produced a NDI that was 32% higher than those from the other two batches. The possibility that the quality of PHA could influence the formation of micronuclei should be investigated. The high frequency of micronuclei in the 4 Gy gamma-irradiated samples in experiment 1 may have influenced other statistical data.

From the alpha and beta values it is clear that neutron radiation induced a linear dose response while gamma radiation induced a linear-quadratic dose response. The low alpha values observed in the gamma curve, confirms the low-LET quality of gamma radiation with most of the induced damage of the reparable type. The two zero-values observed in the first two experiments were possibly due to large inter-experimental variability. The neutron beam produced higher alpha values in accordance with the more densely ionisation pattern of high-LET radiation where less cells are hit but with more lethal consequences.

The assay was not sensitive enough to detect significant radiation damage below 0.5 Gy in either of the two radiation qualities.

The dispersion of micronuclei was not significantly different for gammas and neutrons and produced μ values of close to one as expected for gamma-exposed cells.

5.5. Conclusion

The CBMN assay is the gold standard as an *ex vivo* measure of chromosome breakage and loss and has been standardised by the HUMN project with respect to methodological variables and scoring criteria (Fenech *et al.*, 2003b). Despite the use of these criteria and an established experimental protocol in this study, the inter-experimental variability between three experiments was unacceptable. It has been suggested that different lots of PHA could induce different micronucleus frequencies; this observation should be investigated thoroughly before any attempt is made to employ the assay in its current format as biological indicator of radiation damage.

The assay was sensitive enough to distinguish between low- and high-LET radiation doses above 0.5 Gy and therefore the potential exists to use the assay as a biomarker of radiation damage for radiation doses above 0.5 Gy. Lymphocytes responded to both radiation qualities in a dose-responsive manner.

Chapter 6

Apoptosis

6.1. Introduction and literature review

When a cell is subjected to stress signals, e.g. radiation, chemotherapeutic drugs or withdrawal of growth factors, a range of gene products are activated to prepare the cell to either repair the damage or to die (Ross, 1999). These stimuli can activate a variety of pathways, depending on the specific cell type and stress signal.

Apoptosis is defined as "programmed cell death", and can either be a normal physiological process whereby tissue homeostasis is maintained or it can be induced by radiation. Apoptosis is important, not only in tissue development, but also in the immune defence and in the elimination of cancerous cells (Lewin, 2000). Defects in genes that control apoptosis and the rescue of cells destined for destruction can promote cancer development or result in autoimmune disease. In contrast, excessive activation of apoptosis can lead to neurodegenerative diseases, myocardial infarction, and AIDS (Tannock and Hill, 1998).

Apoptosis is still regarded as an uncommon mechanism for radiation-induced cell death (Fajardo *et al.*, 2001). However, in several tissues apoptosis may be the main mechanism of cell death. The high level of radiosensitivity and rapid loss of certain lymphocytes may be explained by interphase cell death due to apoptosis (Fajardo *et al.*, 2001).

Ionising radiation induces two types of cell death: mitotic (clonogenic) cell death or apoptosis (interphase cell death). Mitotic cell death results when a cell is unable to divide any further and therefore loses its clonogenicity (Shinomiya, 2000). Apoptosis is highly cell type dependent. Cells from the haematopoietic- and lymphoid systems are particularly sensitive to radiation and cells from epithelial origin less sensitive (Steel, 2002).

Radiation activates signalling pathways in the nucleus and/or the plasma membrane. Proteins involved in the recognition of nuclear damage include poly (ADP ribose) polymerase (PARP), DNA dependent protein kinase and p53 (Fajardo *et al.*, 2001). Radiation-induced apoptosis may be p53 dependent or independent. The later events of the apoptosis process are similar for various triggers and involve the activation of a group of calcium-magnesium-dependent enzymes, including an endonuclease that cleaves nuclear chromatin at select internucleosomal linker sites.

The morphological changes during apoptosis is characterised by membrane blebbing and nuclear and cytoplasmic condensation. In the final stages, the dying cells become fragmented into apoptotic bodies that are ultimately removed by phagocytes.

A

B

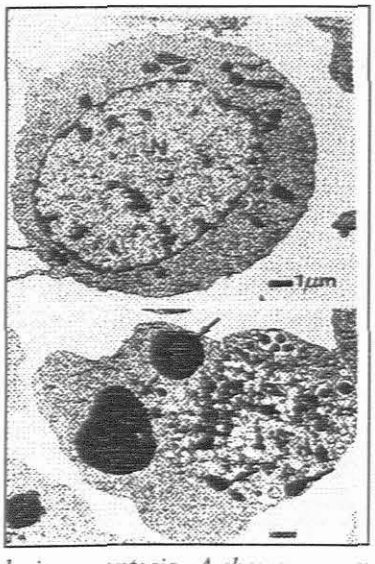

Figure 6-1: *Changes in cell structure during apoptosis. A shows a normal cell while B shows an apoptosing cell. Arrows indicate condensed nuclear fragments (Lewin, 2000)*

Molecularly, apoptosis is a complex process, involving different biological systems. Tannock and Hill (1998) divided the process into three phases. The **induction** phase is activated by different stress stimuli and involves the triggering of the apoptosis cascade by caspases (cysteine-dependent, aspartate-specific proteases). Caspases lie in a latent state in cells but become activated in response to cell death signals, manifesting as the **effector** phase. The last phase of the apoptotic cascade involves the **degradation** of DNA by various enzymes that prepare the cell for phagocytosis.

Two major pathways of caspase activation have been identified, namely the **receptor**-mediated pathway and the **mitochondria**-mediated pathway. Both pathways culminate in the activation of caspase-3, a major downstream effector caspase (Schimmer *et al.*, 2001). A third minor pathway has also been identified whereby **Granzyme B**, synthesised by cytotoxic T-cells, directly activates caspase-3 (Schimmer *et al.*, 2001). A simplified version of the major pathways of apoptosis is given in **Figure 6-2**.

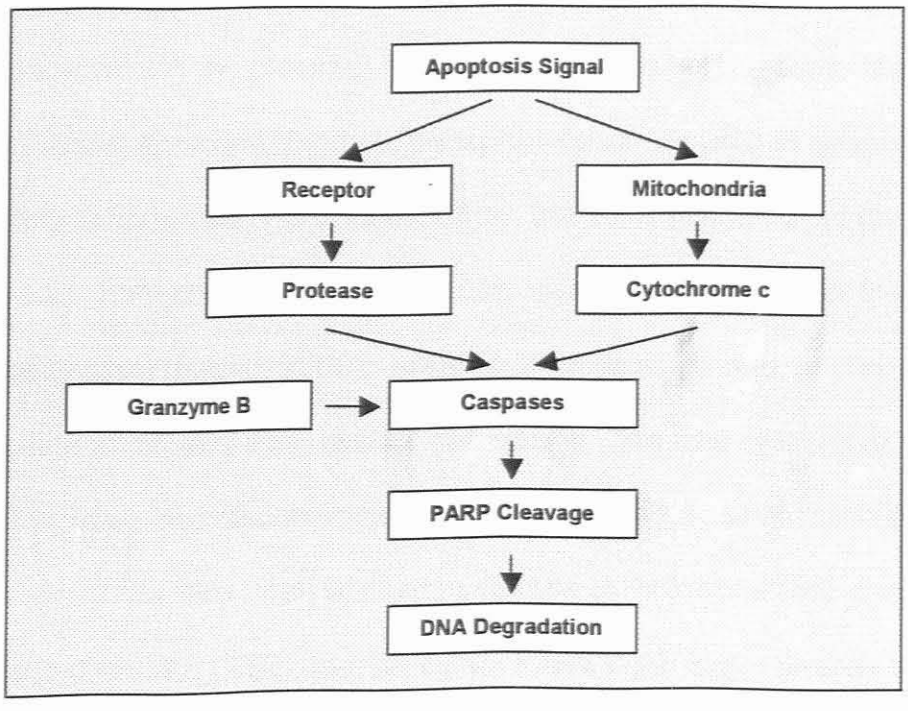

***Figure 6-2**: A simplified representation of the major pathways involved in apoptosis.*

In addition to the caspase family of proteases, another proteolytic system is involved in cell death. Although this system is not well understood the ubiquitin-proteasome degradation system has been proved to be involved in the degradation of most short-lived cytoplasmic and nuclear proteins (Lewin, 2000). Many of these proteins are involved in the regulatory functions of cells and so the ubiquitin system itself is a vital regulatory system controlling the concentration of key proteins by selective degradation. This system has been positively associated with the control of apoptosis in human lymphocytes (Masdehors *et al.*, 2000).

The sequence of events described above is induced by death receptors such as tumour necrosis factor (TNF) or Fas, a cell surface receptor. In contrast, radiation-induced apoptosis is less well studied and the processes following radiation of cells are still being investigated.

Different aspects of the apoptotic cascade have been studied in recent years, resulting in the development of novel techniques for the detection of key enzymes and proteins involved in the process. One such technique takes advantage of the fact that the protein Annexin V binds to phosphatidyl serine (PS) in apoptotic cells. Relatively early in apoptosis, PS relocates from the inner phospholipid layer to the outer to the outer phospholipid layer of the cell, signalling the desire of the cell to die and be phagocytosed (Bacso, 2000). Annexin V binds to PS and, in conjunction with propidium iodide as an exclusion dye for cell viability, this flow cytometric assay can detect apoptotic cells and discriminate between apoptosis and necrosis (Wilkins, 2002). This assay has also been applied in studies of radiosensitivity of lymphocyte subpopulations (Schmitz, 2003), human cervix tumour cell lines (Sheridan, 2001), and patients receiving radiotherapy treatment (Crompton, 1999).

Another flow cytometric assay measuring the degradation phase of apoptosis is the TUNEL (terminal deoxynucleotidyltransferase [TdT] dUTP nick end labelling) assay. TdT recognises breaks in DNA and by adding a fluorescin-labelled nucleotide to the free 3' hydroxyl end, quantification of apoptosis by flow cytometry is possible (Bebb, 2001; Barber, 2000).

Caspase 3/7 activation is one the key events in the apoptosis cascade of most cells and is mostly detected with a fluorescent caspase substrate and analysis by spectrofluorometry. The amount of fluorescent product is proportional to the amount of caspase 3/7-cleavage activity present in the sample (Louagie *et al.*, 1999).

Fluorescent inhibitor of caspases (FLICA) is used to arrest cells in apoptosis, preventing their disintegration and loss from analysis (Smolewski, 2002a and 2002b). By using this method, it was possible to study cumulative apoptosis in human promyelocytic leukaemic HL-60 cells, detecting three different stages of apoptosis. However, the time frame of the TUNEL, Annexin V and FLICA methods are different and the apoptotic index measured by these methods may thus differ, particularly in the later stages of apoptosis.

There is some disagreement on the best marker for apoptosis; therefore it could be advantageous to include an analysis of the morphological features of cells undergoing apoptosis by fluorescence-, light-, or electron microscopy (Vral *et al.*, 1998; Cortese, 2001).

6.2. Aim of study

Radiation-induced apoptosis is characterised by a variety of morphological, biochemical and genetic markers. The complexity of the apoptosis cascade and the varied manner in which cells respond to stress signals necessitates a study design that measures multiple aspects of apoptosis. The aim of this study was thus to analyse the apoptotic response of isolated lymphocytes during different phases of apoptosis after exposure to different qualities and doses of low-level ionising radiation. The study was structured to investigate the ability of the assays to detect the induction of apoptosis by low-level radiation in a dose- and time-responsive manner and ultimately to validate the assays for use as predictors of intrinsic radiosensitivity and as possible biological dosimeters in the low-dose region.

6.3. Overview of methods

6.3.1 Assay principles

The activation of the various phases of the apoptotic cascade was studied by measuring the endpoints after different post-irradiation incubation periods. Unless otherwise stated, three independent experiments were performed for each endpoint and time interval.

The effector phase of apoptosis, marked by the activation of caspases, was studied by using the Apo-ONE ™ Homogeneous Caspase-3/7 Assay (Cat G7791), developed by Promega Corporation (Promega, 2002). The caspases-3/7 substrate rhodamine 110 (Z-DEVD-R110) exists as a profluorescent substrate prior to the assay. Upon sequential cleavage and removal of the DEVD peptides by

caspases-3/7 activity and excitation at 499 nm, the rhodamine 110 leaving group becomes intensely fluorescent. The amount of fluorescent product is proportional to the amount of caspases-3/7 cleavage activity present in the sample (Promega, 2002).

The degradation phase of apoptosis was investigated by employing a novel TUNEL method, the Apo-Direct™ Assay (Cat. 55631), developed by BD Biosciences (2001). This assay is a single-step method for labelling DNA breaks with FITC (fluorescein isothiocyanate) -dUTP, followed by flow cytometric analysis. Non-apoptotic cells do not incorporate significant amounts of the FITC-dUTP owing to the lack of exposed 3'-hydroxyl DNA ends (BD Biosciences, 2001). **Figure 6-3** shows how the DNA breaks are labelled by addition of FITC-dUTP at break sites.

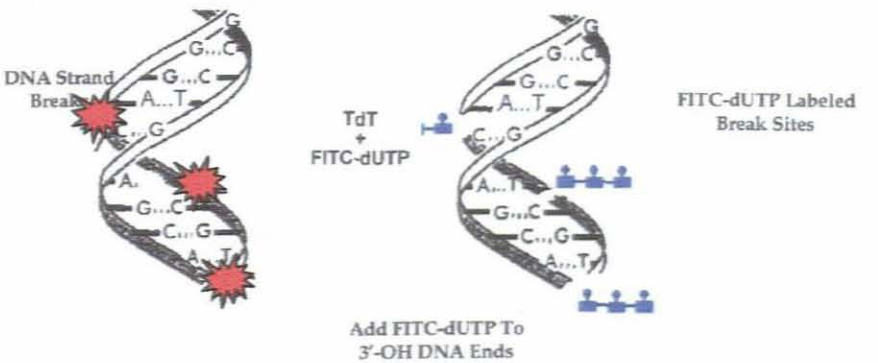

***Figure 6-3**: Diagrammatic representation of the APO-DIRECT TUNEL assay. TdT catalyses the addition of FITC-dUTP at the 3'-OH sites of DNA strand breaks of apoptotic cells (BD Biosciences, 2001).*

As cellular morphology has always been the gold standard for detection of apoptotic features in cells, this method was included in the study to complete the apoptotic picture of isolated lymphocytes.

6.3.2 Cell preparation for all assays

Blood from one healthy female donor was drawn into a 4.5 ml Vacutainer tube containing either EDTA- or lithium heparin as anticoagulant. Peripheral lymphocytes were isolated with Histopaque 1077 (Sigma), washed with PBS and diluted in 10 ml RPMI 1640, supplemented with 15% heat inactivated foetal calf serum, 2 g/l $NaHCO_3$ and 1% Penstrep. Five millilitres of cell suspension were pipetted into round-bottom culture tubes for radiation treatment.

6.3.3 Irradiation procedure and equipment

Gamma irradiation was performed using a ^{60}Co γ-source (Eldorado 76, Atomic Energy of Canada Ltd.), delivering a dose-rate of 0.29 Gy/min at a source surface distance (SSD) of 70 cm, a field size of 30 x 30 cm^2 and a gantry angle of 180°. Tubes were placed side-by-side in the centre of the radiation beam on a 0.5 mm-thick Perspex sheet with a 5 cm thick Perspex block on spacers serving as backscatter material. The dose at the position of the tubes was verified by using a 0.6 cm^3 thimble Farmer ionisation chamber, type 2571 and a Farmer electrometer, model 2570/1 (NE Technology). The dosimetry system was calibrated against a national standard at the CSIR in Pretoria.

The experimental set-up was also verified by irradiating seventeen calibrated thermoluminescent dosimeters (TLDs) to a dose of 2 Gy. The average TLD-dose registered after read-out in a TOLEDO dosimetry system was 2.055 Gy.

Neutron irradiation was performed using the cyclotron at iThemba LABS at Faure, using a dose rate of 0.35 Gy/min delivered by 66 MeV protons bombarding a 19.6

mm thick beryllium target. The p(66)/Be(40) neutron beam generated had a large spectrum of energy with a maximum value of 64.15 MeV (Schreuder, 1992). A field size of 20 x 20 cm^2 and SSD of 150 cm was used at a gantry angle of 0°. Tubes were placed side-by-side in the centre of the beam on a 10 cm thick perspex block with 2 cm nylon as build-up material and 6 cm Perspex as backscatter. The dose at the position of the cells was verified by means of an 80 cm^3 Far West (model IC-80) ionisation chamber (Far West Technology) and a BNC Portanim (model AP-2H) current digitiser (Berkeley Nucleomics, Corporation, USA).

6.3.4 Incubation

Cultures were incubated at 37°C in 5% CO_2 in a QUEUE water-jacketed Co_2 incubator (Model 2710, Q-Systems Inc., New Jersey) until required for further processing.

6.3.5 Statistical analysis

Dose-response curves were generated with Microsoft ® Excel 2000 (9.0.2720). Standard deviations and averages were calculated using the STDEV and AVERAGE statistical functions respectively. Coefficients of variation were calculated using the following formula:

$$CV = SD/Mean \times 100$$

p-Values were calculated using the two-sample student's t-test (TTEST function). assuming unequal variances.

6.4. Methodology

6.4.1 Caspase-3/7 Activity

6.4.1.1 Pilot study

A pilot study was conducted to optimise the Apo-ONE ™ Homogeneous Caspase-3/7 Assay for the detection of caspase activity in lymphocytes isolated from EDTA blood by irradiating cell suspensions (0.2 $x10^6$ cells/ml) with ^{60}Co-gamma doses of 0, 0.25, 0.5, 1.0, 2.0 and 4.0 Gy at different time intervals in order for analysis to take place simultaneously. Cell cultures were incubated in round bottom culture tubes with loose lids for 12, 24, 36, 48, 72, and 96 hours.

Prior to starting the assay, the Homogeneous Caspase-3/7 reagent supplied with the kit was prepared by thawing the reagents and mixing 100 µl of Caspase Substrate Z-DEVD-R110 (100X) with 10 ml Apo-ONE ™ Homogeneous Caspase-3/7 Buffer. One hundred millilitres of Homogeneous Caspase-3/7 reagent was added to each well of a white 96-well plate containing 100 µl of cell suspension, blank (reagent plus medium) or control (0 Gy sample plus reagent). Samples were performed in duplicate. The plates were gently shaken on a plate shaker at room temperature for 3 hours after which it was covered and taken to the Cary Eclipse Fluorescence Spectrophotometer (Installation category 11, Varian Instruments, Australia) for analysis. An excitation filter with a wavelength of 485 to 530 nm was used to collect data.

6.4.1.2 Time-response study

Cell samples were prepared according to the experimental protocol for the pilot study but the cell count was raised to 0.6 x 10^6/ml to improve the fluorescence signal. One culture tube was prepared per radiation quality per dose point. All samples were irradiated simultaneously with gamma- and neutron doses of 0 to 4 Gy (see pilot study) and incubated for 6, 12, 24, 30, 36, 42, 48, 60, 72 and 90 hours. To ensure a homogeneous cell suspension, culture tubes were vortexed at each time interval before samples were removed for the assay. Samples, blanks, and negative controls were pipetted into triplicate wells and shaken for 30 seconds in an automatic plate shaker before it was incubated for 2.5 hours at room temperature. Samples were analysed as for the pilot study.

6.4.1.3 Dose-response study

The protocol for the time response study described above was followed to establish dose-response curves for neutron and gamma irradiation doses of 0, 0.25, 0.5, 1.0, 2.0, and 4 Gy after an incubation period of 36 hours. The experiment was performed in triplicate. One of the experiments included a blood sample from a second donor to verify the results.

6.4.2 DNA fragmentation

Blood was drawn into 5 ml Vacutainer tubes containing either EDTA or Lithium heparin as anticoagulant Lymphocytes were isolated and irradiated as described for the caspase experiments and incubated for 48 hours before treatment with the APO-DIRECT ™ TUNEL Assay (BD Biosciences, Pharmingen, USA).

6.4.2.1 Cell fixation

Irradiated cell samples were taken from the incubator, centrifuged for 5 min at 300 x g after which the supernatant was discarded. Two and a half millilitres of fresh 1% (w/v) paraformaldehyde in PBS were added drop-wise and cells were placed on ice for 45 minutes. Cells were washed twice in PBS after which 2.5 ml of ice cold 70% ethanol were added. Cells were stored at –20°C until required for flow cytometric analysis.

6.4.2.2 DNA labelling procedure

One-millilitre aliquots of the positive and negative control cell suspension (lymphoblastoid cell line) supplied with the kit were resuspended and centrifuged for 5 min at 300 x g with the test samples. All samples were transferred to plastic test tubes suitable for flow cytometric analysis (Falcon 2054, Beckton Dickinson). Ethanol was carefully removed by aspiration and 1 ml of wash buffer supplied by the manufacturer was added to each sample. Samples were washed twice with the wash buffer after which 50 µl of fresh labelling solution was added. The labelling solution for one sample consisted of 10 µl reaction buffer, 0.75 µl TdT enzyme, 8 µl FITC-dUTP and 32.25 µl of distilled water. The manufacturer supplied all reagents except the distilled water. Samples isolated from EDTA-blood were covered and placed on a shaker overnight at room temperature while samples isolated from heparin blood were covered and incubated for I hour at 37°C.

At the end of the incubation time, samples were washed twice with 1 ml of rinse buffer supplied by the manufacturer. The cell pellet was resuspended in 0.5 ml of the Propidium Iodide/Rnase solution supplied by the manufacturer, covered with tin foil

and incubated for 30 min at room temperature. Samples were analysed within 2 hours.

6.4.2.3 Flow cytometric analysis

Samples were analysed on a dual colour FACSCalibur flow cytometer (Beckton Dickinson) equipped with a 488 nm Argon laser as the light source. PI fluoresces at 623 nm and FITC at 520 nm. A total of 10 000 events were collected in the lymphocyte region on the light scattergram with the DNA area signal displayed on the Y-axis and the DNA width displayed on the X-axis. From the gating display, a region was drawn around the non-clumped cells and a second gated dual parameter display was generated. The DNA (linear red fluorescence) was displayed on the X-axis and the d-UTP (log green fluorescence) on the Y-axis. The percentage of FITC-positive cells was calculated as a percentage of the total number of lymphocytes analysed.

6.4.3 Cellular morphology

6.4.3.1 Cell preparation

EDTA-blood collected from the same donor was prepared according to the protocol followed for caspase measurement. Cell suspensions were irradiated with gamma doses of 0 and 4.0 Gy and incubated at 37°C for 24, 48 and 72 hours after which it was fixed with 5 ml of a fresh Carnoy's fluid (methanol:acetic acid 3:1). The fixative was added drop-wise while vortexed at low speed. Samples were stored at 4°C until slides were prepared. Cell suspensions were spun down and the supernatant aspirated until approximately 0.5 ml of fluid was left in tube. Cells were mixed, dropped onto duplicate slides, and left at room temperature to dry for at least 24 hours before staining. Slides were stained for 1 minute with 40 µg/ml acridine orange

DNA binding dye, rinsed in water and buffer (pH 6.8) for 1 minute each and analysed with fluorescence microscopy.

6.4.3.2 *Microscopic analysis*

Cells were classified into 4 cell types according to the morphological appearance of the nucleus and cytoplasm as described by Gasiorowski *et al.* (2001). The criteria that were used for the classification of cells are summarised in **Table 6–1**.

Table 6–1: *Criteria used for classification of morphological features as analysed by fluorescence microscopy.*

Type 1	Normal cell	Round, green fluorescent nucleus with well-preserved red cytoplasm
Type 2	Nuclear condensation	Nucleus starting to condense with bean-shaped appearance
Type 3	Apoptotic cells	Cells displaying typical round, apoptotic bodies
Type 4	Abnormal morphology	Cell remnants with no distinguishable nucleus or cytoplasm

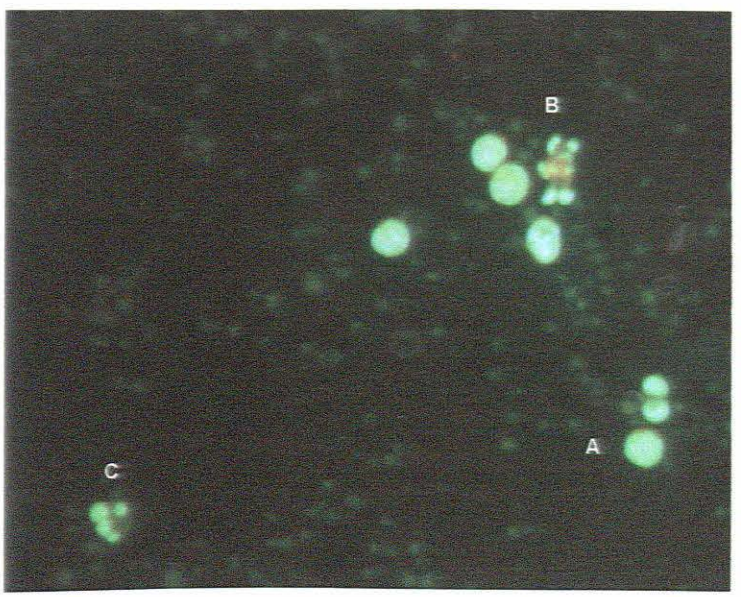

Figure 6-4*: Photomicrograph of normal and apoptotic cells 24 hours after exposure to gamma radiation. A) normal cell, B) typical nuclear blebbing, C) cell with apoptotic bodies in the cytoplasm.*

6.5. Results

6.5.1 Caspase 3/7

6.5.1.1 Pilot study

A pilot study was undertaken to standardise the Apo-ONE ™ Homogeneous Caspase-3/7 Assay and to obtain an overall time- and dose-response of the activation of caspase 3/7 in irradiated lymphocytes. **Figure 6-5** shows caspase activity in isolated lymphocytes after exposure to different doses of gamma radiation. Results are given in terms of a fluorescence ratio, which was calculated by dividing all data points by the control (0 Gy) value. Data points represent the values of one experiment. Duplicate wells were prepared for each data point.

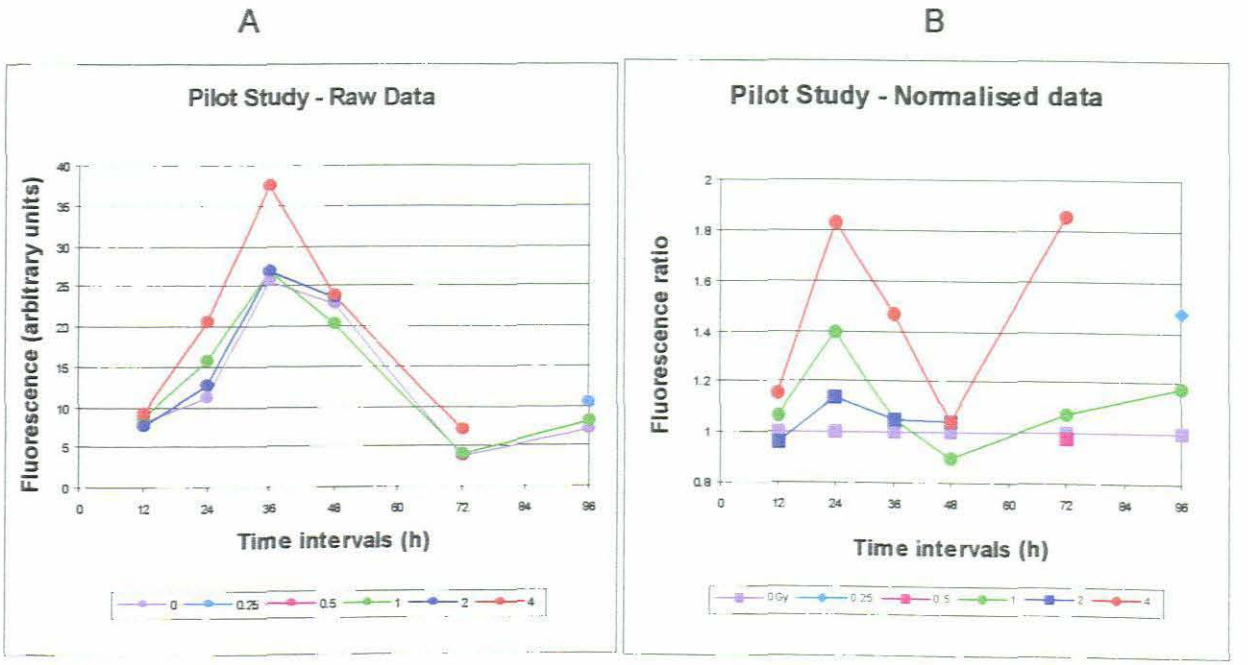

Figure 6-5: *Time-response curves of caspase 3/7 activity for gamma-irradiated isolated lymphocytes. Caspase activity was measured by the Apo-ONE ™ Homogeneous Caspase-3/7 Assay and is expressed as fluorescence (A) or fluorescence ratio (B), compensating for caspase activity present in unirradiated cells (0 Gy) samples.*

With fluorescence ratios of 1.4, 1.1 and 1.8 for doses of 1, 2, and 4 Gy respectively, a peak of caspase activity was observed 24 hours post-irradiation with a second period of caspase increase for 1 Gy (1.1) and 4 Gy (1.9) after 48 hours. The 0.25 and 0.5 Gy samples were incubated for 96 and 72 hours respectively and produced fluorescence ratios of 1.5 and 0.98.

6.5.1.2 Time-response study

An extensive time- and dose-response study was undertaken whereby isolated lymphocytes were exposed to different doses of gamma- and neutron irradiation and incubated for time periods ranging from 6 to 90 hours. Caspase activity was measured using the Apo-ONE ™ Homogeneous Caspase-3/7 Assay after each time interval. Results are given in terms of a fluorescence ratio after compensation for caspase activity present in unirradiated cells (0 Gy samples) as described in section 6.5.1.1. Fluorescence ratios for gammas and neutrons are presented in **Table 6–2** and **Table 6–3** respectively and represent the values of one experiment. Triplicate samples were prepared for each data point.

***Table 6–2**: Fluorescence ratios as measured by the Apo-ONE ™ Homogeneous Caspase-3/7 Assay in a time-response study on caspase activity in gamma-irradiated lymphocytes.*

Gamma Irradiation

	Time (h) after irradiation									
Dose in Gy	**6**	**12**	**24**	**30**	**36**	**42**	**48**	**60**	**72**	**90**
0	1.0	1.0	1.0	1.0	1.0	1.0	1.0	1.0	1.0	1.0
0.25	1.19	1.20	1.12	1.12	1.14	1.10	1.07	1.04	1.08	1.07
0.5	1.03	0.97	1.11	1.15	1.05	1.04	0.98	0.98	1.05	0.97
1.0	1.18	1.19	1.21	1.27	1.18	1.19	1.06	1.12	1.13	1.07
2.0	1.28	1.40	1.34	1.51	1.50	1.38	1.31	1.28	1.23	1.22
4.0	1.29	1.50	1.40	1.64	1.59	1.43	1.34	1.38	1.33	1.31

Table 6–3: *Fluorescence ratios as measured by the Apo-ONE™ Homogeneous Caspase-3/7 Assay in a time-response study on caspase activity in neutron-irradiated lymphocytes.*

Neutron irradiation

	Time (h) after irradiation									
Dose in Gy	**6**	**12**	**24**	**30**	**36**	**42**	**48**	**60**	**72**	**90**
0	1.0	1.0	1.0	1.0	1.0	1.0	1.0	1.0	1.0	1.0
0.25	1.09	1.05	1.07	1.01	0.99	1.04	1.03	1.00	1.02	0.98
0.5	1.16	1.03	1.09	1.01	1.02	1.02	1.02	0.99	1.05	0.96
1.0	1.11	1.04	1.07	1.0	0.97	1.02	0.98	1.14	1.11	1.27
2.0	1.25	1.19	1.13	1.07	1.11	1.13	1.01	1.15	1.70	1.28
4.0	1.33	1.28	1.30	1.30	1.27	1.25	1.22	1.18	1.18	1.27

Figure 6-6 displays the time-response relationship of isolated lymphocytes to gamma radiation after different incubation periods. The 2 and 4 Gy gamma-irradiated samples displayed a peak of caspase activity between 24 (1.34 and 1.40 respectively) and 36 hours (1.50 and 1.59 respectively) post-irradiation, but apart from the slight peak detected in 0.5 Gy and 1.0 Gy-samples at 30 hours (1.15 and 1.27 respectively), isolated lymphocytes exposed to lower doses of gamma radiation did not respond in a time responsive manner.

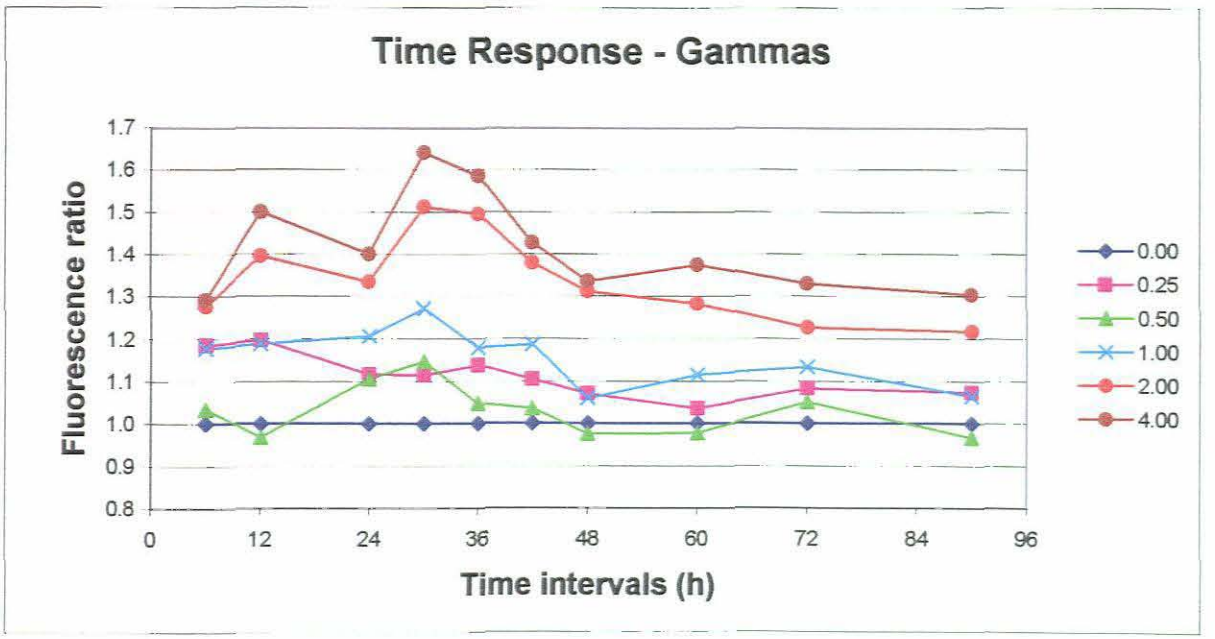

Figure 6-6: *Time-response curves of caspase 3/7 activity for 0 to 4 Gy gamma-irradiated isolated lymphocytes. Caspase activity was measured by the Apo-ONE™ Homogeneous Caspase-3/7 Assay and is expressed as a fluorescence ratio, compensating for caspase activity present in unirradiated cells (0 Gy) samples.*

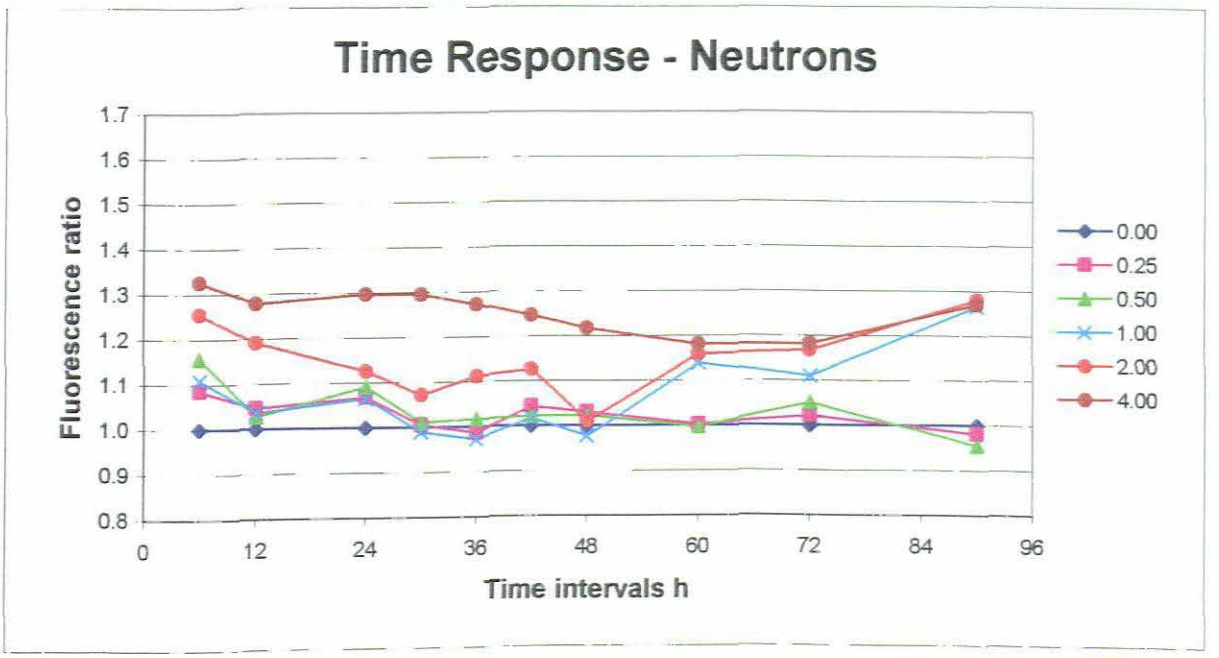

Figure 6-7: *Time-response curves of caspase 3/7 activity for 0 to 4 Gy neutron-irradiated isolated lymphocytes. Caspase activity was measured by the Apo-ONE™ Homogeneous Caspase-3/7 Assay and is expressed as a fluorescence ratio, compensating for caspase activity present in unirradiated cells (0 Gy) samples.*

Figure 6-7 shows the time-response relationship of isolated lymphocytes exposed to neutron radiation after different incubation periods. Neutron-irradiated samples did not respond in a time-responsive manner in any of the dose points. A slight upward trend was detected in samples above 1 Gy, indicating a possible late response to neutron irradiation in these samples.

6.5.1.3 Dose response study

As a peak of caspase activity was identified in the pilot study after 36 hours of incubation, it was decided to conduct a dose response study 36 hours post-irradiation. Isolated lymphocytes were exposed to different doses of gamma-and neutron irradiation and analysed spectrofluorometrically. Fluorescence ratios, averages, standard deviations, coefficients of variation (CV) and p-values of three independent experiments are displayed in **Table 6–4** and **Table 6–5**. The p-values indicate the significance of the difference between the control (0 Gy) value and all other dose points. A p-value of < 0.05 was regarded as significant.

***Table 6–4**: Fluorescence ratios of three independent experiments as measured by the Apo-ONE™ Homogeneous Caspase-3 7 Assay in a dose-response study on caspase activity in gamma-irradiated lymphocytes 36 hours post-irradiation. The p-values indicate the significance of the difference between the control (0 Gy) value and a specific dose point. A p-value of < 0.05 is regarded as significant. SD = Standard Deviation*

Gammas

Dose in Gy	Batch 1	Batch 2	Batch 3	Average	± 1 SD	CV	p-value
0	1.0	1.0	1.0	1.0	0		
0.25	1.16	0.99	1.27	1.14	0.14	12	0.675
0.5	1.08	1.09	1.37	1.18	0.17	14	0.578
1.0	1.32	1.06	1.38	1.26	0.17	13	0.407
2.0	1.53	1.25	1.53	1.44	0.16	11	0.190
4.0	1.69	1.29	1.93	1.64	0.32	20	0.078

Table 6–5: *Fluorescence ratios of three independent experiments as measured by the Apo-ONE™ Homogeneous Caspase-3/7 Assay in a dose-response study on caspase activity in neutron-irradiated lymphocytes. The p-values indicate the significance of the difference between the control (0 Gy) value and a specific dose point. A p-value of < 0.05 is regarded as significant. SD = Standard Deviation*

Neutrons

Dose in Gy	Batch 1	Batch 2	Batch 3	Average	± One SD	%CV	p-values
0	1.0	1.0	1.0	1.0	0		
0.25	1.46	1.14	1.03	1.21	0.22	18	0.911
0.5	1.34	1.23	1.14	1.23	0.10	8	0.939
1.0	1.25	1.13	1.12	1.17	0.07	6	0.837
2.0	1.33	1.27	1.26	1.29	0.04	3	0.971
4.0	1.72	1.25	1.41	1.46	0.24	16	0.900

Figure 6-8 displays the detection of caspase activity in isolated lymphocytes 36 hours after irradiation. Although the ratio of caspase production in gamma-irradiated cells was relatively low (average 1.14 to 1.64) a linear response was observed. However, the response in neutron-exposed cells showed hypersensitivity below 1 Gy with a linear response above 1 Gy.

Isolated lymphocytes responded to both radiation qualities in a dose responsive manner. However, none of the dose points produced significant *p*-values when measured against the control. Similarly, the difference in response between gammas and neutrons was also not significant in any of the dose points. Maximum caspase activity was detected in the 4 Gy gamma-irradiated samples with a fluorescence ratio of just over 1.6. Neutron-irradiated samples displayed a hypersensitivity to doses of 0.25 and 0.5 Gy with fluorescence ratios of 1.21 and 1.23 respectively, reaching a maximum fluorescence ratio of only 1.46 in the 4 Gy sample.

Inter-experimental variability was measured by means of CVs, which ranged between

3 and 20%. The neutron-irradiated samples produced a better average CV (10%) across all dose points compared to gamma-irradiated samples (14%).

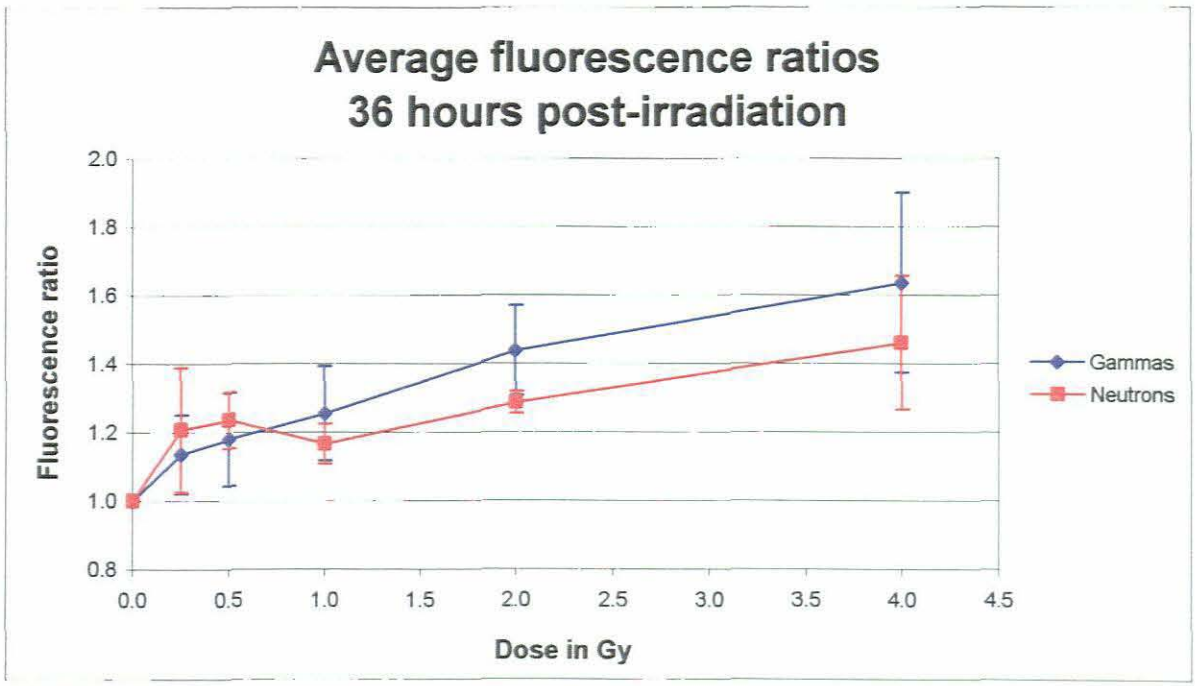

Figure 6-8: *Dose-response curves of caspase 3/7 activity for gamma- and neutron-irradiated isolated lymphocytes. Caspase activity was measured by the Apo-ONE™ Homogeneous Caspase-3/7 Assay and is expressed as a fluorescence ratio, compensating for caspase activity present in unirradiated cells (0 Gy) samples. Data points represent the average values of three experiments and error bars indicate ± one standard deviation.*

Figure 6-9 shows the results of one experiment in which blood from a second male donor (KS) was included. The results show that caspase production in gamma- and neutron-irradiated samples was consistently higher in samples of KS (maximum 1.5 compared to 1.3), indicating possible inter-individual differences in radiation-induced caspase production. However, caspase activity in irradiated samples was still very low for both donors.

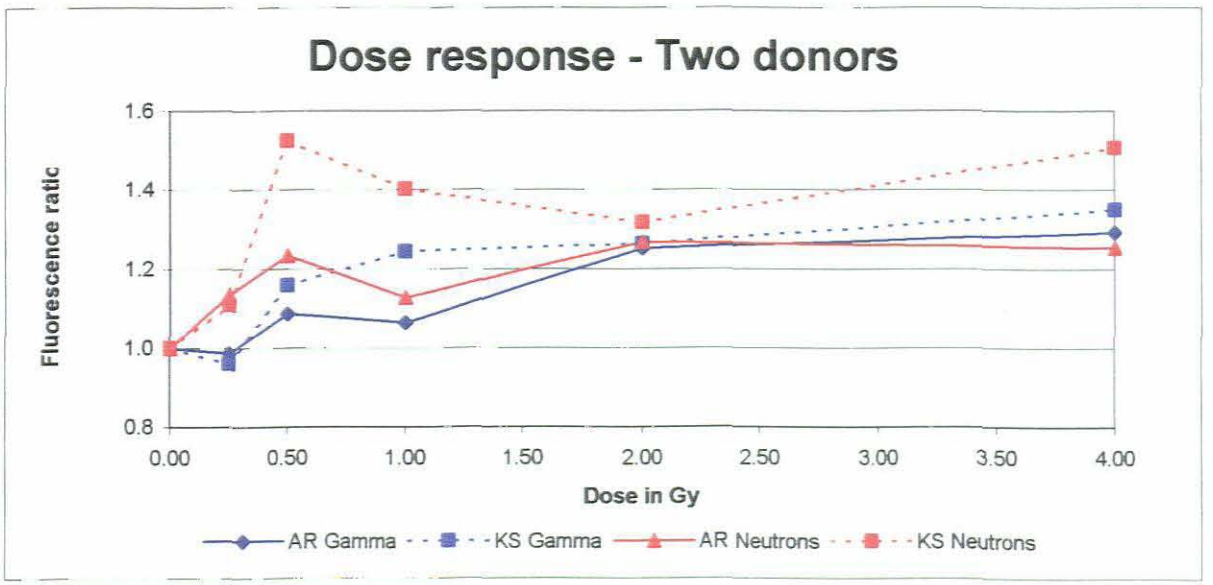

***Figure 6-9**: Dose-response curves of isolated lymphocytes of two donors exposed to gammas and neutrons. Caspase activity was measured by the Apo-ONE ™ Homogeneous Caspase-3/7 Assay and is expressed as a fluorescence ratio, compensating for caspase activity present in unirradiated cells (0 Gy) samples. Data points represent the values of one experiment.*

6.5.2 DNA Fragmentation

Lymphocytes were isolated from EDTA and heparin blood respectively and exposed to different doses of gamma and neutron radiation. Samples were incubated for 48 hours, processed by using the Apo-Direct TUNEL Assay, (BD Biosciences, Pharmingen, 2001) and analysed using a flow cytometer. Three independent experiments were performed on EDTA blood and were processed on separate days. Two experiments were performed on the same day on heparin blood and were processed together. Data were not corrected for spontaneous apoptosis in order to compare the number of FITC-positive cells in unirradiated samples of different experiments.

Apoptotic populations of cells are presented by means of scatter plots and histograms generated by the FACSCalibur software during sample analysis (**Figure 6-10** and **Figure 6-11**). The percentage of FITC-positive cells (with fragmented DNA) calculated from these data is summarised in **Table 6–6** to **Table 6–9** and is graphically displayed in **Figure 6-12** as function of radiation dose.

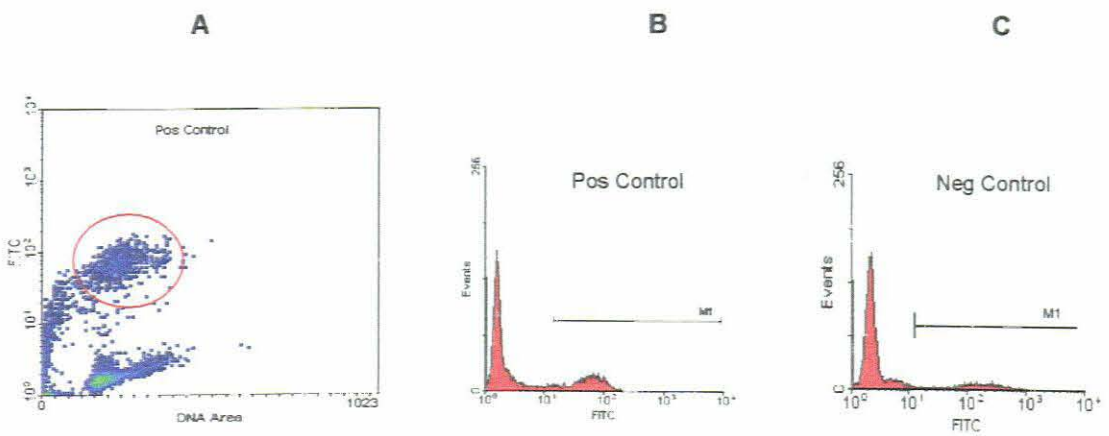

***Figure 6-10**: Flow cytometry data of control cells supplied by the manufacturer of the Apo-Direct TUNEL Assay. The cell population in the red circle in A represents the FITC-positive apoptotic cells. The M1 region in B and C indicates the percentage of FITC-positive cells.*

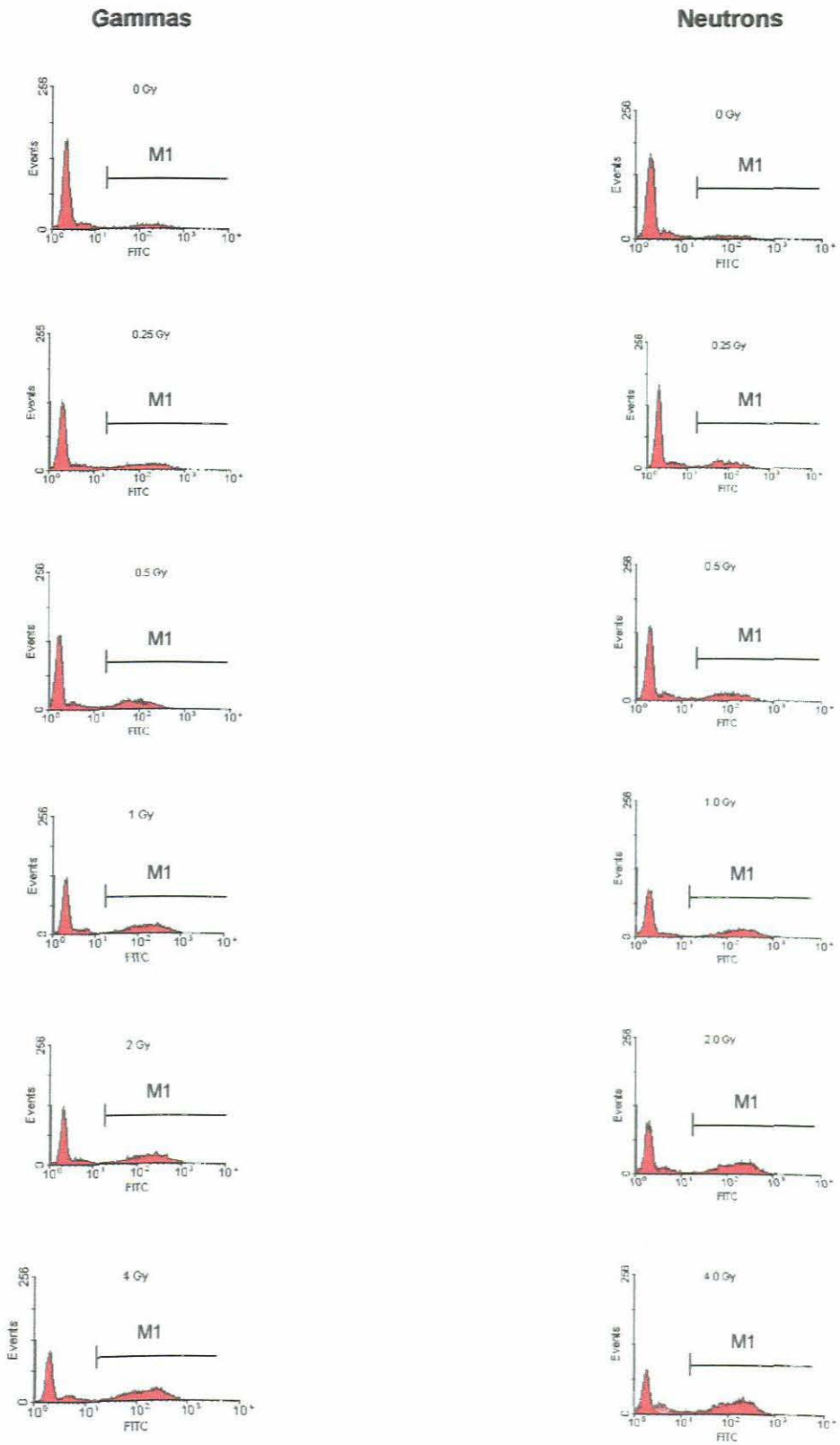

***Figure 6-11**: Flow cytometry data of irradiated lymphocytes as measured by the Apo-Direct TUNEL Assay. The intensity of FITC-positive calls is displayed on the x-axis while the number of events analysed are displayed on the y-axis. The fraction of FITC-positive cells is the number of cells in the M1 region as percentage of the total population.*

Table 6–6: *Results of three independent experiments in which lymphocytes in EDTA blood were isolated and exposed to gamma radiation. The percentage of FITC-positive cells was measured by the Apo-Direct TUNEL Assay. p-Values indicate the significance of the difference between the control (0 Gy) value and a specific dose point. A p-value of < 0.05 was regarded as significant and is printed in red. SD = Standard Deviation*

Gammas – EDTA blood							
Dose in Gy	**Batch 1**	**Batch 2**	**Batch 3**	**Average**	**± 1 SD**	**CV**	**p-Value**
0	18.66	22.32	9.72	16.90	6.48	38	
0.25	14.79	20.30	14.77	16.62	3.19	19	0.951
0.5	22.49	24.75	18.01	21.75	3.43	16	0.334
1.0	18.97	28.05	21.52	22.85	4.68	21	0.273
2.0	29.35	22.72	21.42	24.50	4.25	17	0.176
4.0	23.90	27.71	26.61	26.07	1.96	8	0.124
Pos control	33.78	24.94	32.77	30.50	4.84	16	
Neg control	2.82	2.85	3.09	2.92	0.15	5	

Table 6–7: *Results of three independent experiments in which lymphocytes in EDTA blood were isolated and exposedto neutron radiation. The percentage of FITC-positive cells was measured by the Apo-Direct TUNEL Assay. p-Values indicate the significance of the difference between the control (0 Gy) value and a specific dose point. A p-value of < 0.05 was regarded as significant and is printed in red. SD = Standard Deviation*

Neutrons – EDTA blood							
Dose in Gy	**Batch 1**	**Batch 2**	**Batch 3**	**Average**	**± One SD**	**CV**	**p-Value**
0	16.69	13.57	8.37	12.88	4.20	33	
0.25	16.67	24.16	14.95	18.59	4.90	26	0.201
0.5	30.46	27.43	16.56	24.82	7.31	30	0.086
1.0	21.63	25.67	24.44	23.91	2.07	9	0.028
2.0	32.82	21.16	24.80	26.26	5.97	23	0.039
4.0	35.01	33.92	31.60	33.51	1.71	5	0.006
Pos control	33.78	24.94	32.77	30.50	4.84	16	
Neg control	2.82	2.85	3.09	2.92	0.15	5	

Table 6–8: *Results of two experiments in which lymphocytes in heparin blood were isolated and exposed to gamma radiation. The percentage of FITC-positive cells was measured by the Apo-Direct TUNEL Assay. p-Values indicate the significance of the difference between the control (0 Gy) value and a specific dose point. A p-value of < 0.05 was regarded as significant and is printed in red. SD = Standard Deviation*

Gammas – Heparin blood						
Dose in Gy	**Batch 1**	**Batch 2**	**Average**	**± 1 SD**	**CV**	**p-Value**
0	12.25	10.51	11.38	1.23	11	
0.25	22.10	17.27	19.69	3.43	17	0.149
0.5	24.97	24.47	24.72	0.35	1	0.029
1.0	33.34	31.07	32.21	1.61	5	0.006
2.0	36.73	31.29	34.01	3.85	11	0.055
4.0	43.25	44.87	44.06	1.15	3	0.001
Pos control	24.10	30.22	27.16	4.33	16	
Neg control	1.17	1.14	1.16	0.02	2	

Table 6–9: *Results of two experiments in which lymphocytes in heparin blood were isolated and exposed to neutron radiation. The percentage of FITC-positive cells was measured by the Apo-Direct TUNEL Assay. p-Values indicate the significance of the difference between the control (0 Gy) value and a specific dose point. A p-value of < 0.05 was regarded as significant and is printed in red. SD = Standard Deviation*

Neutrons – Heparin blood						
Dose in Gy	**Batch 1**	**Batch 2**	**Average**	**± 1 SD**	**CV**	**p-Value**
0	10.61	10.86	10.74	0.18	2	
0.25	22.27	18.61	20.44	2.59	13	0.117
0.5	25.20	26.33	25.77	0.80	3	0.018
1.0	25.80	33.58	29.69	5.50	19	0.129
2.0	41.01	40.40	40.71	0.43	1	0.002
4.0	46.67	51.57	49.12	3.46	7	0.040
Pos control	24.10	30.22	27.16	4.33	16	
Neg control	1.17	1.14	1.16	0.02	2	

6.5.2.1 *Inter-experimental variability*

Data displayed in **Table 6–6** to **Table 6–9** represent the results derived from scatter plots generated by flow cytometrical analysis. The percentage of FITC-positive cells was regarded as a measure of DNA fragmentation and was statistically analysed.

Three experiments were carried out in which lymphocytes isolated from EDTA- and heparin blood were exposed to gamma and neutron radiation. Inter-experimental variability was analysed by means of coefficient of variations (CV) calculated for each dose point. Inter-experimental variability in EDTA samples was consistently higher than in heparin blood with CVs ranging from 5% in cells exposed to 4.0 Gy neutrons to 38% in unirradiated samples. CVs for heparin blood ranged from 1% (2.0 Gy neutrons) to 19% (1 Gy gammas). Unirradiated samples produced CVs of 11% and 2% for gammas and neutrons respectively. The CV for the positive control was 16% in both blood preparations and could be considered as true measure of experimental variability for the Apo-Direct TUNEL Assay as positive cells were provided by the manufacturer and did not go through the same cell preparations as the other blood samples.

6.5.2.2 *Dose-response relationships*

Figure 6-12 displays the dose response relationships of lymphocytes in response to gamma- and neutron radiation. Lymphocytes were isolated from EDTA- and heparin blood and were analysed in different experiments. Data is displayed on the same graph for comparison of results. Control values (0 Gy) have not been subtracted from data points in order to compare background apoptosis in different cell

suspensions.

Lymphocytes responded to both radiation qualities in a dose-responsive manner with a maximum of almost 50% TUNEL-positive cells in the 4 Gy neutron-exposed heparin cells. EDTA cells did not respond to the same degree with a maximum of only 33% TUNEL-positive cells in the 4 Gy neutron-exposed sample.

With the exception of the EDTA gamma-exposed samples, all other cell preparations expressed an area of low-dose hypersensitivity to both radiation qualities between 0 (11%) and 1 Gy (32%) while the gamma-irradiated EDTA-samples reached a plateau at only 26% (4 Gy). Neutron-irradiated samples produced consistently higher TUNEL-positive cells (33.5 and 49.1% for EDTA and heparin blood respectively) while gamma-irradiated samples reached a maximum of 44% in the 4 Gy heparin sample.

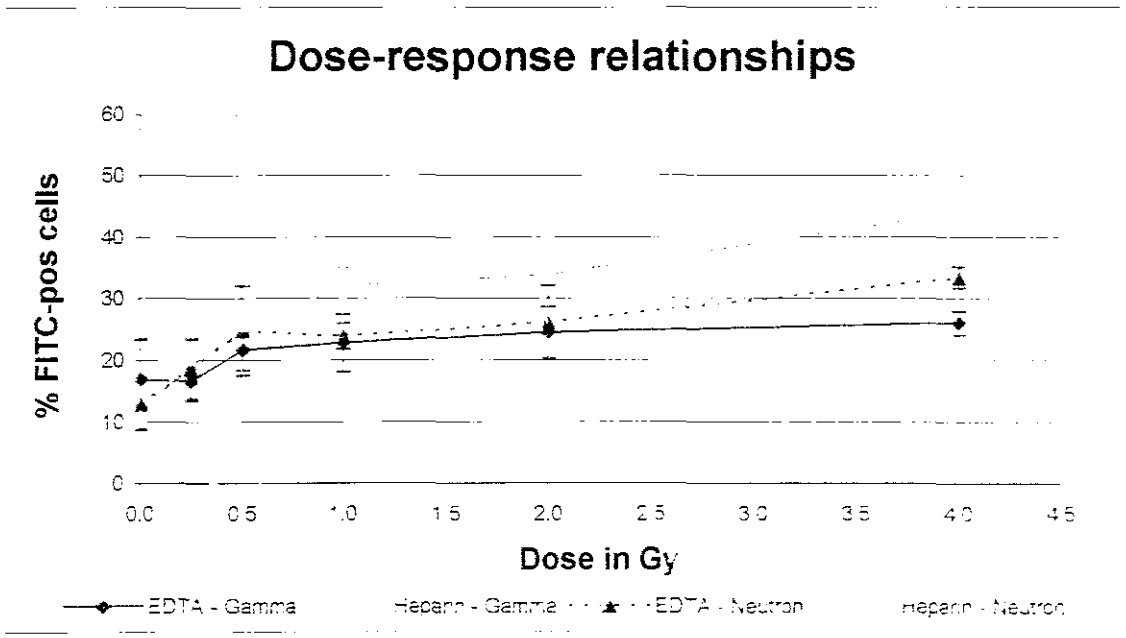

Figure 6-12: Dose response relationships of lymphocytes measured 48 hours after exposure to gamma- and neutron radiation. Lymphocytes were isolated from EDTA- and heparin blood respectively. Error bars indicate ± one standard deviation.

p-Values have been calculated to determine the significance of cell response to different qualities of radiation (**Table 6–10**) and between control cells and exposed cells (**Table 6–6** to **Table 6–9**). The dose-response curve for heparin blood was significantly different from the control samples with p-values ranging from 0.001 to 0.040 for gamma and neutron doses above 0.5 Gy. The dose-response curve for EDTA blood was only significantly different from control samples above 1 Gy neutrons with p-values ranging from 0.006 to 0.028.

The only dose point that showed a significant difference between the induction of DNA fragmentation by gammas and neutrons was the 4 Gy sample of EDTA blood

(p=0.008). Other p-values ranged between 0.242 and 0.828 (**Table 6–10**).

***Table 6–10**: p-Values indicating the significance of the difference in apoptotic response between gamma- and neutron irradiated cells. P-values were obtained by performing the TTEST function of Microsoft Excel 2000. P-values of < 0.05 was regarded as significant and is printed in red.*

Dose in Gy	EDTA Blood	Heparin Blood
0	0.426	0.593
0.25	0.595	0.828
0.5	0.560	0.285
1.0	0.744	0.634
2.0	0.700	0.242
4.0		0.264

6.5.3 Cellular morphology

The results of one experiment in which cell samples were exposed to 0 and 4 Gy gamma radiation are summarised in **Table 6–11** in graphically displayed in **Figure 6-13** and **Figure 6-14**. Cells were stained with ethidium bromide and analysed by fluorescence microscopy during which cells were classified into four cell types according to the criteria tabulated in **Table 6–1**. A minimum of 200 cells was randomly scored per dose point.

Table 6–11: Percentage of gamma-irradiated cells classified into each cell type after analysis with a fluorescence microscope. A minimum of 200 cells was scored per dose point.

	Dose in Gy	Normal cells	Condensed DNA	Apoptotic bodies	Cell remnants
24 hours	0	72	16	12	0
	4	65	16	16	3
48 hours	0	50	35	14	1
	4	32	34	32	3
72 hours	0	41	20	27	13
	4	8	13	13	66

The percentage of normal cells in control samples decreased from 72% at 24 hours to 41% at 72 hours post-irradiation. This decrease in normal cells was noticeable in irradiated samples with 65% at 24 hours and only 8% at 72 hours post-irradiation. Apoptotic cells in control samples increased up to 72 hours (12 to 27%) while apoptotic cells in irradiated samples reached a peak at 48 hours (32%) and decreased to 13% at 72 hours. No cell remnants were visible in unirradiated samples at 24 hours, but increased to 13% at 72 hours while irradiated cells produced 66% cell remnants at the same time interval.

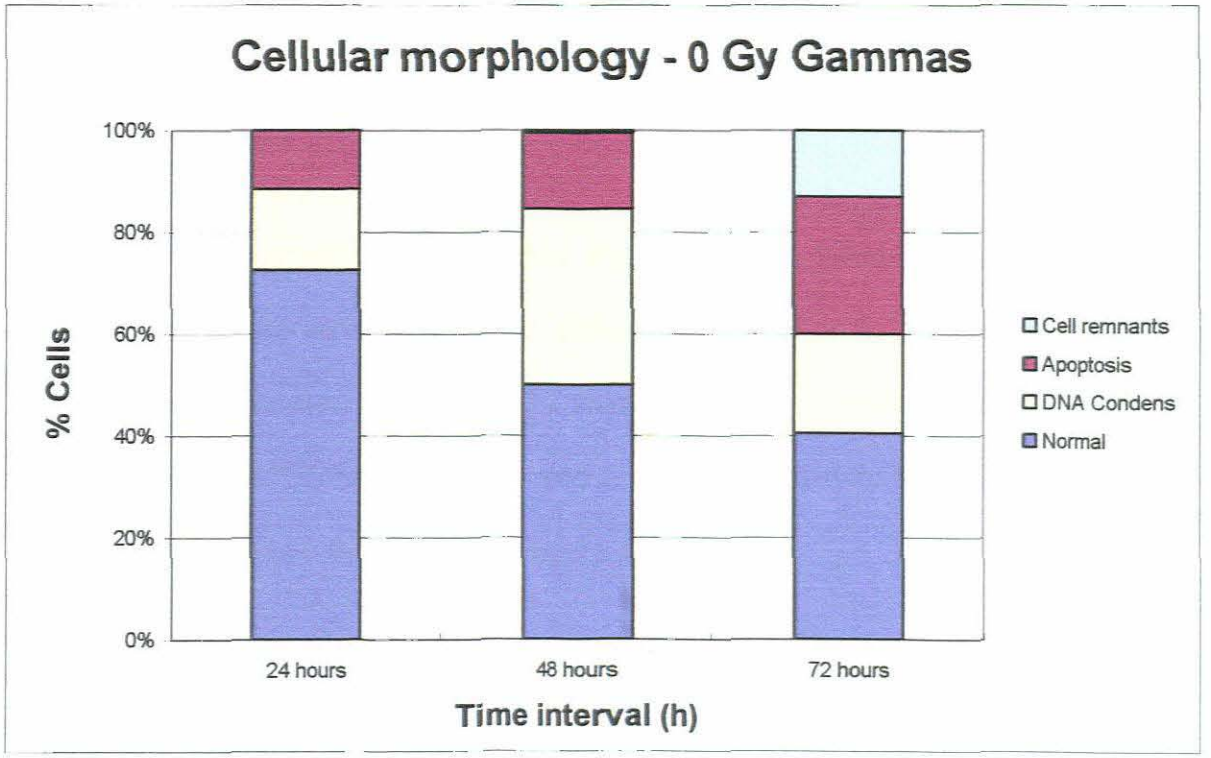

Figure 6-13: *Dose- and time-response of unexposed isolated lymphocytes in terms of microscopic cellular morphology.*

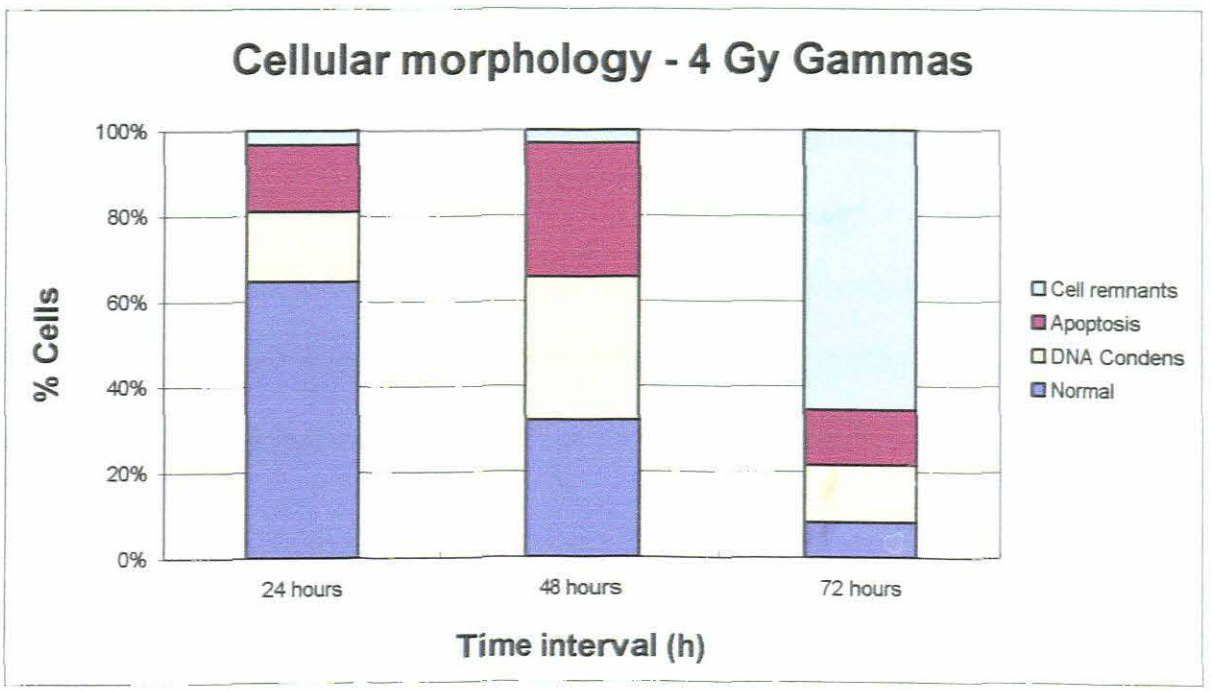

Figure 6-14: *Dose-and time-response of isolated lymphocytes exposed to 4 Gy gamma irradiation in terms of cellular morphology.*

6.6. Discussion

6.6.1 Caspase 3/7 activity

The induction of caspase 3/7 activity was measured in isolated lymphocytes by irradiating cell suspensions *in vitro* with different qualities and doses of radiation. Only a low concentration of caspase 3/7 was detected in irradiated cells after an incubation period of 36 hours and showed a hypersensitivity to high-LET radiation (neutrons) in the 0 to 0.5 Gy region (**Figure 6-8**).

Louagie *et al.* (1999) investigated caspase activity in irradiated lymphocytes and found only a low activation of caspase 3 after 5 Gy of gamma radiation. In addition, they found no cytochrome-c release at any time after irradiation, despite the presence of high amounts of mitochondrial cytochrome-c in total cell lysates. In contrast, staurosporin-treated lymphocytes showed a pronounced cytochrome-c release. Although the addition of caspase inhibitors decreased TUNEL-positive cells from 40% to 20%, Louagie *et al.* (1999) concluded that caspase-3-like proteases had only a limited involvement in the apoptotic process of lymphocytes after radiation. From these results it was evident that radiation-exposed lymphocytes follow another apoptosis pathway than cytochrome-c release and caspase activation.

Masdehors *et al.* (2000) shed more light on this observation with their investigation of the ubiquitin-dependent proteolytic pathway of apoptosis in irradiated lymphocytes. They found that poly ADP-ribose polymerase (PARP), usually cleaved by caspases, was regulated by a **caspase-independent** "N-end rule" pathway. By using dipeptide competitors for the NH_2-terminal amino acids, they proved that only substrates of

ubiquitination with the same basic NH_2-terminal amino acids are involved in lymphocyte apoptosis. Wójcik (1999) confirmed these findings by stating: "Ubiquitin antisense inhibition considerably diminished the proportion of apoptotic lymphocytes after γ-irradiation, which clearly implied an active role for this system in cell death". Delic *et al.* (1993) investigated whether ubiquitin could be associated with apoptotic cells by means of anti-ubiquitin immunostaining and showed that ubiquitin was increased only in apoptotic cells and not all irradiated cells. They suggested that the ubiquitin gene is one of the genes that are activated during apoptosis and that ubiquitination of nuclear proteins might be involved in chromatin disorganisation and oligonucleosomal fragmentation.

The results of this study clearly show that caspases are not significantly activated in irradiated lymphocytes; the findings of this study are thus in agreement with Wójcik *et al.* (1999) and Delic *et al.* (1993) that a ubiquitin-dependent proteolytic pathway may well regulate the cleavage of PARP and subsequent DNA degradation in radiation-exposed lymphocytes. From the evidence of the literature and the results of this study, a possible sequence of events is proposed in **Figure 6-15**, although it is not suggested that the exact mechanism and time frame of events are fully understood. The ubiquitin-pathway (printed in green) is given in relation to the well known receptor- and mitochondria-mediated pathways.

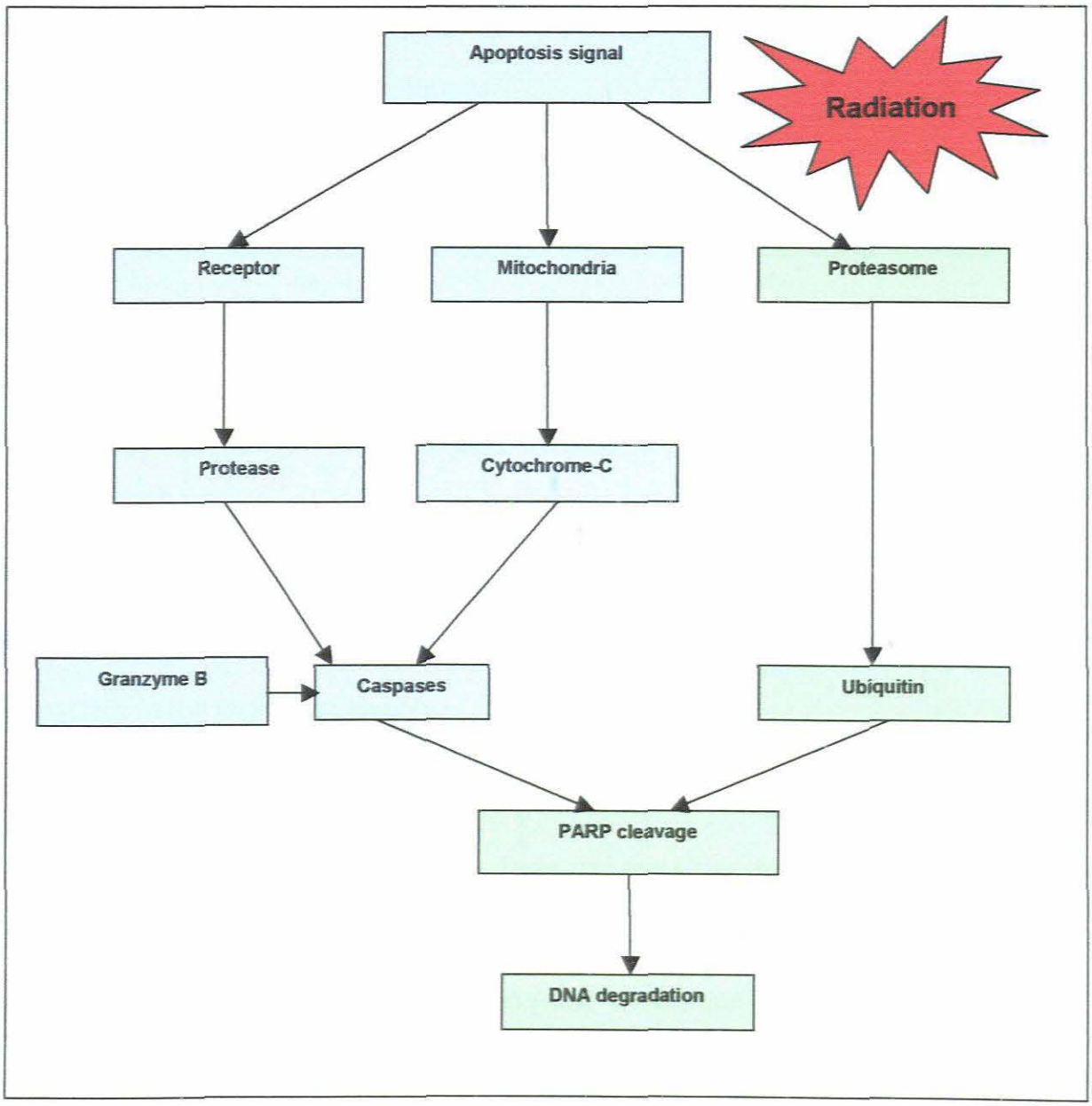

***Figure 6-15**: Schematic representation of the major pathways involved in apoptosis. The ubiquitin-pathway involved in radiation-induced apoptosis in lymphocytes is given in relation to the classical pathways involving death receptors and mitochondria.*

The observation of low-dose hypersensitivity of lymphocytes to high-LET radiation may be as a result of the bystander effect as it has been shown that radiation

damage could be induced in cells not traversed by radiation (Mothersill and Seymour 2003). Although the actual mechanism is still unclear, cellular communication seems to play a key role in this phenomenon.

Although caspase activity was low in exposed cells, it was clear that caspase activity increased as the radiation dose increased. Dose-response curves for gamma- and neutron-exposed lymphocytes did not differ significantly at any dose point. It is surprising however that the neutron-exposed cells showed lower caspase activity above 1 Gy than gamma-exposed cells. This could be explained by the fact that low-LET radiation produces mainly indirect DNA damage, resulting in the production of free radicals in the cell, while high-LET radiation produces more direct DNA damage. Being active in the cellular medium, free radicals could initiate caspase activation, especially in the high-dose region.

The aim of this study was to validate the Apo-ONE ^{TM} Homogeneous Caspase-3/7 Assay for use as biological dosimeter. From the results of the study it is clear that this assay is not suitable as biological dosimeter as only low levels of caspase 3/7 activity were present in irradiated lymphocytes. In addition it was shown that irradiated lymphocytes do not activate caspases as major route of apoptosis; this would mean that no assay measuring caspase activity in lymphocytes would be suitable as biological indicator of radiation damage.

6.6.2 DNA Fragmentation

The presence of fragmented DNA in lymphocytes after exposure to different qualities and doses of radiation was investigated by employing the Apo-Direct TUNEL Assay.

Samples were incubated for 48 hours after which it were analysed by flow cytometry.

The decision to use heparinised blood in addition to EDTA-blood was taken after low levels of DNA fragmentation was observed in the initial experiments on EDTA blood and some researchers used heparinised blood in their studies (Crompton *et al*, 1999; Louagie *et al*, 1999). Favourable results obtained from the positive and negative control cells supplied by the manufacturer confirmed a sound methodology. In addition, the incubation period for FITC-labelling was changed from overnight incubation on a shaker to 60 min in a 37°C incubator to rule out the possibility that the extended period of shaking could have damaged the cells.

These changes proved to be successful. Although two experiments could not be regarded as a true measure of inter-experimental variability the results obtained with heparin blood were in agreement with those from other studies performed on irradiated lymphocytes (Masdehors *et al.*, 2000; Louagie *et al.*, 1999). Results obtained from EDTA-blood were not considered in the discussion.

Dose response curves for gamma- and neutron-exposed cells were not significantly different at any dose point when p-values are taken into consideration (**Table 6–10**). The two curves followed the same slope up to 1 Gy after which the gamma curve reached a slight plateau between 1 and 2 Gy and slowly increased to 4 Gy. The neutron curve followed a constant increase to 4 Gy with 11% more TUNEL-positive cells at 4 Gy (49% for neutrons and 44% for gammas).

The Apo-Direct TUNEL Assay could be useful as biological dosimeter once it has been standardised and a standard curve established from the population to be monitored. It was sensitive enough to detect DNA fragmentation in

lymphocytes below 0.5 Gy of gamma- and neutron radiation although it could not distinguish between the two radiation qualities.

6.6.3 Cellular morphology

Cellular morphology is the hallmark of apoptosis and by including one experiment in which cells were exposed to 4 Gy gamma radiation, the typical morphological features of irradiated cells were analysed after incubation periods ranging from 24 to 72 hours.

As expected, most of the control cells appeared normal after 24 hours of incubation (73%) although it was clear that 4 Gy of gamma radiation had an adverse effect on lymphocytes at 24 hours after irradiation (65% normal cells). After 72 hours of incubation though, only 41% and 8% cells displayed normal morphology in control and exposed cells respectively. The largest fraction of apoptotic cells in the control sample appeared after 72 hours, while a peak of apoptotic cells in the irradiated samples was detected after 48 hours. This is not surprising as highly damaged cells in irradiated samples disintegrate and are only visible as cell remnants at 72 hours (66%).

Cellular morphology was not validated for use as indicator of radiation damage, but it confirmed the apoptotic response of lymphocytes to radiation.

6.7. Conclusion

From the three apoptosis assays evaluated in this study only the Apo-Direct TUNEL Assay could be considered as biological dosimeter. Much was learnt from the Apo-ONE ™ Homogeneous Caspase-3/7 Assay, but the observation that lymphocytes do not follow the caspase proteolytic pathway of apoptosis rules out the possibility of using this assay as biological indicator of radiation damage.

Neither the Apo-ONE ™ Homogeneous Caspase-3/7 Assay nor the Apo-Direct TUNEL Assay displayed a significant difference between the dose-response relationships of gamma- and neutron radiation although distinctly different slopes were visible at higher doses. Further experiments of one assay would be necessary to confirm this tendency. Neither of these assays would thus be suitable for the discrimination of DNA damage induced by different radiation qualities.

The difference between control values and other dose points were significantly different above 0.5 Gy for the Apo-Direct assay but was not significant in any of the dose points for the Apo-One Assay.

Crompton *et al.* (1999) proposed a rapid assay of intrinsic radiosensitivity based on apoptosis in human CD4 and CD8 T-lymphocytes. The leukocyte apoptosis assay (LAA) provides a rapid screen for genetically hypersensitive cancer patients identified to receive radiation therapy. The Apo-Direct TUNEL Assay could fulfil the same role as predictor of radiosensitivity although it would be more expensive than LAA. It provides the advantage of measuring multiple features of apoptotis such as cell size and DNA fragmentation where the LAA only relies on changes in cell size and

granularity.

Before implementing the Apo-Direct TUNEL Assay as predictor of intrinsic radiosensitivity, it would be necessary to establish a standard curve from the population to be analysed by irradiating lymphocytes with different doses of gamma radiation and determining the percentage of TUNEL-positive cells in the sample after different incubation periods. Should the radiation doses be expanded to cover doses from 0.1 to 8 Gy, the same standard curve could be utilised as predictor of *radiosensitivity and biological dosimeter.*

Chapter 7

Discussion and Conclusion

In the past, radiobiological research was largely focused on the effects of high doses of radiation. Recent developments in molecular biology and genetics have provided new insights on the effects of low doses of radiation on different biological systems and as a result new techniques have been developed to measure these effects.

Some of these novel techniques have been included in this study, i.e. the spectrofluorometric measurement of caspases and the detection of fragmented DNA by flow cytometric analysis. With the inclusion of the more established comet and micronucleus assays, a range of biological endpoints could be analysed for the detection of radiation-induced DNA damage in peripheral lymphocytes.

In addition to the more available low-LET gamma radiation beams, a high-energy neutron beam was used as a second radiation quality to provide the added advantage of high-LET radiation. This approach added a unique flavour to the study, as radiobiological data on low-dose high-energy neutrons are not freely available.

The comet assay was performed on different cell preparations: whole blood proved to be the more sensitive indicator of radiation-induced DNA damage. Lymphocyte isolation added a certain measure of uncertainty to the assay as an agent other than radiation induced the formation of highly damaged cells and hedgehogs in unirradiated cells. In contrast to the deductions from other research groups (Roser *et al*, 2001; Lankoff *et al*, 2004), the results of this study proved that hedgehogs are not

induced as a result of apoptosis. As the literature is unclear on the influence if the isolation procedure, it would be useful to investigate this phenomenon before an attempt is made to use the comet assay as biomarker of radiation damage.

The alkaline comet assay is sensitive and reliable to detect DNA damage in lymphocytes induced by gamma- and neutron doses above 1 Gy. The difference in the mechanism of DNA breakage between low- and high-LET radiation was detected with the observation that neutrons induced less DNA fragments at higher doses than gammas. Due to the high density of particles produced by neutrons, more energy was deposited in the same cell with less fragmented DNA to migrate away from the nucleus, resulting in lower tail factors.

The CBMN assay confirmed the difference in energy deposition between low- and high-LET radiations. Damage induced by radiation doses above 0.5 Gy were detected in a dose-responsive manner although it seemed as if the quality of PHA could induce a positive correlation with the NDI and micronucleus frequency. As only one experiment was performed with each lot of PHA, it was not possible to investigate this observation in depth, but it is a tendency that needs to be clarified in the future.

Although not in large quantities, caspase 3/7 showed a hypersensitivity to high-LET doses below 0.5 Gy. This tendency could possibly be explained by the bystander phenomenon. The principle is based on cellular communications in which irradiated cells transfer a message to unirradiated cells that they were hit by radiation, eliciting the same response in neighbouring cells. This low-dose hypersensitivity was only observed in neutron-irradiated cells.

The Apo-Direct TUNEL Assay detected a high percentage of TUNEL-positive cells in a clear dose-responsive manner and was extremely sensitive to low doses of gamma- and neutron radiation. This assay has the potential to serve as biological indicator of low-doses of radiation damage as well as predictor of radiosensitivity. The Leukocyte Apoptosis Assay measures apoptotic features in irradiated cells and has been proved to be a good predictor of radiosensitivity in radiotherapy patients. The Apo-Direct Assay should be even more sensitive in such a role, as more features of apoptosis such as DNA fragmentation and changes in cells size are measured. Although the cost implications could be a barrier the possibility of employing this technique in radiotherapy centres should be investigated.

The detection of very low levels of caspase 3/7 in irradiated lymphocytes as measured by the Apo-ONE Homogeneous Caspase 3/7 Assay was somewhat surprising, but it has recently been elucidated that irradiated lymphocytes do not follow the classical pathway of apoptosis in which caspases induce DNA fragmentation, but rather the more unknown proteasome/ubiquitin route (Masdehors *et al*, 2000; Delic *et al*, 1993). However, both pathways induce the cleavage of PARP and subsequent DNA fragmentation as was evident in this study. The activation of ubiquitin in irradiated lymphocytes needs to be investigated further by means of immunostaining, polyacrylamide gel electrophoresis, Western blotting, or flow cytometry.

Various endpoints have been validated and discussed as biological indicators of low-dose radiation damage. Of these, the Apo-Direct TUNEL Assay is the only assay sensitive enough to detect the effect of low- and high-LET radiation doses below 0.5 Gy in lymphocytes. This assay has the potential to be standardized as a biological

indicator of low-level radiation damage as well as a predictor of intrinsic radiosensitivity.

References

ALBERTINI RJ, 1999, Biomarker responses in human populations: toward a worldwide map, *Mutation Research,* 428, 217-226.

ANDERSON D; KARAKAYA, AE; SRÁM RJ, 2000, Human monitoring after environmental and occupational exposure to chemical and physical agents. NATO science series, Series A, *Life Sciences*, 1387-6687, vol.313, IOS Press, Amsterdam

BACSO Z; EVERSON RB; ELIASON JF, 2000, The DNA of Annexin V-binding Apoptotic cells is highly Fragmented, *Cancer Research,* 60, 4623-4628

BALLARINI F; BIAGGI M; OTTOLENGHI A; SAPORA C, 2002, Cellular communication and bystander effects: a critical review for modelling low-dose radiation action, *Mutation Research,* 501, 1-12

BANÁTH JP; FUSHIKI M; OLIVE PL, 1998, Rejoining of DNA single- and double-strand breaks in human white blood cells exposed to ionising radiation, *Int. J. Rad. Biol.,* 73(6), 649-660

BARBER JBP; WEST CML; KILTIE AE; Roberts SA; Scott D, 2000, Detection of individual differences in radiation-induced apoptosis of peripheral blood lymphocytes in normal individuals, ataxia telangiectasia homozygotes and heterozygotes, and breast cancer patients after radiotherapy, *Radiation Research,* 153, 570-578

BEBB DG; WARRINGTON PJ; DE JONG G; YU Z; MOFFAT JA; SKOV K; SPACEY S; GELMON K; GLICKMAN BW, 2001, Radiation induced apoptosis in ataxia telangiectasia homozygote, heterozygote and normal cells, *Mutation Research,* 476, 13-20

BERGQVIST M; BRATSTRÖM D; STALBERG M; VAGHEF H; BRODIN O; HELLMAN B, 1998, Evaluation of radiation-induced DNA damage and DNA repair in human lung cancer cell lines with different radiosensitivity using alkaline and neutral single cell gel electrophoresis, *Cancer Letters,* 133(1), 9-18

CAMPAROTO M L; RAMALHO A T; NATARAJAN A T; CURADO MP; SAKAMOTO-HOJO E T, 2003, Translocation analysis by the FISH-painting method for retrospective

dose reconstruction in individuals exposed to ionising radiation 10 years after exposure, *Mutation Research,* 530, 1-7

CARERE A; ANDREOLI C; GALATI R; LEOPARDI P; MARCON F; ROSATI MV; ROSSI S; TOMEI F; VERDINA A; ZIJNO A; CREBELLI R, 2002, Biomonitoring of exposure to urban air pollutants: analysis of sister chromatid exchanges and DNA lesions in peripheral lymphocytes of traffic policemen, *Mutation Research,* 518, 215-224

CHANG WP; TSAI M; HWANG J; LIN Y; HSIEH WA; SHAO-YI H, 1999, Follow-up in the micronucleus frequencies and its subsets in human populations with chronic low-dose gamma irradiation exposure, *Mutation Research,* 428, 99-105

CHOUCROUN P; GILLET D; DORABGE G; SAWICKI B; DEWITTE JD, 2001, Comet assay and early apoptosis, *Mutation Research,* 478, 89-96

COLLINS A; AI-GAO M; DUTHIE SJ, 1995, The kinetics of repair of oxidative DNA damage (strand breaks and oxidised pyrimidines) in human cells, *Mutation Research,* 336, 69-77

COLLINS A; DOBSON VL; DUSINSKA M; KENNEDY G; STETINA R, 1997, The comet assay: what can it really tell us?, *Mutation Research,* 183-193

CORTESE J, 2001, Death Watch II: Caspases and apoptosis, *The Scientist,* 15(13), 24

CROMPTON NEA; MIRALBELL R; RUTZ H-P; ERSOY F; SANAL O; WELLMANN D; BIERI S; COUCKE PA; SHI Y-Q; EMERY GC; BLATTMANN H; OZSAHIN M, 1999, Altered apoptotic profiles in irradiated patients with increased toxicity, *Int. J. Radiation Oncology Biol, Phys,* 45(3), 707-714

CUNNINGHAM R; ILARI O; ISHIGURO H; METIVIER H; PARETZKE H; PRETRE S; SUGIER A; SUSANNA A, 1994, Radiation protection today and tomorrow - An assessment of the present status and future perspectives of radiation protection, [Online]. Available: *http://www.nea.fr/html/rp/reports/1004/rp.html.* [2003, July 28]

DAINAIK N, 2002, Hematological consequences of exposure to ionising radiation, *Experimental Hematology,* 30, 513-528

DE BOECK M; TOUIL N; DE VISSCHER G; AKA VANDE P; KIRSCH-VOLDERS M, 2000, Validation and implementation of an internal standard in comet assay analysis, *Mutation Research,* 469, 181-197

DELIC J; MORANGE M; MAGDELENAT H, 1993, Ubiquitin pathway involvement in human lymphocyte γ-irradiation-induced apoptosis, *Molecular and Cellular Biology*, Aug. 1993, 4875-4883

FAJARDO LF; BERTHRONG M; ANDERSON RE, 2001, *Radiation Pathology*, Oxford University Press, New York

FENECH M; AITKEN C; RINALDI J, 1998, Folate, vitamin B12, homocysteine status and DNA damage in young Australian adults, *Carcinogenesis*, Vol. No 7, 1163-1171

FENECH M, 2000, The *in vitro* micronucleus technique, *Mutation Research,* 455, 81-95

FENECH M; CHANG WP; KIRSCH-VOLDERS M; HOLLAND N; BONASSI S; ZEIGER E, 2003a, HUMN project: detailed description of the scoring criteria for the cytokinesis-block micronucleus assay using isolated lymphocyte cultures, *Mutation Research,* 534, 65-75

FENECH M; *et al*, 2003b, Intra- and inter-laboratory variation in the scoring of micronuclei and nucleoplasmic bridges in binucleated human lymphocytes Results of an international slide-scoring exercise by the HUMN project, *Mutation Research,* 534, 45-64

FENECH M; HOLLAND N; CHANG WP; ZEIGER E; BONASSI S, 1999, The HUman MicroNucleus Project - An international collaborative study on the use of the micronucleus technique for measuring DNA damage in humans, *Mutation Research,* 428, 271-283

FENECH M; MORLEY AA, 1985, Measurement of micronuclei in lymphocytes, *Mutation Research,* 147, 29-36

FLOYD DN; CASSONI AM, 1994, Intrinsic radiosensitivity of adult and cord blood lymphocytes as determined by the micronucleus assay, *European Journal of Cancer,* 30A(5), 615-620

FOWLER JF, 1981, Nuclear particles in cancer treatment, *Medical Physics Handbooks 8*, Adam Hilger Ltd., Bristol.

GIOVANNELLI L; PITOZZI V; RIOLO S; DOLARA P, 2003, Measurement of DNA breaks and oxidative damage in polymorphonuclear and mononuclear white blood cells: a novel approach using the comet assay, *Mutation Research*, 538, 71-80

GRAY JW; MOORE D; PIPER J; JENSEN R. 1995, Molecular cytogenetic approaches to the development of biomarkers, *Biomarkers and Occupational Health: Progress and Perspectives*, 194-214

GUITIÉRREZ S; CARBONELL E; GALOFRÉ P; CREUS A; MARCOS R, 1999, Cytogenetic damage after 131-iodine treatment for hyperthyroidism and thyroid cancer, *European Journal of Nuclear Medicine,* 26(12), 1589-1596

GUTIERREZ S; CARBONELL E; GALOFRE P; CREUS A; MARCOS R, 1998, The alkaline single cell gel electrophoresis (SCGE) assay applied to the analysis of radiation-induced DNA damage in thyroid cancer patients treated with 131I, *Mutation Research,* 413, 111-119

HALL EJ, 2000, *Radiobiology for the Radiologist,* 5th Edition, Philadelphia: Lippincott Williams & Wilkins

HE JL; CHEN WL; JIN LF; JIN HY, 2000, Comparative evaluation of the *in vitro* micronucleus test and the comet assay for the detection of genotoxic effects of X-ray radiation, *Mutation Research,* 469, 223-231

HENDRY JH; LORD BI, 1995, Editors of Radiation Toxicology. Bone Marrow and Leukaemia, Taylor and Francis, London

HILL MA, 1999, Radiation damage to DNA: The importance of track structure, *Radiation Measurements*, 31, 15-23

HODGSON KO AND COMMITTEE, No date, Research program Plan: Biological effects of low dose and dose rate radiation, *[Online]. Available: http://lowdose.tricity.wsu.edu/pubs/progplan.html [2004, April 7]*

ICRP 1991, ICRP Publication 60: The 1990 Recommendations of the International Commission on Radiological Protection, Pergamon Press, Oxford

ICRP 1997, ICRP Publication 75: General principles for the radiation protection of workers, Pergamon Press, Oxford

IVANCSITS S; DIEM E; SCHAFFER A; RÜDIGER HW; 2002a, Vanadate induces DNA strand breaks in cultured human fibroblasts at doses relevant to occupational exposure, *Mutation Research,* 519, 25-35

IVANCSITS S; DIEM E; PILGER A; RÜDIGER HW; JAHN O, 2002b, Induction of DNA strand breaks by intermittent exposure to extremely-low-frequency electromagnetic fields in human diploid fibroblasts, *Mutation Research,* 519, 1-13

JONES LA; CLEGG S; BUSH C; MCMILLAN C; PEACOCK JH, 1994, Relationship between chromosome aberrations, micronuclei and cell kill in two human tumour cell lines of widely differing radiosensitivity, *Int. J. Rad. Biol.,* 66(5), 639-642

JONES LA; SCOTT D; COWAN R; ROBERTS SA, 1995, Abnormal radiosensitivity of lymphocytes from breast cancer patients with excessive normal tissue damage after radiotherapy: chromosome aberrations after low dose-rate irradiation, *Int. J. Rad. Biol.,* 67,5, 519-528

KIRSCH-VOLDERS M; SOFUNI T; AARDEMA M; ALBERTINI S; EASTMOND D; FENECH M; ISHIDATE M JR; KIRCHNER S; LORGE E; MORITA T; NORPPA H; SURRALLÉS J; VANHAUWAERT A; WAKATA A, 2003, Report from the in vitro micronucleus assay working group, *Mutation Research,* 540, 153-163

KRYSCIO A; MÜLLER W-Ü; WOJCIK A; KOTSCHY N; GROBELNY S; STREFFER C, 2001, A cytogenetic analysis of the long-term effect of uranium mining on peripheral lymphocytes using the micronucleus-centromere assay, *Int. J. Rad. Biol.,* 77(11), 1087-1093

KUMAR V; COTRAN RS; ROBBINS SL, 1997, *Basic Pathology*, 6th Edition, W B Saunders Company, Philadelphia

LAFFON B; PÁSARO E; MÉNDES J, 2002, Evaluation of genotoxic effects in a group of workers exposed to low levels of styrene, *Toxicology,* 171, 175-186

LANKOFF A; KRZOWSKI L; GLAB J; BANASIK A; LISOWSKA H; KUSZEWSKI T; GÓZDZ S; WÓJCIK, 2004, DNA Damage and repair in human peripheral blood lymphocytes following treatment with microcystin-LR, *Mutation Research*, 559, 131-142.

LEBAILLY P; VIGREUX C; GODARD T; SICHEL F; BAR E; LETALAËR JY; HENRY-AMAR M; GAUDUCHON P, 1997, Assessment of DNA damage induced *in vitro* by

etoposide and two fungicides (carbendazim and chlorothanolil) in human lymphocytes with the comet assay, *Mutation Research,* 375, 205-217

LEWIN B, 2000, *Genes VII,* Oxford University Press, USA

LOONEY SW, 2002, Statistical methods for assessing biomarkers, *Methods in Molecular Biology: Statistical methods, Vol 184,* 81-110

LOUAGIE H; PHILIPPE J; VRAL A; CORNELISSEN M; THIERENS H; DE RIDDER L, 1998, Induction of micronuclei and apoptosis in natural killer cells compared to T Lymphocytes after gamma-irradiation, *Int. J. Rad. Biol.,* 73 (2), 179-185

LOUAGIE H; SCHOTTE P; VRAL A; CORNELISSEN M; THIERNES H; BEYAERT R; DE RIDDER L; PHILIPPE J, 1999, Apoptosis induced by γ- irradiation in peripheral blood mononuclear cells is not mediated by cytochrome-c release and only partially involves caspase-3-like proteases, *Cell Biology International, 23 (9), 611-617*

MALCOLMSON AM; DAVIES G; HANSON JA; DEELEY JOT; GAFFNEY CC; MCGREGOR AD; KERBY IJ, 1995, Determination of radiation-induced damage in lymphocytes using the micronucleus and microgel electrophoresis "comet" assays, *European Journal of Cancer,* 31A(13/14), 2320-2323

MASDEHORS P; GLAISNER S; MARCIOROWSKI Z; MAGDELENAT H; DELIC J, 2000, Ubiquitin-dependent protein processing controls radiation-induced apoptosis through the N-end rule pathway, *Experimental cell Research,* 257, 48-57

MEDICAL RADIATION PHYSICS, No date, Radiobiological effects and adaptive response (Hormesis), [Online], Available: *http://www.medical-physics.com/hormesis.htm*, [2003, July 31]

MENDIOLA-CRUZ MT; MORALES-RAMIREZ P, 1999, Repair kinetics of gamma-ray induced DNA damage determined by the single cell gel electrophoresis assay in murine leukocytes *in vivo, Mutation Research,* 433, 45-52

MOTHERSILL C; SEYMOUR C, 2003, Low-dose radiation effects: Experimental hematology and the changing paradigm, *Experimental Hematology,* 31, 437-445

MUSTONEN R; BOUVIER G; WOLBER G; STÖHR M; PESCHKE P; BARTSCH H, 1999, A comparison of gamma and neutron irradiation on Raji cells: effects on DNA

damage, repair, cell cycle distribution and lethality, *Mutation Research,* 429, 169-179

OLIVE PL, 1999, DNA damage and repair in individual cells: applications of the comet assay in radiobiology, *Int. J. Rad. Biol.,* 75(4), 395-405

ÖSTLING O; JOHANSON KJ, 1984, Micro-electrophoretic study of radiation-induced DNA damage in individual mammalian cells, *Biochemical and Biophysical Research Communications,* 123(1), 291-298

PIZZARELLO DJ; WITCOFSKI RL, 1982, *Medical Radiation Biology,* 2nd Edition, Lea & Febiger: Philadelphia

PROMEGA CORPORATION, 2002, Apo-ONE™ Homogeneous Caspase-3/7 Assay, Technical Bulletin, 295, 1-12

RIGAUD O; MOUSTACCHI E, 1996, Radio-adaptation for gene mutation and the possible molecular mechanism of the adaptive response, *Mutation Research,* 358, 127-134

ROJAS E; LOPEZ MC; VALVERDE M, 1999, Single cell gel electrophoresis assay: methodology and applications, *Journal of Chromatography B,* 722, 225-254

ROSER S; POOL-ZOBEL B-L; RECHKEMMER G. 2001, Contribution of apoptosis to responses in the comet assay, *Mutation Research,* 497, 169-175

ROSS GM, 1999, Induction of cell death by radiotherapy, *Endocrine-related Cancer,* 6, 41-44

SAMARIN A, 2001, Absorption and biological effects of ionising radiation, [Online]. Available: *http://www.atse.org.au/publications/occasional/occ-samarin.htm.* [2003, December 3]

SARI-MINODIER I; ORSIERE T; BELLON L; POMPILI J; SAPIN C; BOTTA A, 2002, Cytogenetic monitoring of industrial radiographers using the micronucleus assay, *Mutation Research,* 521, 37-46

SCHIMMER AD; HEDLEY DW; PENN LZ; MINDEN MD, 2001, Receptor- and mitochondrial-mediated apoptosis in acute leukemia: a translational view, *Blood,* 98, 3541-3553

SCHMITZ A; BAYER J; DÉCHAMPS N; THOMAS G, 2003, Intrinsic susceptibility to radiation-induced apoptosis of human lymphocyte subpopulations, *Int. J. Radiation Oncology Biol. Phys.*, 57(3), 769-778

SCHREUDER AN, 1992, Characterisation of the NAC's p(66)/Be(40) neutron therapy beam in terms of primary and scattered dose components, *M.Sc Thesis, University of Stellenbosch,* 13-14

SHERIDAN M T; WEST CML, 2001, Ability to undergo apoptosis does not correlate with the intrinsic radiosensitivity (SF2) of human cervix tumour cell lines, *Int. J. Radiation Oncology Biol, Phys,* 50(2), 503-509

SHINOMIYA N; KUNO Y; YAMAMOTO F; FUKASAWA M; OKUMURA A; UEFUJI M; ROKUTANDA M, 2000, Different mechanisms between premitotic apoptosis and post mitotic apoptosis in x-irradiated U937 cells, *Int. J. Radiation Oncology Biol, Phys,* 47(3), 767-777

SINGH NP; MCCOY MT; TICE RR; SCHNEIDER EL, 1988, A simple technique for quantitation of low levels of DNA damage in individual cells, *Experimental cell research,* 175, 184-191

SINGH NP; STEPHENS RE, 1997, Microgel electrophoresis: Sensitivity, mechanisms. and DNA electro stretching, *Mutation Research,* 383

SLABBERT JP, 2004, Personal communication.

SMOLEWSI P; GRABAREK J; HALICKA HD; DARZYNKIEWICZ Z, 2002a, Assay of caspase activation *in situ* combined with probing plasma membrane integrity to detect three distinct stages of apoptosis, *Journal of Immunological Methods,* 265, 111-121

SMOLEWSKI P; GRABAREK J; LEE JG; JOHNSON GL; DARZYNKIEWICZ Z, 2002b, Kinetics of HL-60 cell entry to apoptosis during treatment with TNF-alpha or Camptothecin assayed by the stathmo-apoptosis method, *Cytometry,* 47, 143-149

SPEIT G; TRENZ K; SCHÜTZ P; ROTHFUSS A; MERK O, 1999. The influence of temperature during alkaline treatment and electrophoresis on results obtained with the comet assay, *Toxicology Letters,* 110, 73-78

STEEL G, 2002, *Basic Clinical Radiobiology,* 3rd Edition, Arnold: London

TANNOCK IF; HILL RP, 1998, *The Basic Science of Oncology*, 3rd Edition, The McGraw-Hill Companies, New York

TESTARD I; SABATIER L, 2000, Assessment of DNA damage induced by high-LET ions in human lymphocytes using the comet assay, *Mutation Research,* 448, 105-115

THIERENS H; VRAL A; BARBÉ M; AOUSALAH B; DE RIDDER L, 1999, A cytogenetic study of nuclear power plant workers using the micronucleus-centromere assay, *Mutation Research,* 445, 105-111

THIERENS H; VRAL A; MORTHIER R; AOUSALAH B; DE RIDDER L, 2000, Cytogenetic monitoring of hospital workers using the micronucleus centromere assay, *Mutagenesis,* 15(3), 245-249

TICE RR; VASQUEZ M, 1999, ILS: Protocol for the application of the pH >13 alkaline single cell (SCG) assay to the detection of DNA damage in mammalian cells, [Online]. Available: *http:// www.cometassay.de/Methode/lab-protocol.html.* [2003, August 30].

TOUIL N; AKA PV; BUCHET J-P; THIERENS H; KIRSCH-VOLDERS M, 2002, Assessment of genotoxic effects related to chronic low level exposure to ionising radiation using biomarkers for DNA damage and repair, *Mutagenesis,* 17(3), 223-232

TOUIL N; ELHAJOUJI A; THIERENS H; KIRSCH-VOLDERS M, 2000, Analysis of chromosome loss and chromosome segregation in cytokinesis-blocked human lymphocytes: non-disjunction is the prevalent mistake in chromosome segregation produced by low dose exposure to ionising radiation, *Mutagenesis,* 15(1), 1-7

TRAVIS EL, 1989, *Medical Radiobiology,* 2nd Edition, Year Book Medical Publishers: Chicago

TUBIANA M; DUTREIX J; WAMBERSIE A, 1990. *Introduction to Radiobiology*, Taylor & Francis, London,

TURAI I, 2000, The IAEA's co-ordinated research project on biodosimetry, 1998-2000, *Applied Radiation and Isotopes,* 52, 1113-1116

UNDEGER U; ZORLU F; BASARAN N, 1999, Use of the alkaline comet assay to monitor DNA damage in technicians exposed to low-dose radiation, 41(8), 693-698

VAN ROOYEN, TJ, 2002, The science of Radiation Protection. iThemba LABS

VIJAYALAXMI; LEAL BZ; DEAHL TS; MELTZ ML, 1995, Variability in adaptive response to low dose radiation in human blood lymphocytes: consistent results from chromosome aberrations and micronuclei, *Mutation Research,* 348, 45-50

VRAL A; CORNELISSEN M; THIERENS H; LOUAGIE H; PHILIPPE J; STRIJKMANS K; DE RIDDER L, 1998, Apoptosis induced by fast neutrons versus 60 Co γ-rays in human peripheral blood lymphocytes, *Int. J. Radiat. Biol.*, 73 (3), 289-295

VRAL A; THIERENS H; BAEYENS A; DE RIDDER L, 2002, The micronucleus and G2-phase assays for human blood lymphocytes as biomarkers of individual sensitivity to ionizing radiation: Limitations imposed by intra-individual variability, *Radiation Research,* 157, 472-477

WASHINGTON STATE UNIVERSITY TRI-CITIES, No date, About low dose radiobiology, *[Online]. Available: http://lowdose.tricity.wsu.edu/radiobio_main.html [2004, April 30]*

WIDEL M; JEDRUS S; LUKASZCZYK B; RACZEK-ZWIERZYCKA K; SWIERNIAK A, 2003, Radiation-induced micronucleus frequency in peripheral blood lymphocytes is correlated with normal tissue damage in patients with cervical carcinoma undergoing radiotherapy, *Radiation Research,* 159, 713-721

WILKINS RC; KUTZNER BC; TRUONG M; SANCHEZ-DARDON J; MCLEAN JRN, 2002, Analysis of radiation-induced apoptosis in human lymphocytes: Flow cytometry using Annexin V and Propidium Iodide versus the neutral comet assay, *Cytometry,* 48, 14-19

WÓJCIK C, 1999, Proteasome in apoptosis: villains or guardians?, *Cellular and Molecular Life Sciences,* 56, 908-917

WOJEWÓDZKA M; KRUSZEWSKI M; IWANENKO T; COLLINS A; SZUMIEL I, 1998, Applications of the comet assay for monitoring DNA damage in workers exposed to chronic low-dose irradiation. I. Strand breakage, *Mutation Research,* 416, 21-35

ZHOU H; XU A; SUZUKI M; RANDERS-PEHRSON G; WALDREN CA; HALL EJ; HEI TK, 2002, The yin and yen of bystander versus adaptive response: lessons from the micro beam studies, *International Congress series,* 1236, 241-247